(2)

NAVAL POSTGRADUATE SCHOOL
Monterey, California

THESIS

USING C-VECTOR METHOD TO DERIVE THE THREE-DIMENSIONAL CIRCULATION PATTERN NEAR THE EAST GREENLAND POLAR FRONT

by

Wei-Szu Li

December, 1992

Thesis Advisor: Peter C. Chu
Second Reader: Robert H. Bourke

REPORT DOCUMENTATION PAGE

1a. REPORT SECURITY CLASSIFICATION UNCLASSIFIED	1b. RESTRICTIVE MARKINGS
2a. SECURITY CLASSIFICATION AUTHORITY	3. DISTRIBUTION/AVAILABILITY OF REPORT Approved for public release; distribution is unlimited.
2b. DECLASSIFICATION/DOWNGRADING SCHEDULE	
4. PERFORMING ORGANIZATION REPORT NUMBER(S)	5. MONITORING ORGANIZATION REPORT NUMBER(S)
6a. NAME OF PERFORMING ORGANIZATION Naval Postgraduate School 6b. OFFICE SYMBOL (*If applicable*) OC	7a. NAME OF MONITORING ORGANIZATION Naval Postgraduate School
6c. ADDRESS (*City, State, and ZIP Code*) Monterey, CA 93943-5000	7b. ADDRESS (*City, State, and ZIP Code*) Monterey, CA 93943-5000
8a. NAME OF FUNDING/SPONSORING ORGANIZATION 8b. OFFICE SYMBOL (*If applicable*)	9. PROCUREMENT INSTRUMENT IDENTIFICATION NUMBER
8c. ADDRESS (*City, State, and ZIP Code*)	10. SOURCE OF FUNDING NUMBERS Program Element No / Project No / Task No / Work Unit Accession Number

11. TITLE (*Include Security Classification*)
USING THE C-VECTOR METHOD TO DERIVE THE THREE-DIMENSIONAL CIRCULATION PATTERN NEAR THE EAST GREENLAND

12. PERSONAL AUTHOR(S) Li, Wei-Szu

13a. TYPE OF REPORT	13b. TIME COVERED	14. DATE OF REPORT (*year, month, day*)	15. PAGE COUNT
Master's Thesis	From To	December 1992	102

16. SUPPLEMENTARY NOTATION
The views expressed in this thesis are those of the author and do not reflect the official policy or position of the Department of Defense or the U.S. Government.

17. COSATI CODES			18. SUBJECT TERMS (*continue on reverse if necessary and identify by block number*)
FIELD	GROUP	SUBGROUP	C-VECTOR, EAST GREENLAND POLAR FRONT, AGEOSTROPHIC PSEUDO-VORTIDITY, TOTAL PSEUDO-VORTICITY

19. ABSTRACT (*continue on reverse if necessary and identify by block number*)

The C-vector method is used to determine the three-dimensional pseudo-vorticity field of the East Greenland Current by using a CTD data set acquired during the 1984 Northwind cruise. The value of the ageostrophic pseudo-vorticity, the total (geostrophic and ageostrophic) pseudo-vorticity and the vertical component of the C-vector curl, Psi, can be calculated by the C-vector method. From these values the pseudo-vorticity can be investigated for the East Greenland Current. Additionally, the positive and the negative vertical motion at each level can be investigated from the Psi value. A two-cell structure with downward motion around the East Greenland Polar Front was found. The C-vector method also demonstrates that the vertical circulation induced by an anticyclonic gyre and the cross-coastal circulation generated by the surface wind can be depicted.

20. DISTRIBUTION/AVAILABILITY OF ABSTRACT	21. ABSTRACT SECURITY CLASSIFICATION	
☒ UNCLASSIFIED/UNLIMITED ☐ SAME AS REPORT ☐ DTIC USERS	Unclassified	
22a. NAME OF RESPONSIBLE INDIVIDUAL Peter C. Chu	22b. TELEPHONE (*Include Area code*) 408-656-3257	22c. OFFICE SYMBOL

DD FORM 1473, 84 MAR — 83 APR edition may be used until exhausted; All other editions are obsolete

Approved for public release; distribution is unlimited.

USING THE C-VECTOR METHOD TO DERIVE THE THREE-DIMENSIONAL CIRCULATION PATTERN NEAR THE EAST GREENLAND POLAR FRONT

by

Wei-Szu Li
Lieutenant Commander,Chinese Navy
B.S., Chung Cheng Institute of Technology

Submitted in partial fulfillment
of the requirements for the degree of

MASTER OF SCIENCE IN PHYSICAL OCEANOGRAPHY

from the

NAVAL POSTGRADUATE SCHOOL
December 1992

Author: Li, Wei-Szu.
Wei-Szu Li

Approved by: Peter C Chu
Peter C. Chu, Thesis Advisor

Robert H Bourke
Robert H. Bourke, Second Reader

Robert H Bourke for
Curtis A. Collins, Chairman,
Department of Oceanography

ABSTRACT

The C-vector method is used to determine the three-dimensional pseudo-vorticity field of the East Greenland Current by using a CTD data set acquired during the 1984 Northwind cruise. The value of the ageostrophic pseudo-vorticity, the total (geostrophic and ageostrophic) pseudo-vorticity and the vertical component of the C-vector curl, Ψ, can be calculated by the C-vector method. From these values the pseudo-vorticity can be investigated for the East Greenland Current. Additionally, the positive and the negative vertical motion at each level can be investigated from the Ψ value. A two-cell structure with downward motion around the East Greenland Polar Front was found. The C-vector method also demonstrates that the vertical circulation induced by an anticyclonic gyre and the cross-coastal circulation generated by the surface wind can be depicted.

TABLE OF CONTENTS

LIST OF FIGURES

ACKNOWLEDGEMENT

I would like to thank my thesis advisor Dr. Peter C. Chu for his support and guidance throughout the research and preparation of this thesis and to my thesis second reader Dr. R. H. Bourke for his kind help and precise revision during the writing of this thesis.

Also, I would like to thank Dr. R. G. Paquette who provided the CTD data for East Greenland Current collected during the 1984 Northwind cruise. In addition, I thank Mr. Padro Tsai for his guidance and instruction in the processing of the data required for this thesis.

Most of all, I thank my wife Hai-Lin for her support and understanding while I worked on this thesis. This work is dedicated to my parents.

I. INTRODUCTION

A. GENERALITY

It has been a long-term effort for physical oceanographers to determine the three dimensional (3-D) circulation of the ocean based upon measurements of its internal density distribution. Two distinct approaches have been developed: (1) the dynamical method, which is widely used by experimentalists, in which one computes the dynamical height of the sea surface relative to a certain depth, from which geostrophic currents can be calculated by assuming a certain level of no motion; and (2) the numerical method, mostly used by modelers, which solves the complete prognostic dynamical equations under some assumptions such that the density field does not change with time. The dynamical method computes only the geostrophic current; no 3-D circulation can be inferred by this method. However, the numerical method of computing the 3-D ocean circulation based upon an observed hydrographic data set presents a difficult problem, i. e., the numerical method does not provide a one-to-one correspondence of the 3-D circulation to the observed hydrographic data set. In order to overcome this difficulty, the C-vector method is proposed in this thesis.

B. TRADITIONAL METHODS OF CURRENT CALCULATION

Traditionally, two methods exist to investigate oceanic currents, the direct method and indirect method. Before the early years of this century, scientists put drift bottles in the ocean. Some of these bottles were found and returned. This is the simplest direct method; however, it provides trajectories of only the surface currents. Another direct method is to moor current meters at fixed positions. This method can obtain current data for several different depths. However, this data pertains only to the immediate vicinity of the current meter.

The indirect method, also known the geostrophic or dynamic method, requires information of the density distribution in the ocean. It is easier to obtain this information from measurements of temperature and salinity than from measurements of currents directly. In fact, most of our knowledge of the ocean circulation below the surface has been obtained in this way.

The geostrophic method uses the density field in the interior of the ocean to calculate the horizontal current field by the geostrophic equation. If the slopes of constant density (or isopycnal surfaces) vary with depth, this indicates that the currents vary with depth. We say that, in this case, there is 'current shear' or 'geostrophic shear'. This is characteristic of the baroclinic situation in which the slopes of the isopycnals vary because the water density

depends on water properties (temperature and salinity) as well as on pressure (depth). The barotropic situation is one in which the density depends on depth only; there will be no current shear, i.e., the current will be the same from top to bottom. This is the barotropic part of geostrophic current and the geostrophic equation gives us no information about it. The barotropic geostrophic currents must be inferred from the trace method (Reid, 1989) or a reference level (level of no motion). The dynamical method only resolves the geostrophic currents; no information about the vertical circulation can be obtained from such methods.

C. THE PURPOSE OF THIS THESIS

In this thesis the author employs a method of calculating the C-Vector that is developed from the geostrophic method in order to obtain more information. The general idea is set out in meteorology by the Q-vector concept (Hoskins et al., 1978). Hoskins et al. determined that the Q-vector derived from the ω equation [the (ω) equation is a very useful diagnostic equation used in mid-latitude cyclogenesis studies as the vertical velocity is important for understanding the observed cloud structure and the development of cyclones and fronts. It describes the vertical velocity distribution that results from dynamical forcing.] can be explained on the synoptician's chart more precisely than earlier studies (Sutcliffe, 1947). This theory is very helpful for learning about and diagnosing

the synoptic and frontal vertical circulation. A disadvantage of this concept is that it ignores the barotropic part of the rotational ageostrophic flow. According to Xu (1992), this problem can be overcome by a new concept, the C-vector concept, which provides a method of resolving the ageostrophic circulation conveniently and a new method of solution which relies on the C-vector equation. The C-vector concept also can be applied in physical oceanography (Chu, 1992). This thesis employs the hydrographic data that was collected from the East Greenland Current by the icebreaker "Northwind" in 1984. A three-dimensional model will be designed to distribute the irregularly spaced hydrographic data on each grid point. The C-Vector will then be computed from these gridded data.

D. ENVIRONMENTAL CONDITIONS IN THE EAST GREENLAND CURRENT

1. Water Masses

Four primary water masses have been recognized historically within the East Greenland Current (EGC) north of the Denmark Strait and in the Greenland Sea (Coachman and Aagaard, 1968 a,b). They are known as Polar Water, Atlantic Water, Atlantic Intermediate Water and Deep Water. Although these water masses are well recognized features of the Greenland Sea, their properties have been variously defined by polar researches. The following discussion of water mass properties follows that of Paquette et al., 1985 and Bourke et al., 1987.

a. Polar Water

Polar Water (PW) is defined as having a temperature of less than 0°C and a salinity of less than 34.5 psu. Water with these characteristics occupies the upper layer of the EGC, and extends over the east Greenland shelf, reaching depths of over 200 m in places (Figure 1.1). Near the East Greenland Polar Front (EGPF) it is pinched off at the surface by the warm water of the Return Atlantic Current(RAC) to the east.

b. Atlantic Water

Atlantic Water (AW) has its origin in the warm, saline Norwegian Atlantic Current and has salinities above 34.9 psu and temperatures above 3°C, sometimes exceeding 5°C even at latitudes north of 75°N.

c. Atlantic Intermediate Water

Atlantic Intermediate Water (AIW) ranges in temperature from 0°C to 3°C and in salinity from 34.5 to 34.9 psu. This water is found over the deeper parts of the shelf and the troughs which cut across it and in the region of the EGPF. It is also found in the upper layer between the West Spitsbergen Current (WSC) and the EGC. In the frontal zone and westward thereof, it lies underneath the PW. The RAC is essentially all AIW. The RAC has its source in the AW of the WSC, part of which turns westward and southward at latitudes between 75°N and 80°N or occasionally even farther north.

d. Deep Water

Deep Water (DW) is found below about 800 m. The temperature of this water is less than 0°C decreasing slowly until it attains a value near -1°C at the bottom. The salinity varies little remaining between 34.88 and 34.90 psu, which represents a decrease from the usually higher salinities of the AIW above it. No DW is found on the shelf.

2. Currents and Circulation

a. General Circulation in the Greenland Sea

The general circulation in the Greenland Sea is presented in Figure 1.1. The surface circulation is dominated by a large cyclonic gyre bounded to the south by the Jan Mayen Current and to the east by the Norwegian Atlantic and West Spitsbergen Currents. In the northern portion of the Greenland Sea, the West Spitsbergen Current splits into two branches, one branch continues to flow northward; the second turns westward, subsequently submerging to about 200 m and turning southward. This second branch of relatively warm water, called the Return Atlantic Current (RAC), together with the East Greenland Current (EGC), which comes from Arctic PW, accounts for the flow of water in the western portion of the Greenland Sea. Figure 1.2 is a map of the estimated near surface circulation pattern in the region of the East Greenland Current based upon the hydrographic data obtain during the

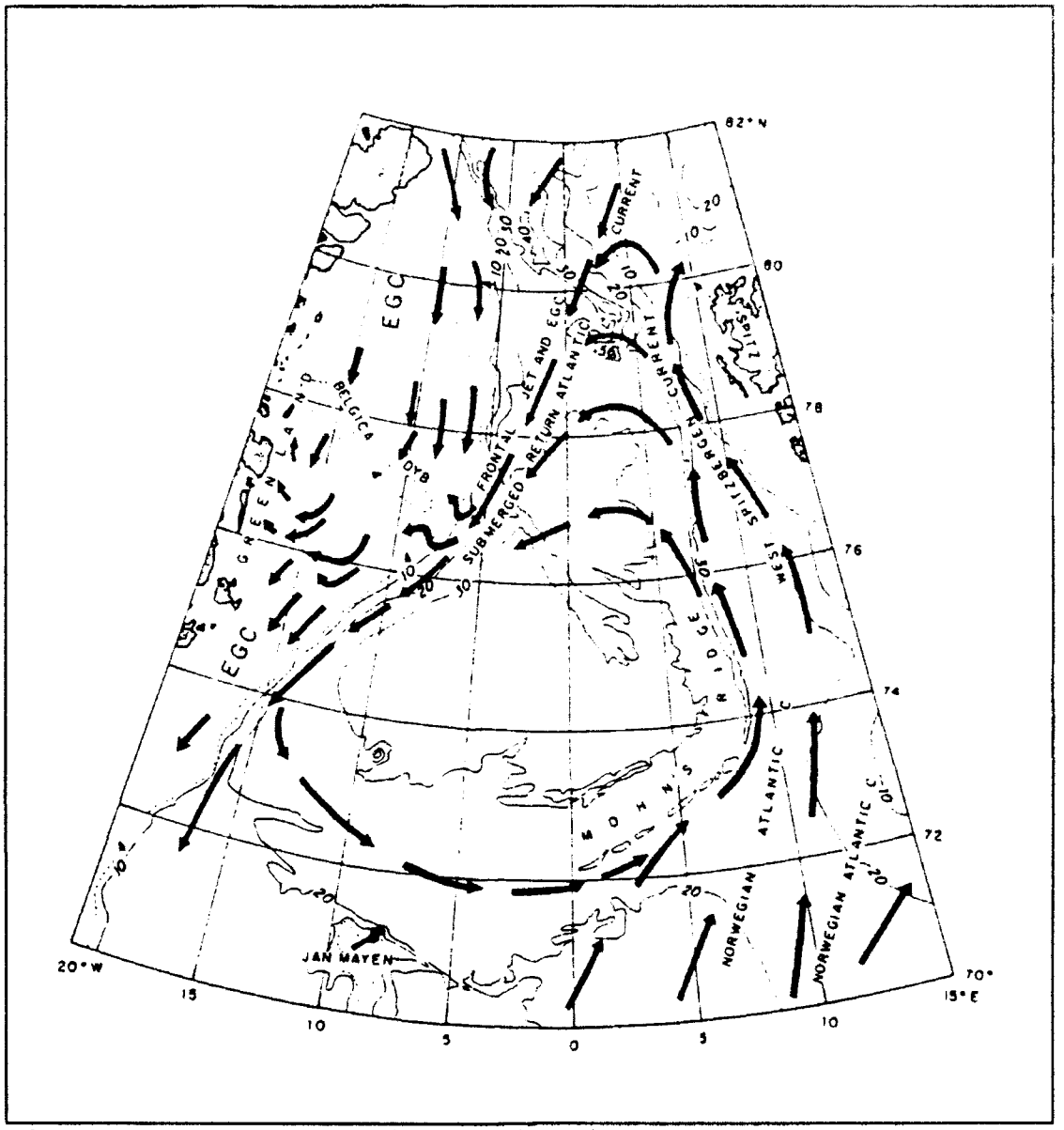

Figure 1.1 General circulation in the Greenland Sea (from Paquette et al., 1985).

1984 Northwind cruise. During the period of this cruise two current meters were moored on the 1000 m isobath near 78.5°N essentially under the jet of the EGC (Muench et al., 1986). The mean speed compared well with the baroclinic current calculated by Bourke et al. (1987), based on geostrophic

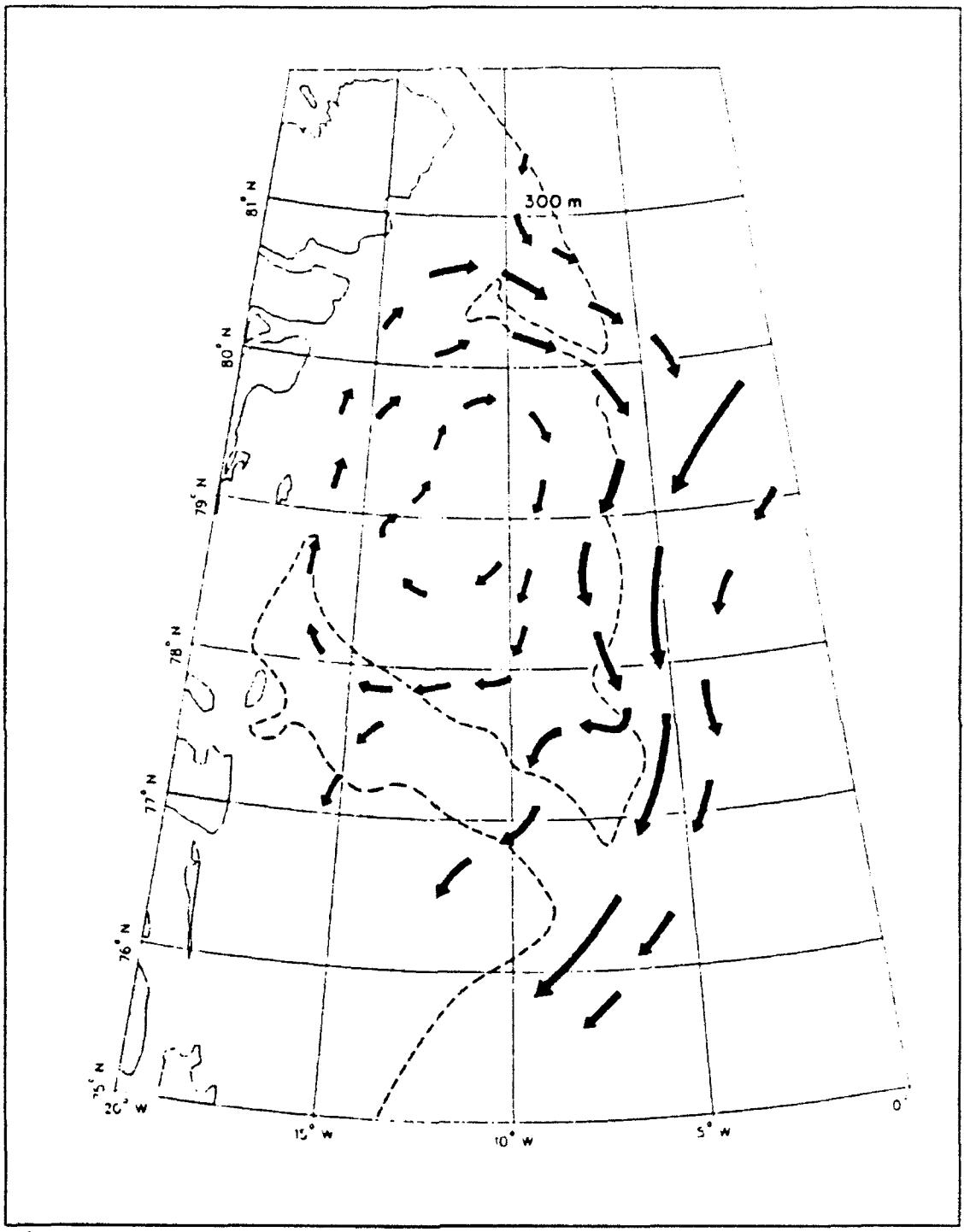

Figure 1.2 Near-surface baroclinic circulation over the east Greenland continental shelf. The length of the arrows is suggestive of the relative speed, with maximum speeds near the EGPF (Bourke et al., 1987)

velocity cross sections referenced to 500 m depth or the bottom. The southward part of the geostrophic transport ranged from 1.33 to 1.61 Sv, with an average of 1.47 Sv. From three sections which extended across the entire shelf, the northward part of the transport ranged from 0.44 to 0.72 Sv, with a mean of 0.58 Sv. These means were subtracted to give a net flow in the EGC of 0.89 Sv southward. The northward flow near the coast turned anticyclonically near 80°N following the depression of the Westwind Trough. This anticyclonic circulation transported about 0.5 Sv, providing a substantial amount of recirculating upper layer shelf water to the frontal zone. The northward flow near the coast also was substantiated by ice drift measurements using NOAA 7 imagery in August - September 1985.

b. Return Atlantic Current

The Return Atlantic Current (RAC) is found to be a notable feature and requires more emphasis than that given in previous work. The current gains its identity from being a core of warm, high-salinity water, often broken into differing filaments, most of it being above 0°C and near the high end of the salinity range for AIW, even overlapping into AW. Property limits for these waters are described later in this paper. The RAC has a width of 100 km or less and lies along the EGPF at depths roughly between 50 to 300 m, commonly at least partly under the PW.

3. East Greenland Polar Front

This front acts as the boundary between cold fresh PW, flowing southward as part of the EGC along the Greenland coast, and the warmer, more saline AIW immediately to the east (Paquette et al.,1985). The warm, saline water to the east of the ice must originate in the AW of the WSC. At the ice edge the horizontal density gradient (i. e., the baroclinic shear) is strongest. It is in this region that a narrow (~50 km wide) southward flowing jet exists. Maximum speeds in excess of 40 cm/s have been observed. The jet decays with depth essentially vanishing by 300 m.

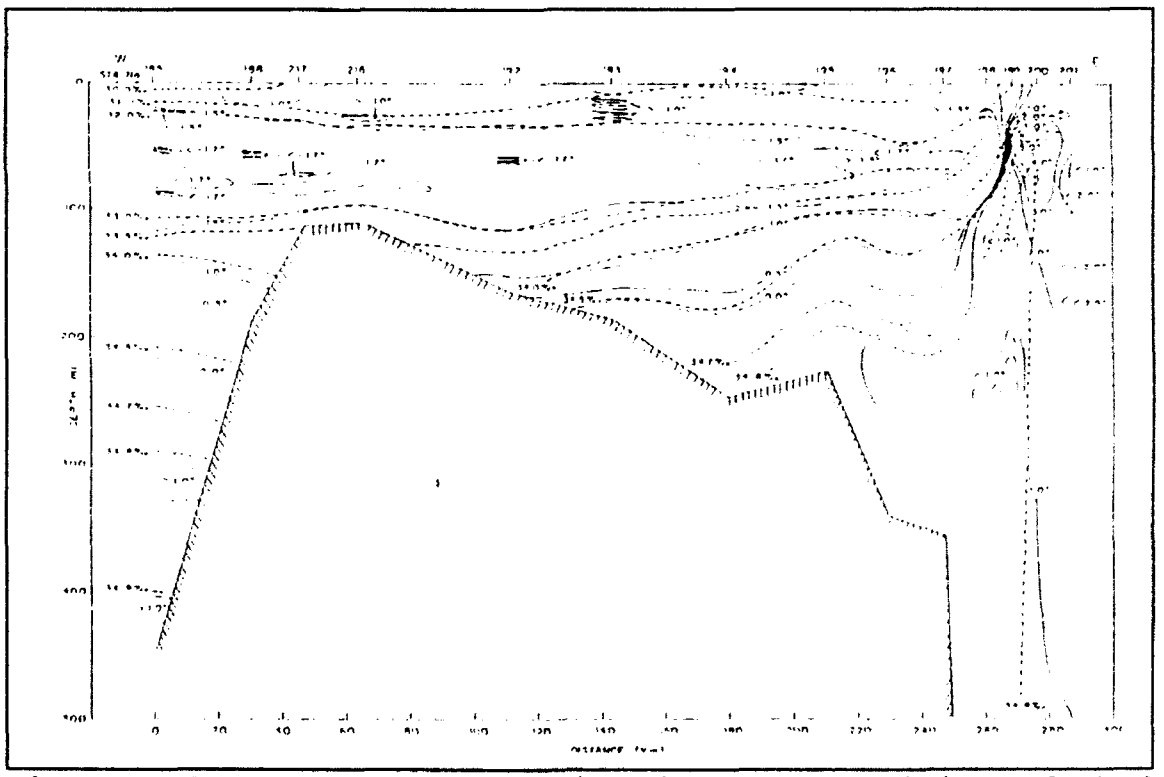

Figure 1.3 Temperature (solid line) and salinity (dashed line) cross section along 78°12´. The EGPF is near the shelf break (Bourke et al., 1987).

Figure 1.3 is a temperature salinity cross section along 78°12 N. In the vicinity of station 199, a sharp temperature and salinity gradient can be seen. This feature marks the core of the EGPF. The cold and dilute PW can be seen to the left of the EGPF; the warm and saline AW and AIW are to the right of the EGPF.

Figure 1.4 is a similar cross section farther southward aligned along the axis of Belgica Trough. In this figure, the region of the sharp gradient of temperature and salinity is between stations 265 and 263.

The data in these two figures represent summertime conditions prevalent during 1984.

E. DATA BACKGROUND

1. Original Hydrographic Survey Data and Grid Point Area

a. Original Hydrographic Survey Area

During August and September 1984, the icebreaker Northwind visited the northern part of the Greenland Sea, the east Greenland shelf and the EGPF region. A hydrographic survey was conducted in the region bounded by 17°W and 10°E, and 75.5°N and 81.5°N. More than 300 CTD stations were occupied during this four week cruise (Figure 1.5). This study uses the data from 237 stations from this cruise (Figure 1.6). In addition to temperature and salinity data, density (σ_t) and wind speed are also used.

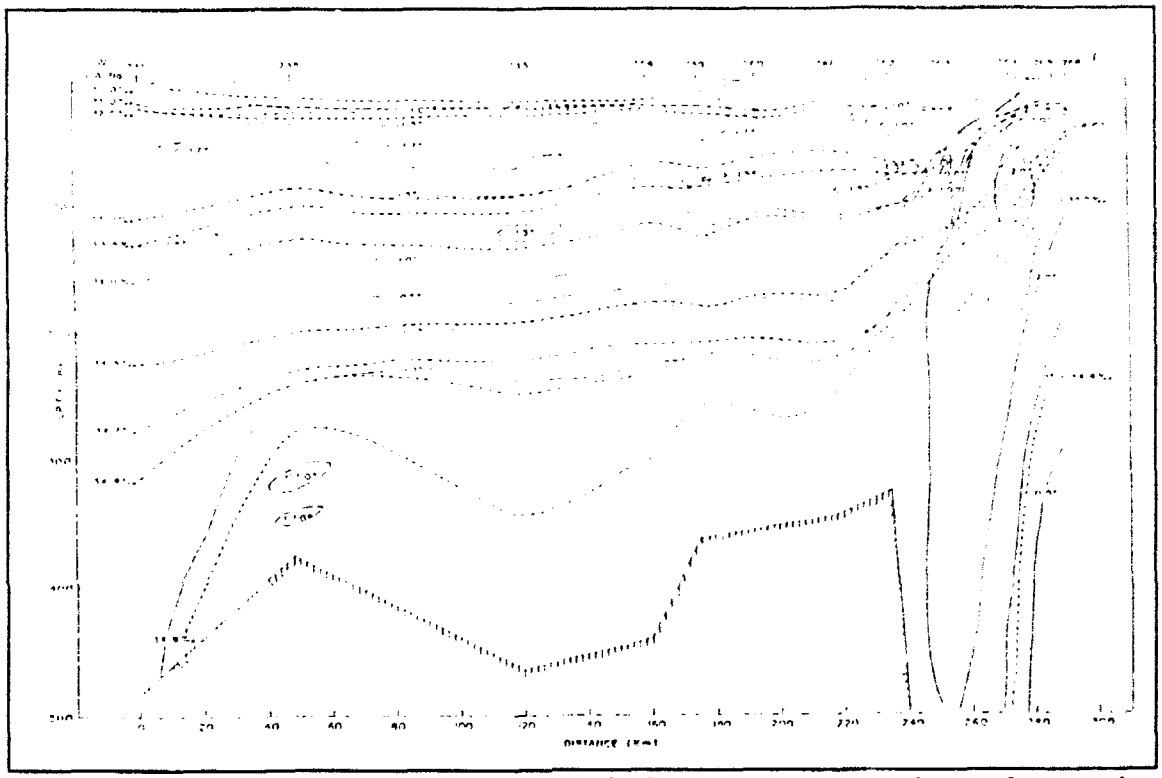

Figure 1.4 Temperature and salinity cross section along the axis of Belgica Trough and across the EGPF (Bourke et al., 1987).

b. Grid Point Area

The region encompassed by the Northwind cruise was gridded to provide a spatially-smooth data field. The grid extended from 15°W to 5°W and from 76.5°N to 81°N. The rectangular grid area contains 10 x 21 grid points with the distance between each point being about 25 km. The northwest corner of this grid area is on land. Excluding the points on land, the grid contains 195 points (Figure 1.8).

2. Bathymetry

Johnson and Eckhoff (1966) collected previously acquired bathymetric data from the Greenland Sea to make a bathymetric map of that region. According to their

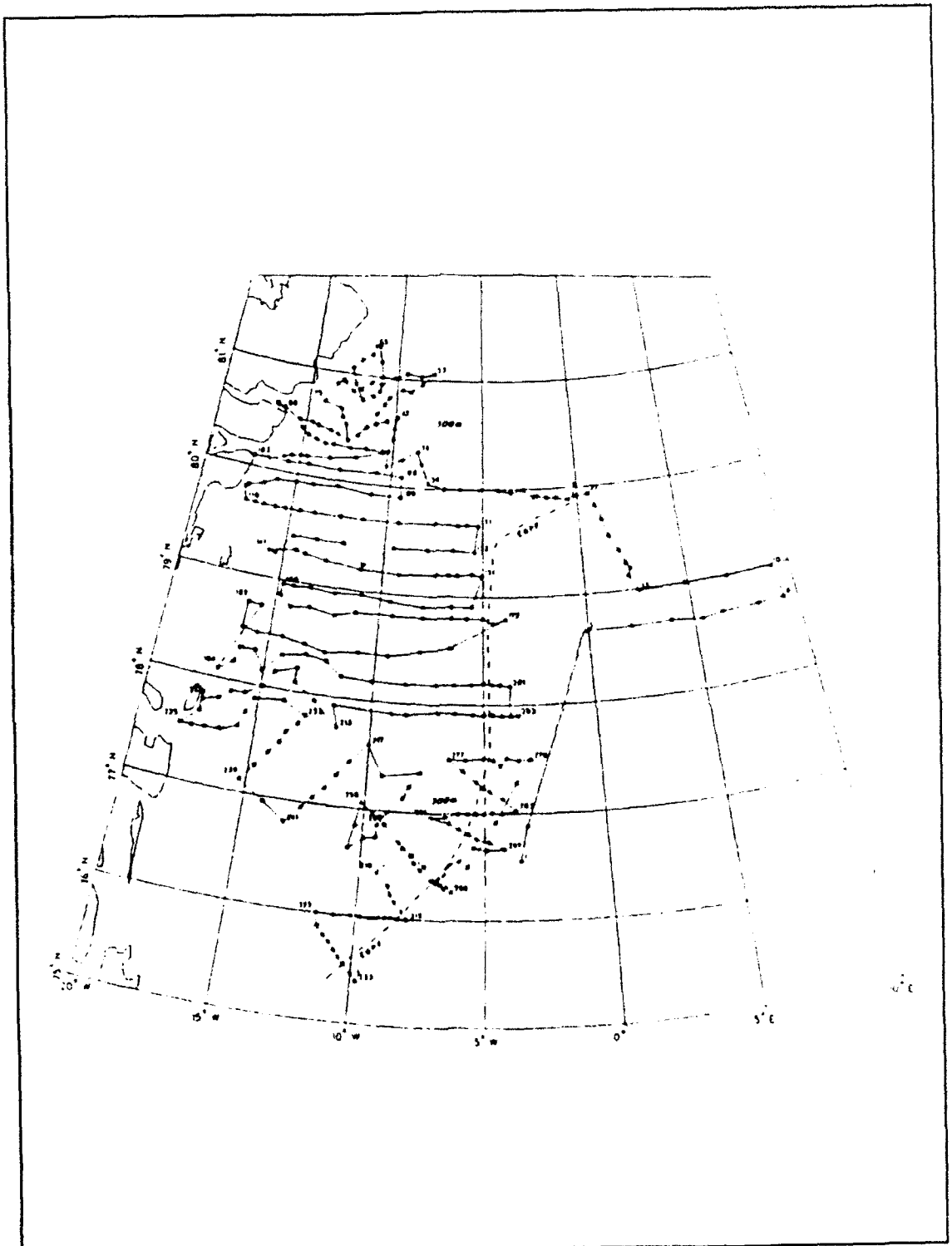

Figure 1.5 CTD stations during the Northwind 1984 MIZEX cruise. The 300 m isobath is shown dotted. The ice edge and EPGF are shown dashed (Tunnicliffe, 1985).

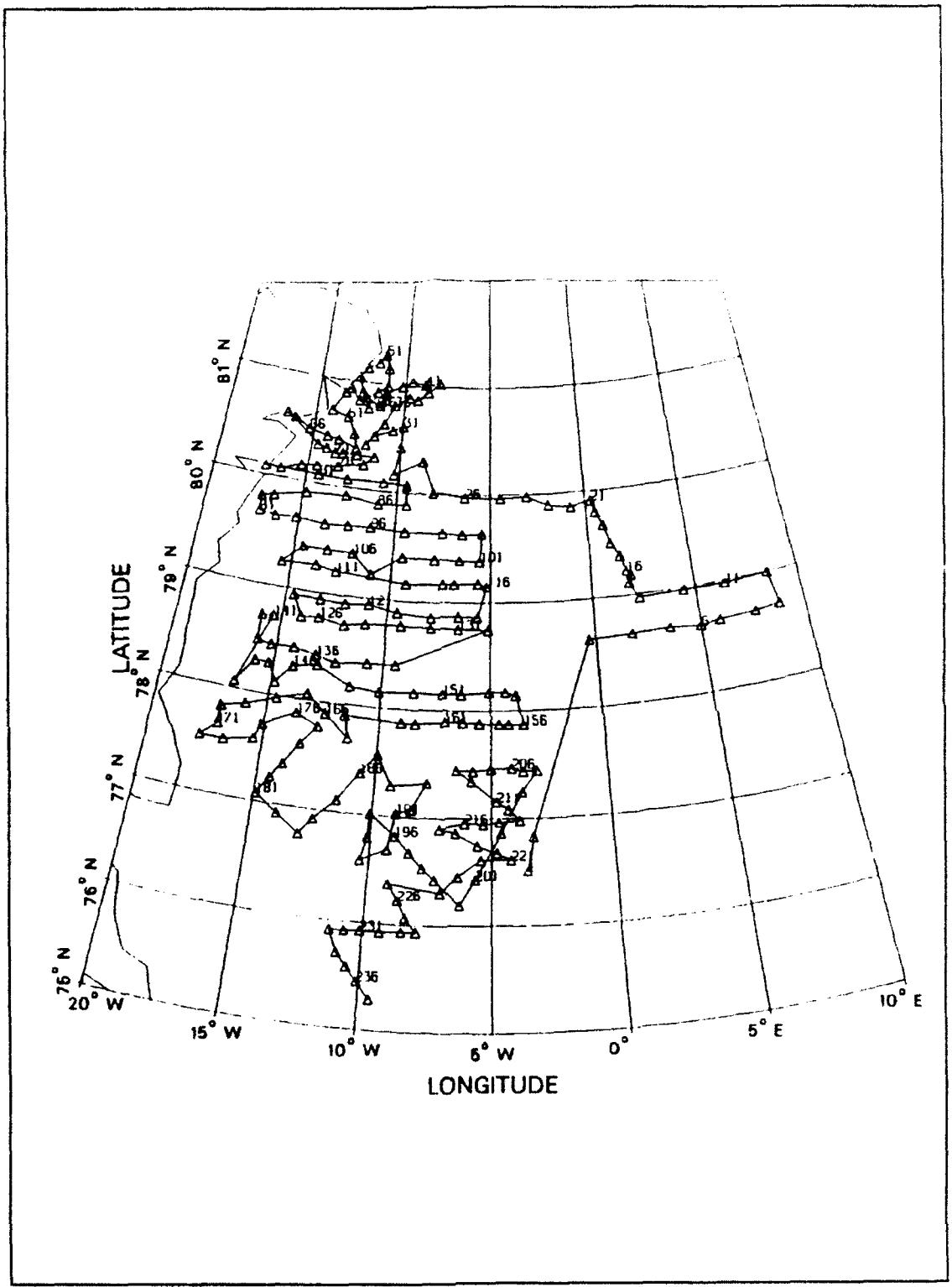

Figure 1.6 The stations chosen from the Northwind 1984 cruise for distributing the data to grid points.

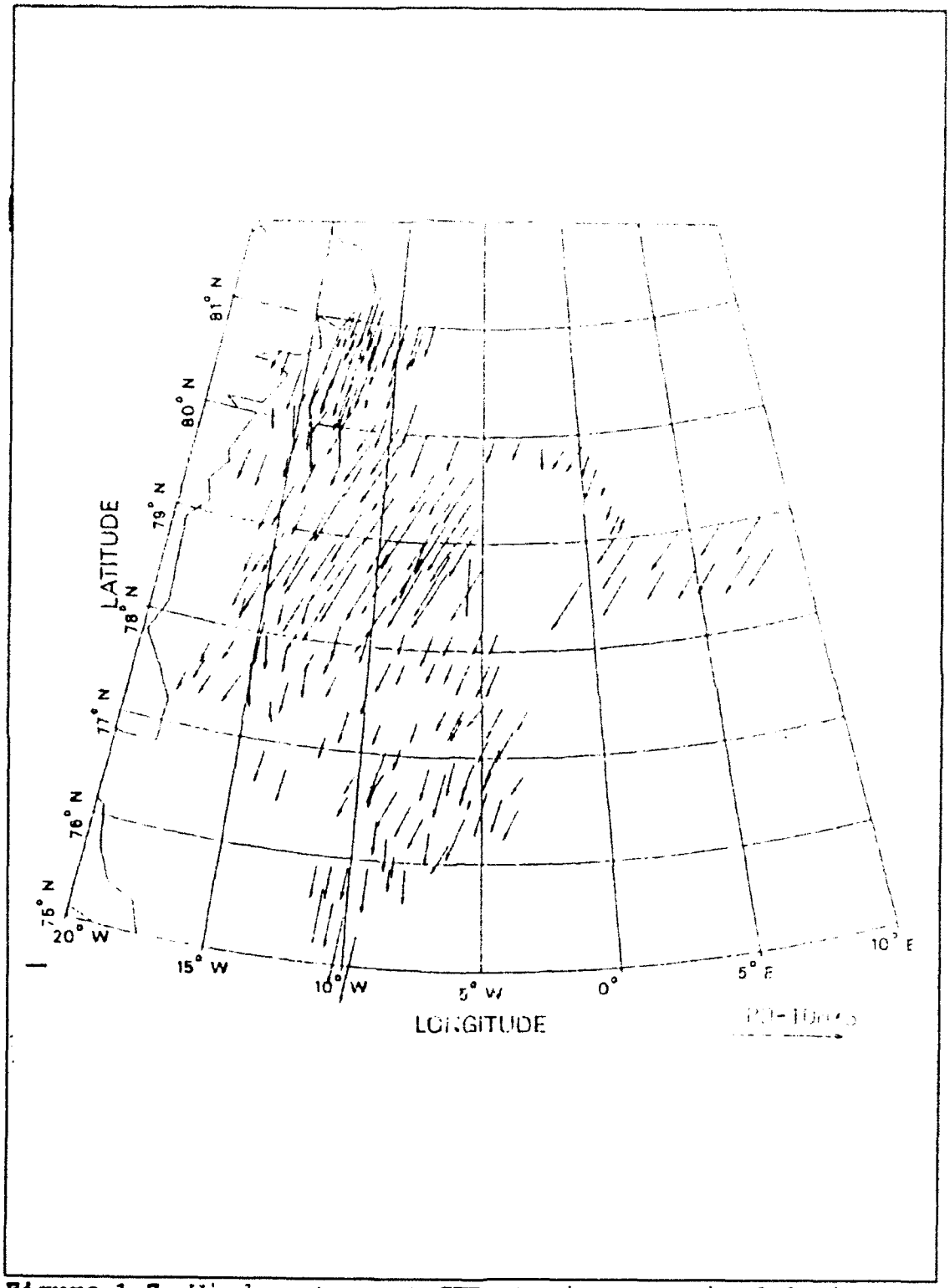

Figure 1.7 Wind vectors at CTD stations acquired during the Northwind 1984 cruise.

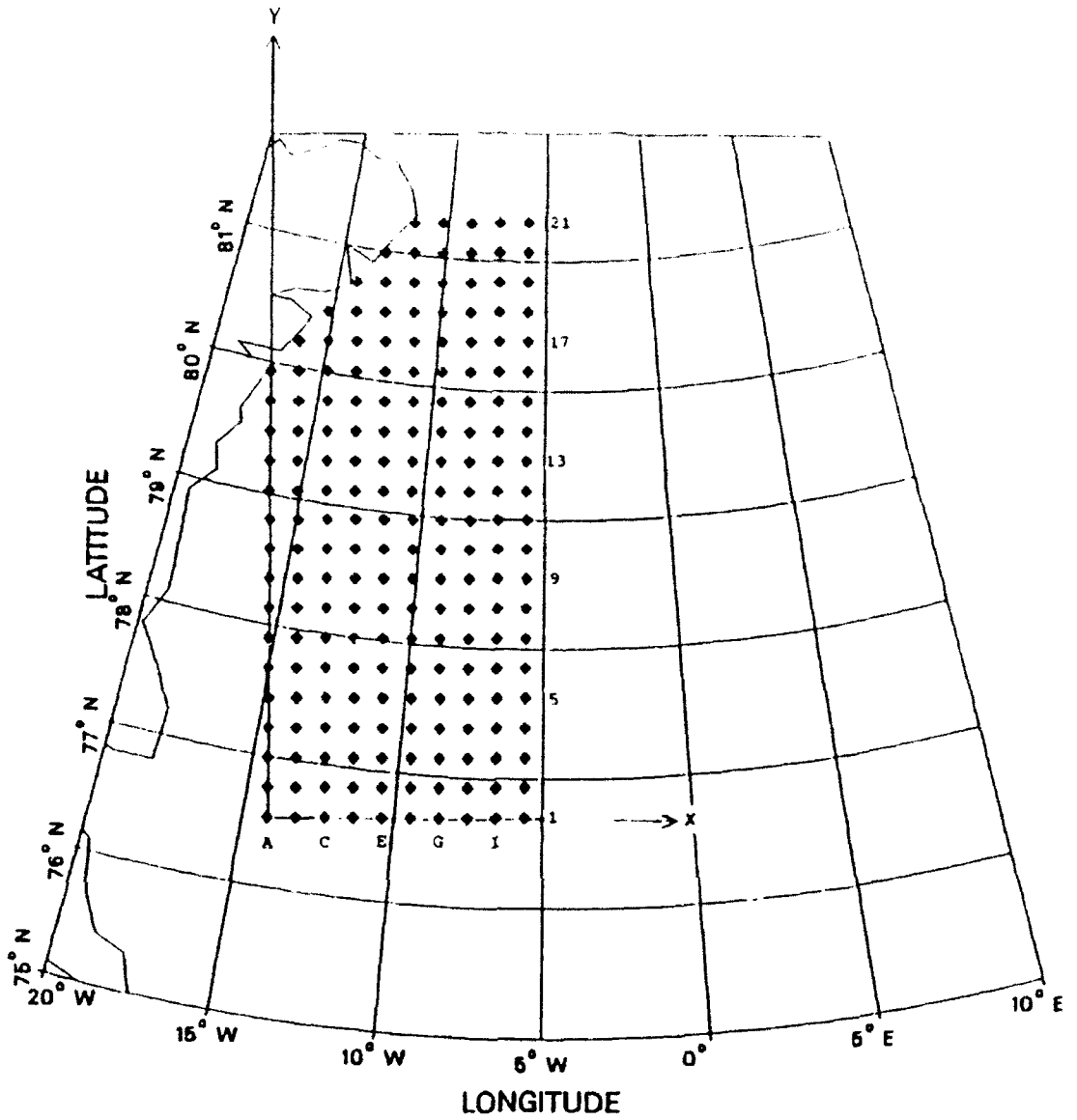

Figure 1.8 Positions of grid points in the three-dimensional C-vector model of the western part of the Greenland Sea.

description, the Greenland shelf, as is typical with most high latitude continental shelves, is broad, irregular, and fairly deep. The continental shelf is approximately 100 km wide at 70°N and broadens to 240 km at 76°45'N. It then narrows with increased latitude being only 150 km wide at 80°30'N. The continental shelf is typically rough with an approximate 9-m

amplitude and 700-m wave length relief superimposed on a rather uneven platform. Troughs are present on shelves near the coast. Some of these appear to parallel the coast of Greenland while others are nearly normal to the shoreline.

A detailed map of the east Greenland shelf bathymetry is shown in Figure 1.9. It is derived from the map of Perry et al. (1980) but significantly updated by depth measurements made at CTD stations during the Westwind 1979 and the Northwind 1981 and 1984 cruises and produced by Tunnicliffe (Bourke et al., 1987). The bathymetry of the Greenland continental shelf is cut by three troughs or depressions:

- Belgica Trough:

  Belgica Trough cuts the shelf from the shelf break at 77°N westward to just north of Ile de France at 78°N. The greatest depth is in excess of 500 m at the shoreward end.

- Norske Trough:

  Norske Trough runs from the west end of Belgica Trough, to the west end of Westwind Trough and parallels the coastline.

- Westwind Trough:

  Westwind Trough is located at the north end of the Greenland continental shelf and extends southeasterly from Engolf's Fjord. It is somewhat shallower than Belgica Trough.

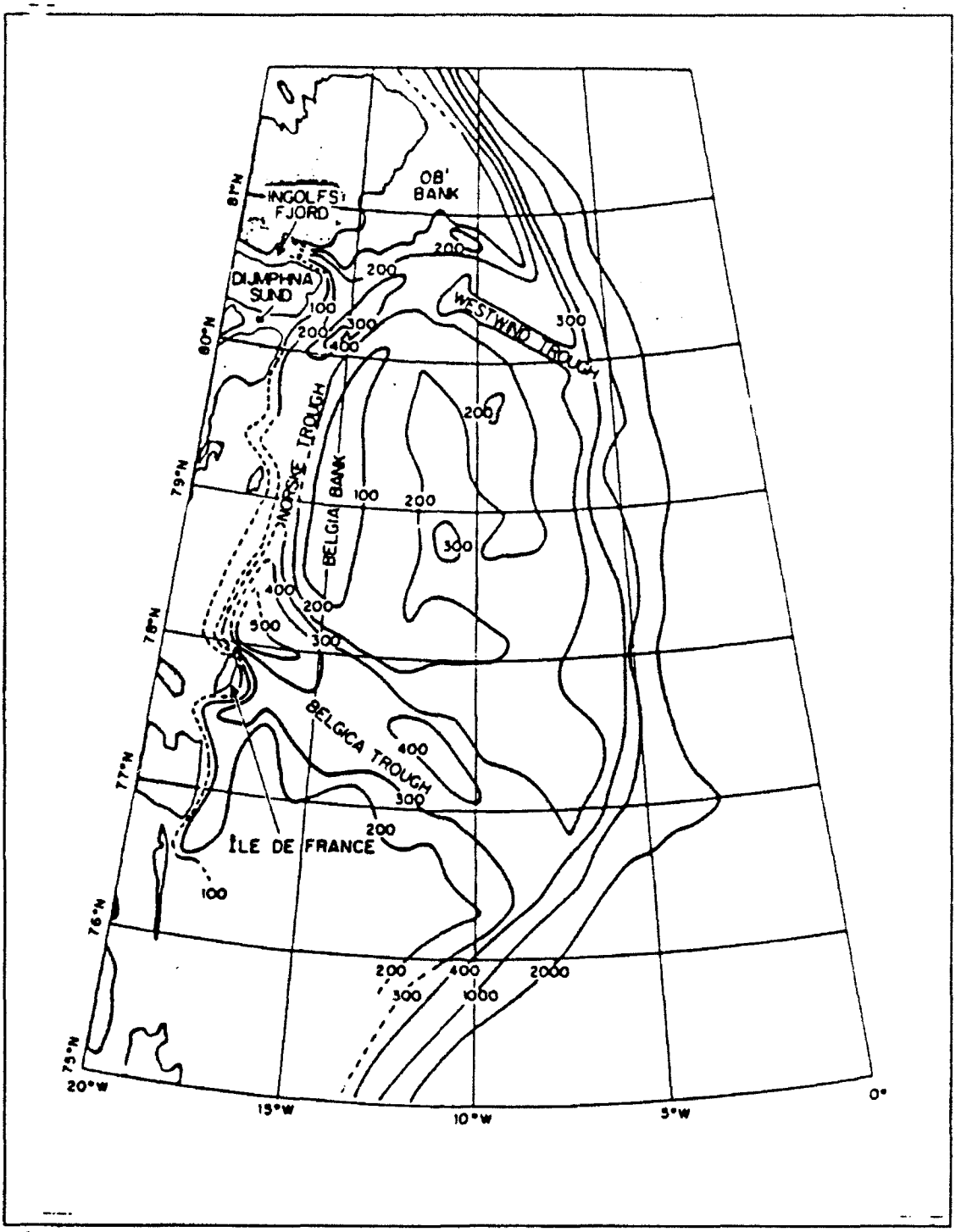

Figure 1.9 The bathymetric map of the Greenland continental shelf was produced by contouring depths measured at CTD stations during the 1979 Westwind and the 1981 and 1984 Northwind cruises (Bourke et al., 1987).

II. BASIC THEORY

A. "C-VECTOR" CONCEPT

1. Geostrophic and Ageostrophic Circulation

The ocean currents, as mentioned in Chapter I, are not truely geostrophically balanced. When we compute the velocity in the ocean by the geostrophic method, we depict the major movement of the oceanic waters but the total flow is not represented, particularly in regions having strong fronts near the coast (Arnone et al., 1990). Neither geostrophic currents nor the dynamic height provides any information about the three dimensional flow field near oceanic fronts. In order to diagnose the three dimensional flow field near frontal regions, a new theory, the 'C-vector', is introduced. The flow over most continental shelves contains two parts, geostrophic currents and ageostrophic contributions. The geostrophic currents are obtained from hydrographic data sets while the ageostrophic circulation includes the non-geostrophic contribution, namely the flow driven by the surface wind field. The C-Vector is a new technique which can calculate the three-dimensional ageostrophic circulation by incorporating hydrographic and surface wind data sets (Chu, 1992).

Assuming the Boussinesq approximation, the geostrophic

currents in the north-south and east-west directions are computed from the density data derived from CTD observations by

$$f\frac{\partial U_g}{\partial z} = \frac{g}{\rho_0}\frac{\partial \rho}{\partial y} = \frac{g}{\rho_0}\frac{\partial \sigma_t}{\partial y} = -\frac{\partial b}{\partial y} \qquad \textbf{(1a)}$$

$$f\frac{\partial V_g}{\partial z} = -\frac{g}{\rho_0}\frac{\partial \rho}{\partial x} = -\frac{g}{\rho_0}\frac{\partial \sigma_t}{\partial x} = \frac{\partial b}{\partial x} \qquad \textbf{(1b)}$$

where

ρ_0 : the characteristic value (a constant) representing the mean density

ρ : the density deviation from ρ_0 (i.e., $\rho_0+\rho$ is the observed density field)

σ_t : $\rho + \rho_0 - 1000$

b : the buoyancy force ($-g\rho/\rho_0$)

As stated previously, the geostrophic current does not represent the entire water motion. To determine this we must consider the non-geostrophic contributions. The basic non-geostrophic equations, describing the coastal water flow without an adiabatic source of buoyancy and induced by the wind stress, are

$$\left(\frac{\partial}{\partial t} + \vec{V}\cdot\nabla\right) u - f(v - V_g) = \frac{\partial Y^x}{\partial z} \qquad \textbf{(2a)}$$

$$\left(\frac{\partial}{\partial t} + \vec{V}\cdot\nabla\right) v + f(u - U_g) = \frac{\partial Y^y}{\partial z} \qquad \textbf{(2b)}$$

$$(\frac{\partial}{\partial t}+\vec{V}\cdot\nabla)\, b+N^2 w=0 \qquad (2c)$$

$$\frac{\partial u}{\partial x}+\frac{\partial v}{\partial y}+\frac{\partial w}{\partial z}=0 \qquad (2d)$$

where

V : (u, v, w)

f : Coriolis parameter [$2\Omega\sin$(latitude)]

N : Brunt-Vaisala frequency

(Y^x, Y^y) : turbulent momentum flux caused by the surface wind stress (τ_x, τ_y)

$$Y^x|_{z=0}=\frac{\tau^x}{\rho_0}\ , \quad Y^y|_{z=0}=\frac{\tau^y}{\rho_0} \qquad (3)$$

We decompose the three-dimensional flow into two parts: the geostrophic current (V_g) and the ageostrophic circulation (V_a)

$$\vec{V} = \vec{V}_g+\vec{V}_a \ . \qquad (4)$$

After the decomposition, the basic equations (2a)-(2d) should have the following form:

$$\mathbf{H}(\vec{V}_a) = \mathfrak{R}(\vec{V}_g, \rho, Y^x, Y^y) \qquad (5)$$

where $\mathbf{H}$ and $\mathfrak{R}$ are differential operators. If the real forms of these operators are obtained, we can use (5) to compute the three-dimensional ageostrophic circulation (V_a) from the

hydrographic data (V_g, ρ) and the surface wind data.

2. The C-vector

If a quasi-geostrophic (QG) system is employed, this leads to

$$\frac{\partial}{\partial t} + \vec{V} \cdot \nabla \approx \frac{\partial}{\partial t} + \vec{V}_g \cdot \nabla \qquad \textbf{(6b)}$$

The basic equations for the coastal water (2a)-(2d) on an f-plane can be transformed to the following equations:

$$-fV_a = \frac{\partial Y^x}{\partial z} - (\frac{\partial}{\partial t} + \vec{V}_g \cdot \nabla) U_g \qquad \textbf{(7a)}$$

$$fu_a = \frac{\partial Y^y}{\partial z} - (\frac{\partial}{\partial t} + \vec{V}_g \cdot \nabla) V_g \qquad \textbf{(7b)}$$

$$N^2 w_a = -(\frac{\partial}{\partial t} + \vec{V}_g \cdot \nabla) b \qquad \textbf{(7c)}$$

$$\frac{\partial u_a}{\partial x} + \frac{\partial v_a}{\partial y} + \frac{\partial w_a}{\partial z} = 0 \qquad \textbf{(7d)}$$

Using the cross-derivatives with equations (7a) - (7c), the ageostrophic pseudo-vorticity equations become

$$-\frac{\partial}{\partial z}(f^2 v_a) + \frac{\partial}{\partial y}(N^2 w_a) = 2C_1 \qquad \textbf{(8a)}$$

$$\frac{\partial}{\partial z}(f^2 u_a) - \frac{\partial}{\partial x}(N^2 w_a) = 2C_2 \qquad \textbf{(8b)}$$

$$\frac{\partial}{\partial x}(f^2 v_a) - \frac{\partial}{\partial y}(f^2 u_a) = 2C_3 \qquad \textbf{(8c)}$$

where

$$C_1 \equiv -f\left(\frac{\partial U_g}{\partial y}\frac{\partial V_g}{\partial z} - \frac{\partial V_g}{\partial y}\frac{\partial U_g}{\partial z}\right) + \frac{f}{2}\frac{\partial^2 Y^x}{\partial z^2} \qquad \textbf{(9a)}$$

$$C_2 \equiv -f\left(\frac{\partial U_g}{\partial z}\frac{\partial V_g}{\partial x} - \frac{\partial V_g}{\partial z}\frac{\partial U_g}{\partial x}\right) + \frac{f}{2}\frac{\partial^2 Y^y}{\partial z^2} \qquad \textbf{(9b)}$$

$$C_3 \equiv -f\left(\frac{\partial U_g}{\partial x}\frac{\partial V_g}{\partial y} - \frac{\partial V_g}{\partial x}\frac{\partial U_g}{\partial y}\right) - \frac{f}{2}\frac{\partial}{\partial z}\left(\frac{\partial Y^x}{\partial x} + \frac{\partial Y^y}{\partial y}\right) \qquad \textbf{(9c)}$$

$$\vec{C} \equiv (C_1, C_2, C_3) \qquad \textbf{(9d)}$$

C_1, C_2 and C_3 are the three components of the C-Vector. The C-vector can be computed from the oceanic and wind geostrophic currents (U_g, V_g) which are obtained from the hydrographic data set and the wind data (Y^x, Y^y).

In addition, we have another important vector, the pseudo-vorticity of total flow (C_x, C_y, C_z), which is induced from the geostrophic and the ageostrophic currents. These three components are found by following process:

We decompose v and w into $v = v_g + v_a$, $w = w_g + w_a$ but $w_g = 0$, so $w = w_a$, then we get

$$-\frac{\partial}{\partial z}(f^2 v) + \frac{\partial}{\partial y}(N^2 w)$$

$$= -\frac{\partial}{\partial z}(f^2 v_a) - \frac{\partial}{\partial z}(f^2 v_g) + \frac{\partial}{\partial y}(N^2 w_a)$$

$$= -\frac{\partial}{\partial z}(f^2 v_g) + 2C_1 \equiv 2C_x f^2$$

$$\Rightarrow \qquad C_x \equiv \frac{C_1}{f^2} - \frac{1}{2}\frac{\partial v_g}{\partial z} \qquad \textbf{(10a)}$$

After a similar operation, we can get the other components, C_y and C_z :

$$C_y \equiv \frac{C_2}{f^2} + \frac{1}{2}\frac{\partial u_g}{\partial y} \qquad \textbf{(10b)}$$

$$C_z \equiv \frac{C_3}{f^2} + \frac{1}{2}\left(\frac{\partial v_g}{\partial x} - \frac{\partial u_g}{\partial y}\right) \qquad \textbf{(10c)}$$

3. Three Important Physical Characteristics of the C-vector

a. C-vector as an ageostrophic vortex line

The mathematical connection between the C-Vector and the ageostrophic pseudo-vorticity is most clearly seen in the nondimensional form for flows with constant f and N:

$$\nabla \times \vec{V}_a = 2R_0\vec{C} \tag{11}$$

$$\nabla \cdot \vec{V}_a = 0 \tag{12}$$

where $R_0 \equiv U/(FL)$ is the Rossby number, $H/L = W/U = f/N$ is chosen for the scaling, and C is nondimensional here. The ageostrophic vorticity is proportional to the C-vector; therefore, a C-vector streamline can be viewed as an ageostrophic vortex line (Figure 2.1).

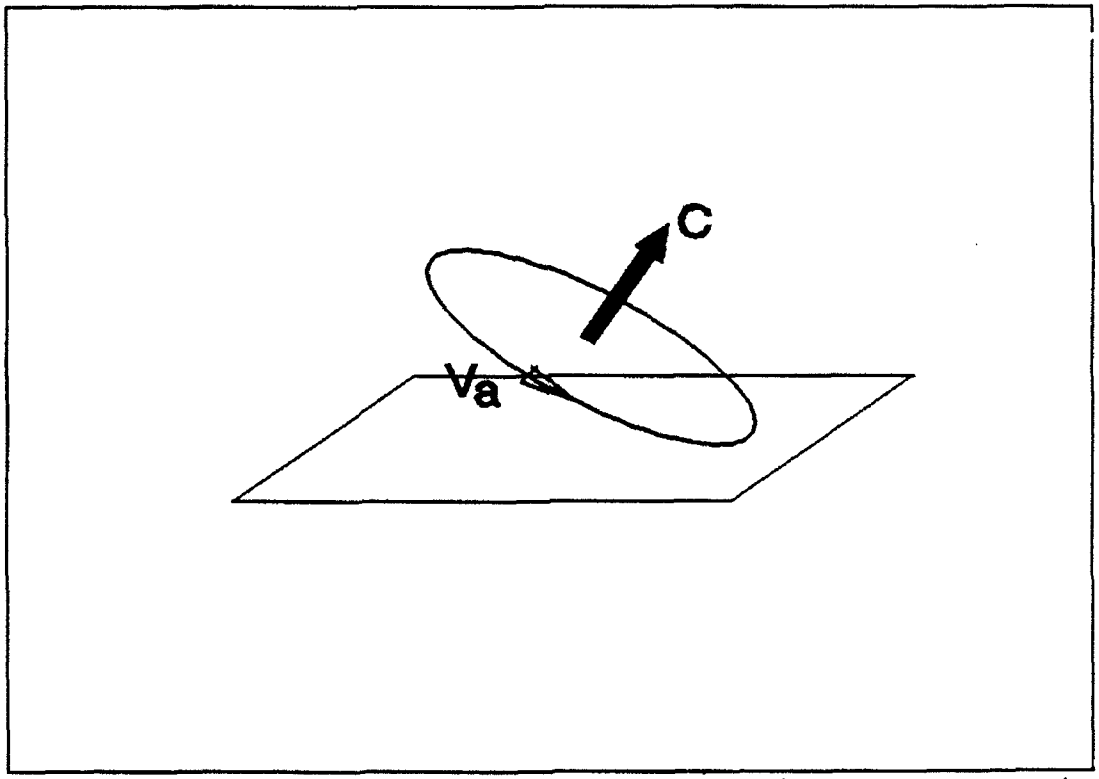

Figure 2.1 Ageostrophic circulation induced by C in three-dimensional space.

b. Inducing vertical velocity from the vertical vorticity of the C-vector

The vertical velocity equation is obtained from $-k\bullet\nabla\times$[eq(12)] :

$$\nabla^2 w_a = -2R_o \vec{k}\cdot\nabla\times\vec{C} \qquad \textbf{(13)}$$

This indicates that the vertical velocity is induced by the vertical vorticity of C (Figure 2.2).

If we define

$$\psi \equiv 2\left(\frac{\partial C_y}{\partial x} - \frac{\partial C_x}{\partial y}\right) \quad , \textbf{(14a)}$$

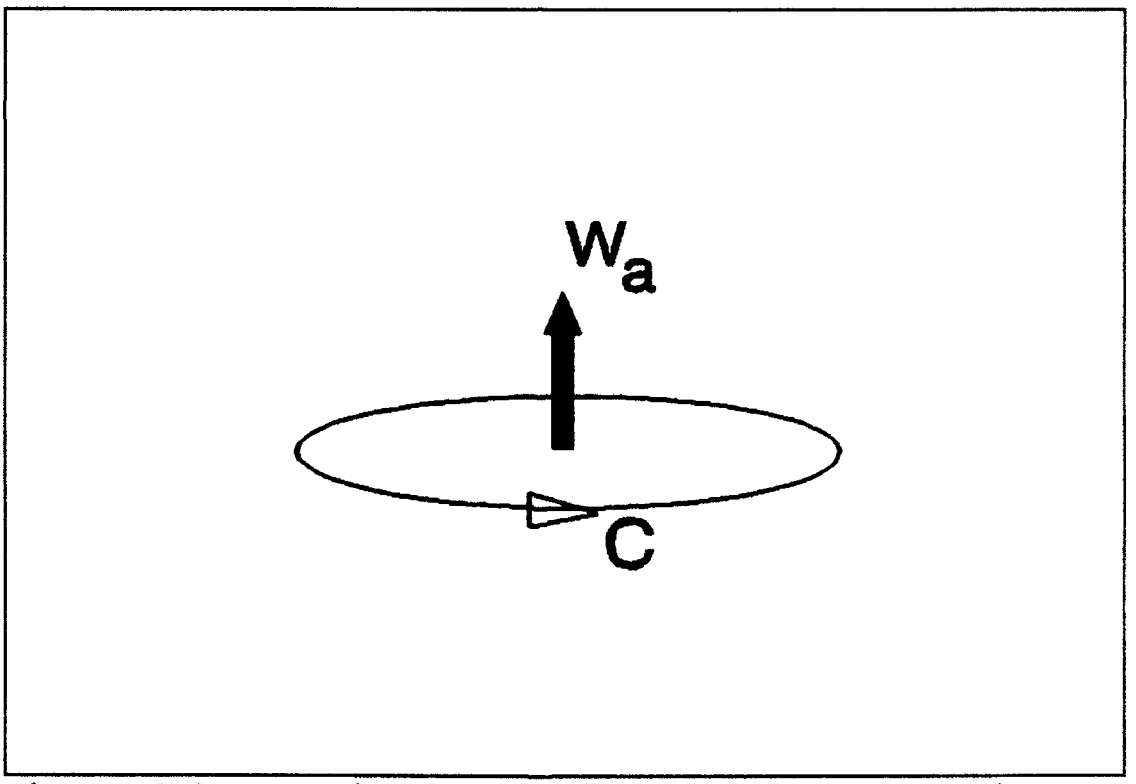

Figure 2.2 Vertical velocity w_a induced by horizontal rotation(vorticity) of C.

then equation (14) becomes

$$\nabla^2 w_a = -2R_0\psi \quad . \quad \textbf{(14b)}$$

If the normal modes are considered, the vertical velocity w_a has the same sign as Ψ.

c. Non-divergence of the C-vector

To add the differential of equation (9a) with respect to x, (9b) with respect to y and (9c) with respect to z, we can get the following equation:

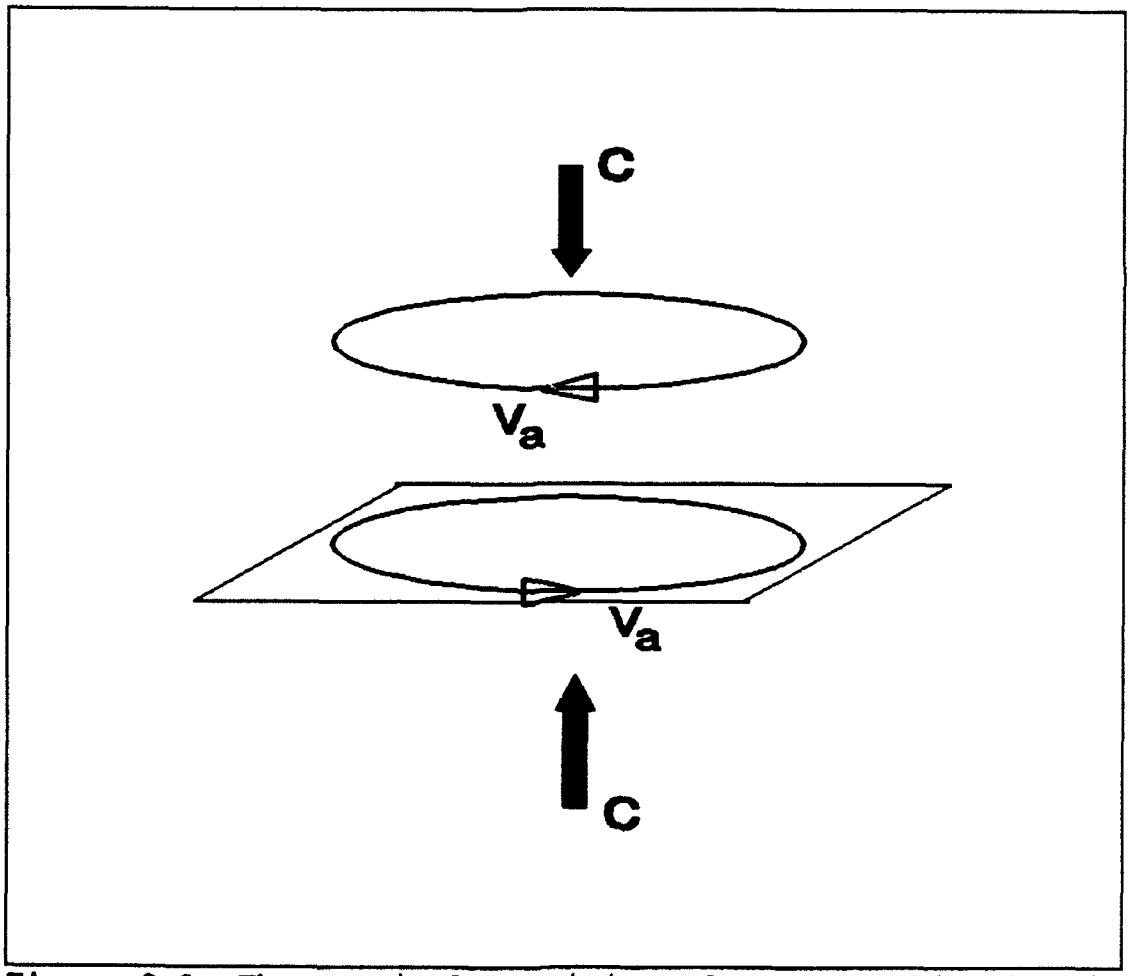

Figure 2.3 The vertical vorticity of ageostrophic flow is inferred from the vertical component of the C-Vector.

$$\nabla \cdot \vec{C} = 0 \qquad (15)$$

which indicates that the C-vector is non-divergent, i.e., the horizontal divergence (convergence) should be balanced by the vertical convergence (divergence). Figure (2.3) shows that the vertical vorticity of ageostrophic flow can be inferred from the vertical component of the C-vector.

B. WEIGHTING FUNCTION

To compute the C-Vector three-dimensionally in the ocean, the hydrographic data on a gridded surface are necessary. Since the CTD stations acquired during the Northwind 1984 cruise were not on grid points, a weighting function is used to distribute the original CTD data onto the grid points. The data, after processing by this method, will still retain the original characteristics of this particular special region of the ocean.

Barnes(1964) used a Gaussian weighting function to develop an objective analysis and filtering technique for application to a two-dimensional meteorological field. He modified this method in 1973 for scale separation. Maddox(1980) developed this analysis technique to study atmospheric circulations associated with a large complex of thunderstorms. This scale separation has been used successfully to isolate different subsynoptic meteorological phenomena. Tintoré et al. (1990) used this technique to investigate mesoscale dynamics and

vertical motion in the Alboran Sea. This technique is also useful in the analysis of oceanographic phenomena.

The two-dimensional values of a parameter, e. g., temperature, $f^0(i,j)$ at each incremental depth at the grid point (i,j) are computed from the observed data from a total of N stations. There are four basic steps.

The first step is to calculate the first guess value at each grid point from the observed data at each station.

$$f^0(i,j) = \frac{\sum_{n=1}^{N} W_n(i,j)\, f_n(x,y)}{\sum_{n=1}^{N} W_n(i,j)} \qquad (16)$$

where

$f_n(x,y)$: the observed data

$f^0(i,j)$: the first guess value at each grid point from the observed data at each station.

The weighting function $w_n(i,j)$ is

$$W_n(i,j) = \exp[-d_n(i,j)^2/4c] \qquad (17)$$

where

$d_n(i,j)$: the separation distance between the grid point (i,j) and the nth station.

c : 1000 (analysis parameter).

The second step is to calculate the first guess value at each station considering all the stations. The weighting

function in eq(21) is

$$f_n^0(x,y) = \frac{\sum_{n=1}^{N} W_n^*(x,y)\, f_n(x,y)}{\sum_{n=1}^{N} W_n^*(x,y)} \qquad (18)$$

$$W_n^*(x,y) = \exp[-d_n(x,y)^2/4c] \qquad (19)$$

where

$d_n(x,y)$: the distance between a station and all other stations.

The third step is to calculate the difference between the original station data and the first guess value at each station.

$$\Delta f_n(x,y) = f_n(x,y) - f_n^0(x,y) \qquad (20)$$

where

$f_n(x,y)$: the observed data at each station.

$f_n^0(x,y)$: first guess value of the nth station determined from adjusting the observed data at all stations.

$\Delta f_n(x,y)$: the difference between the observed data and the first guess value at the same point.

The fourth step is to compute the resulting grid point data as following :

$$f(i,j) = f_n^0(i,j) + \frac{\sum_{n=1}^{N} W_n^{**}(i,j)\Delta f_n(x,y)}{\sum_{n=1}^{N} W_n^{**}(i,j)} \qquad (21)$$

where the modified weighting function, w_n^{**}, is

$$w_n^{**}(i,j) = \exp[-d_n(i,j)^2/4cg],\ 0<g<1 \qquad (22)$$

Advantages of Using Weighting Functions:

Barnes(1973) listed the advantages of this Gaussian weighting, objective analysis and filtering technique as the following :

- The weighting function constants c and g are chosen prior to the analysis so that pattern scales, resolvable by the data distribution, will be revealed to a known response amplitude.
- If w_n approaches zero asymptotically, the influence of data may be extended to any distance without changing the weighting function and response characteristics.
- Small-scale noise is suppressed so that further smoothing with numerical filters is not necessary.
- Desired scale resolution is achieved with only one iteration.

III. DATA PROCESSING

As previously mentioned, there were 333 CTD stations acquired during the 1984 Northwind cruise. Of these, the density (σ_t) data from 237 stations were chosen for use in this thesis. These data can be used to compute the σ_t at each grid point. After determining the σ_t data at each grid point, the geostrophic velocity and the C-vector at each grid point can then be computed.

A. COMPUTING THE ASSUMED σ_t VALUE AT EACH GRID POINT

The weighting function described in the previous chapter can be used to compute the assumed σ_t value at each grid point from the σ_t data of the original CTD station. The following steps constitute the procedures for obtaining the σ_t data at each grid point:

(1) choose the grid area;

(2) set the relative coordinate for each grid point and each CTD station;

(3) compute the distance between each grid point and each CTD station, as well as between each CTD station and every other CTD station from the relative coordinate;

(4) obtain the 'grid to station' weighting value from the 'grid to station' distance data file;

(5) obtain the 'station to station' weighting value from the 'station to station' distance data file;

(6) calculate the first guess of the σ_t value at each grid point in every layer by using the 'grid to station' weighting value;

(7) calculate the guessed station σ_t value from the original σ_t value of the other stations by using the 'station to station' weighting value;

(8) obtain the differences by subtracting the guessed σ_t value at each CTD station from the guessed station σ_t value;

(9) obtain the assumed differences between the first guessed σ_t value at each grid point and the resulting guessed σ_t value by using the weighting function to calculate the differences in (8);

(10) obtain the resulting guessed σ_t at each grid point by adding the first guessed σ_t at each grid point and the assumed differences in (9).

B. COMPUTATION OF GEOSTROPHIC VELOCITY

The baroclinic velocity can be calculated from σ_t data by using equations (1a) and (1b). The constants in these equation are $g = 9.81\ m\ s^{-2}$, $\rho_0 = 1026\ kg\ m^{-3}$, the Coriolis parameter $f = 2\Omega\sin\phi$ $\Omega = 7.29\times10^{-5}\ sec^{-1}$ and $\phi = 75°$. The geostrophic method requires the assumption of a level of no motion. Because the bottom depths vary considerably over the study area, the weighting function can produce an assumed σ_t

value below the bottom, that is, a shallow station can refer to the σ_t value of a deeper station around it to assume the σ_t value below the bottom by calculating the weighting function. The assumed σ_t value above 300 m at each station can be computed. The geostrophic velocities, U_g and V_g, can be calculated by using the assumed σ_t value at 300 m, chosen to be the level of no motion.

C. COMPUTATION OF THE C-VECTOR

After U_g and V_g are obtained by using the geostrophic method, C_1, C_2 and C_3, the three components of the C-vector, can be computed continuously by using equations (9a), (9b) and (9c). The turbulent momentum fluxes Y^x and Y^y are calculated from the following equations:

$$Y^x|_{z=0} = \frac{\tau^x}{\rho_0} , \quad Y^y|_{z=0} = \frac{\tau^y}{\rho_0}$$

where the wind stress τ^x and τ^y is calculated from :

$$\tau^x = \rho_a C_D |\vec{V}_w| u_w, \qquad \tau^y = \rho_a C_D |\vec{V}_w| v_w$$

where the drag coefficient $C_D = 1.3 \times 10^{-3}$ and the air density $\rho_a = 1.293 \times 10^{-1}$ kg m^{-3}. $|V_w|$ is the average wind speed at height 10 m, u_w and v_w are the components of wind speed in the x and y directions at each CTD station. Using the weighting function as before, u_w and v_w at each grid point can be computed. The average depth of the mixed layer in the East Greenland Current during the cruise of Northwind 1984 is about 15 m. We assume

that the turbulent stress linearly decreases with depth in the mixed layer, and there is no stress below the mixed layer. Under these conditions, the C-vector with wind can be computed. After obtaining the C_1, C_2, C_3 components, the total C-Vector (C_x, C_y, C_z) can be calculated continuously by using equations (10a), (10b) and (10c). Once C_x, C_y and C_z have been obtained, the stream function (Ψ) can be computed easily by using equation (11).

IV. RESULTS

A. THE COORDINATE SYSTEM

The coordinate system is chosen such that the origin is located at (76°30'N, 16°30'W); the X-axis is zonal and positive eastward; the Y-axis is meridional and positive northward; and the Z-axis is vertical and positive upward. There are 10 sections along the X-axis(Sections A to J), 21 sections along Y-axis(Sections 1 to 21) and 31 layers in the vertical (each layer is 10 m thick). Figure 1.8 shows this coordinate system.

B. C-VECTOR PLOTS

1. C_1/f^3 and C_x/f in the X and Y direction

The solid contours of C_x/f and C_1/f^3 are the zonal positive total and ageostrophic nondimensional pseudo vorticities, which means the rotational axis is towards the east. The dash contours of C_x/f and C_1/f^3 are the negative total and ageostrophic nondimensional pseudo vorticities, which indicates the rotational axis is towards the west. Appendix I shows these plots. Similar to the above, contours of C_y/f and C_2/f^3 represent longitudinal-directed vorticities, i. e., rotational axies are pointed towards the north (solid lines) or south (dashed lines). These are shown in Appendix II.

2. Ψ plots

The vorticity of the C-vector Ψ is plotted on the horizontal plane for each 10 m layer in the study area. The Ψ function has the same sign as the ageostrophic vertical velocity. Therefore, the positive contours (solid line) mean upwelling and the negative contours (dash line) mean downwelling. Appendix III shows these plots.

C. SIGNIFICANT FEATURES FOUND FROM THE C-VECTOR METHOD

1. Cross-Coastal Circulation Generated by the Surface Wind

The wind data collected from the 1984 Northwind cruise (Figure 1.7) indicates the average wind speed is 5 m/s from NNE to NE. The Ekman transport is directed to the right of the wind. From the continuity equation such a wind field will generate coastal downwelling. This indicates that C_2/f^3 should be negative near the coast. Figure 4.1 shows the relation between the wind direction and the vertical circulation near the east Greenland coast.

Figure 4.2 shows three sections (7, 8 and 9) of C_2/f^3 contours in three dimensional view. The east Greenland coast lies to the negative horizontal vortices are found to the west in these sections, indicating that downwelling was occurring near the coast and upwelling was occurring over the outershelf, strongest near the shelf break.

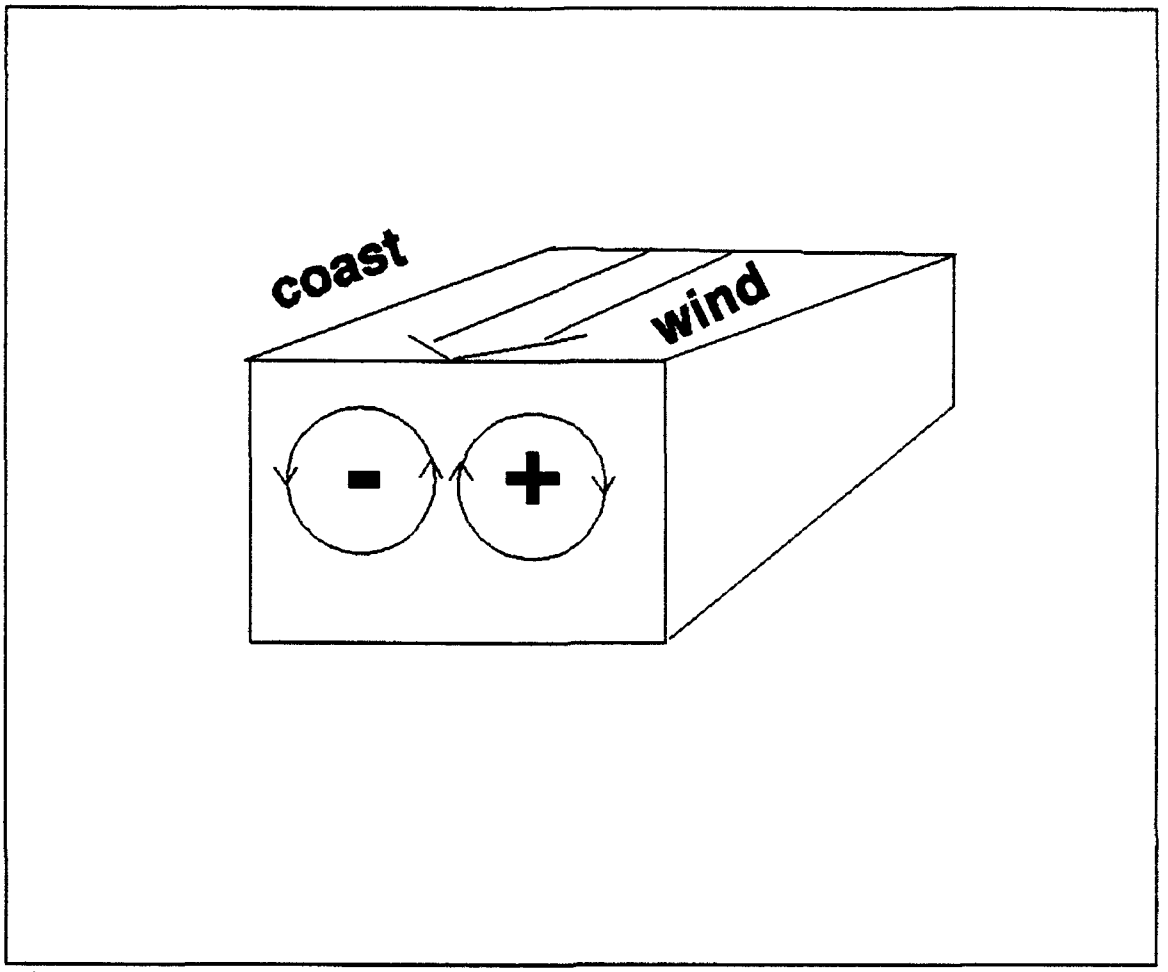

Figure 4.1 The relation between the wind direction and the vertical circulation near the east Greenland coast.

From the plots of C_2/f^3 in Appendix II, we can see that horizontal rows appear from the surface to 40 m depth. This indicates that wind effects dominate the vertical circulation in the upper ocean.

2. Vertical Circulation Induced by the Anticyclonic Gyre

A northward flow in Norske Trough results from a clockwise turning of the current around the southwest corner of Belgica Bank (Tunnicliffe, 1985). Figure 4.3 shows the

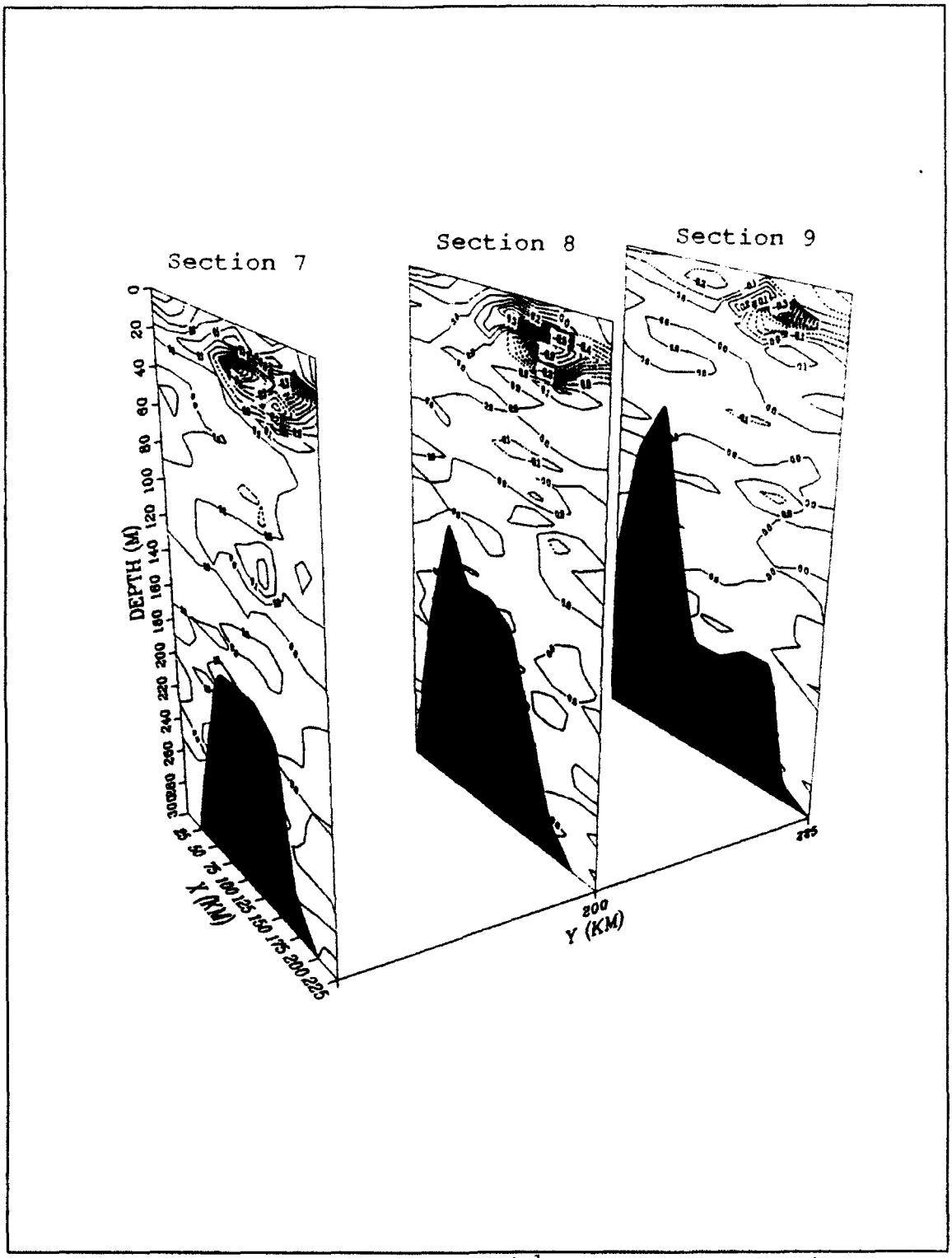

Figure 4.2 Three dimensional C_2/f^3 contours at Sections 7, 8 and 9.

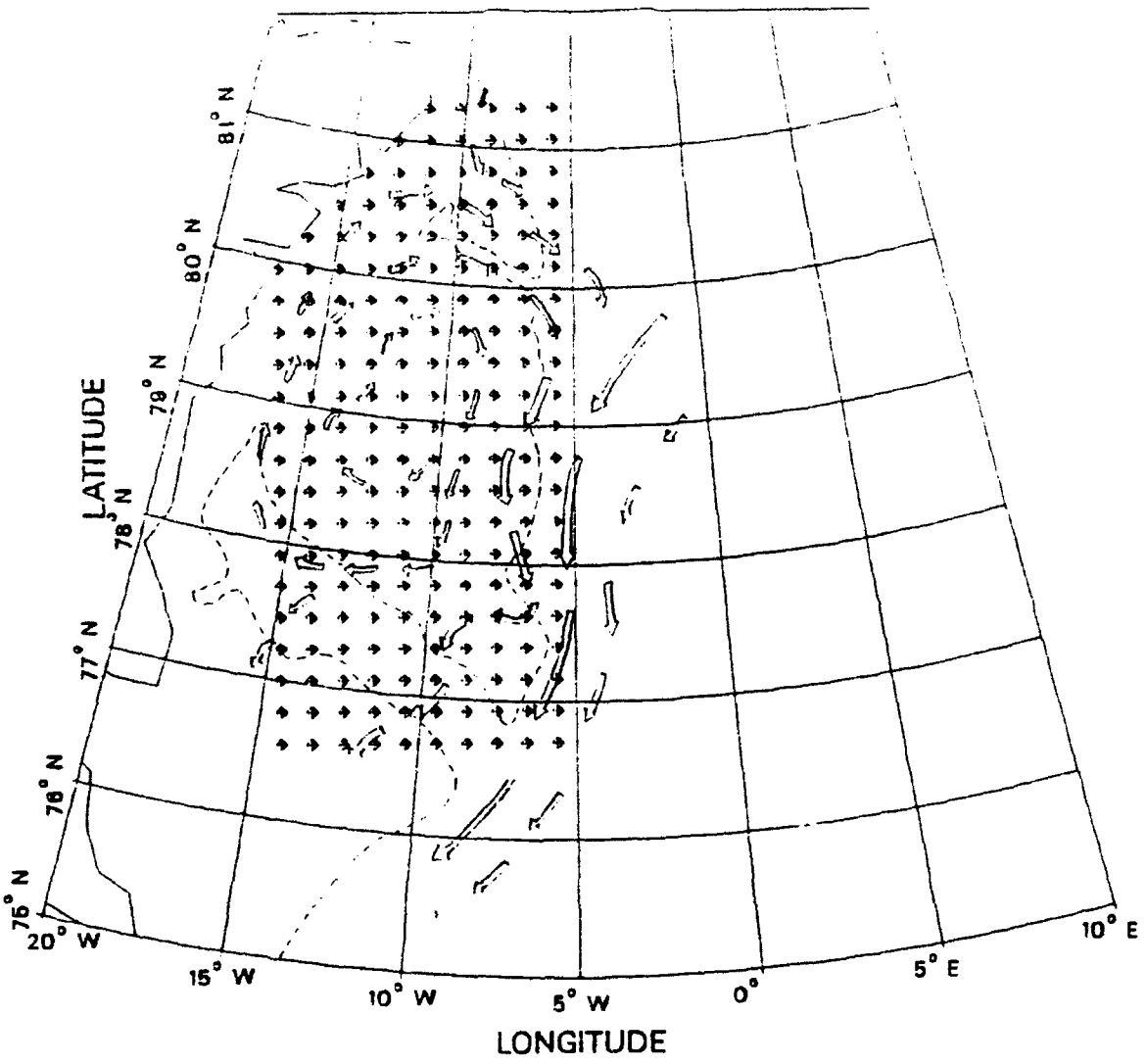

Figure 4.3 The relative position between grid area and the surface circulation.

relative position between the grid points and the surface circulation in EGC. The anticyclonic gyre is found at the center the grid area. The vertical motion should be upward at the gyre center, because the water in the center of gyre will move out from the gyre center to conserve continuity. Hence upwelling should occur in the central part of the gyre. Figure 4.4 shows three dimensional C_y/f contours for Sections 10, 11 and 12.The dashed contours indicate cyclonic or upward motion; conversely for the solid contours. The central part of the gyre is located from X = 75 km to X = 125 km in section 10, from X = 50 km to X = 175 km in section 11, from X = 75 km to X = 175 km in section 12. We can see the surface upwelling in this region, which suggests that the upwelling is induced by the presence of the anticyclonic gyre.

The upwelling induced by the anticyclonic gyre is also seen in the Ψ field. The central part of this anticyclonic gyre is located at X = 50 to 150 km and Y = 200 to 325 (Figure 4.5). The Ψ-values at z = 0, 10, and 20 m in the central part of the gyre are generally positive (upward motion), which also confirms the results obtained from C_y-field.

3. Vertical Circulation Generated by the EGPF

The EGPF was investigated in previous studies. Figures 1.3 and 1.4 (Bourke, et al., 1985) reveal the location and structure of the EGPF from the temperature and salinity contours. From these two figures we can see that a sharp

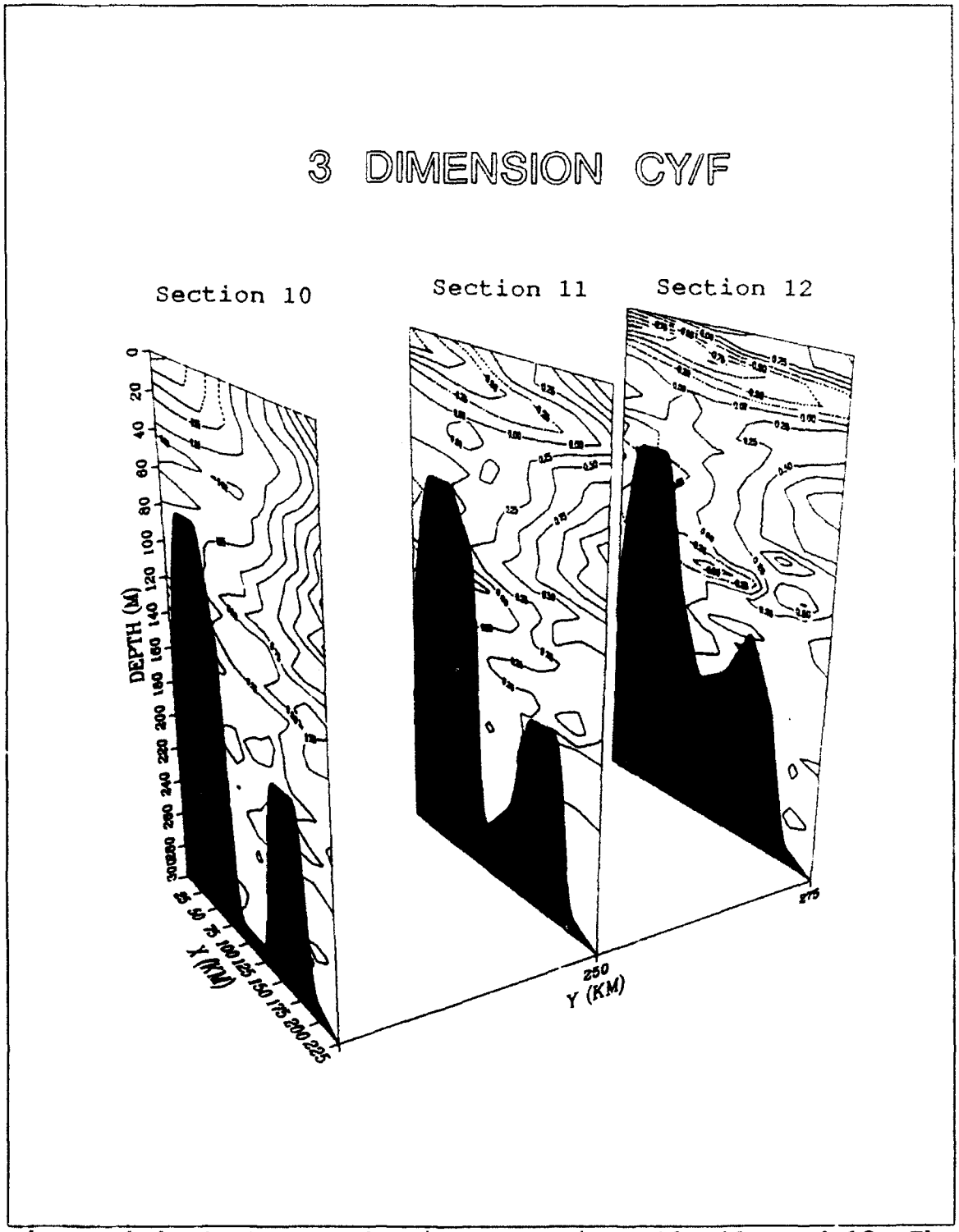

Figure 4.4 Contours of C_y/f at Sections 10, 11, and 12. The dashed line indicates upward motion and the solid line downward motion.

temperature and salinity gradient is present below 40 m (the effect region by wind) and extends from about 60 m to 120 m.

In Figure 4.3 a strong frontal jet flows through Sections 1 and 2 in the Y direction. C_y/f^3 contour plots for these two sections, shows that a two-cell structure is found at a depth about 60 to 120 m near the EGPF. Therefore, this two-cell structure indicates that the AIW of the RAC meets with PW, a feature which can be seen in X-Z cross sections 1 and 2 at a depth of about 60 to 120 m (Figure 4.6). Figure 4.7 shows that a two-cell structure occurs at the front between AIW (warm and saline) and the PW (cold and fresh). We can sketch a frontal model for the EGPF. When AIW and PW are moving toward each other, two horizontal opposite vortices will be formed with a downward motion along the front.

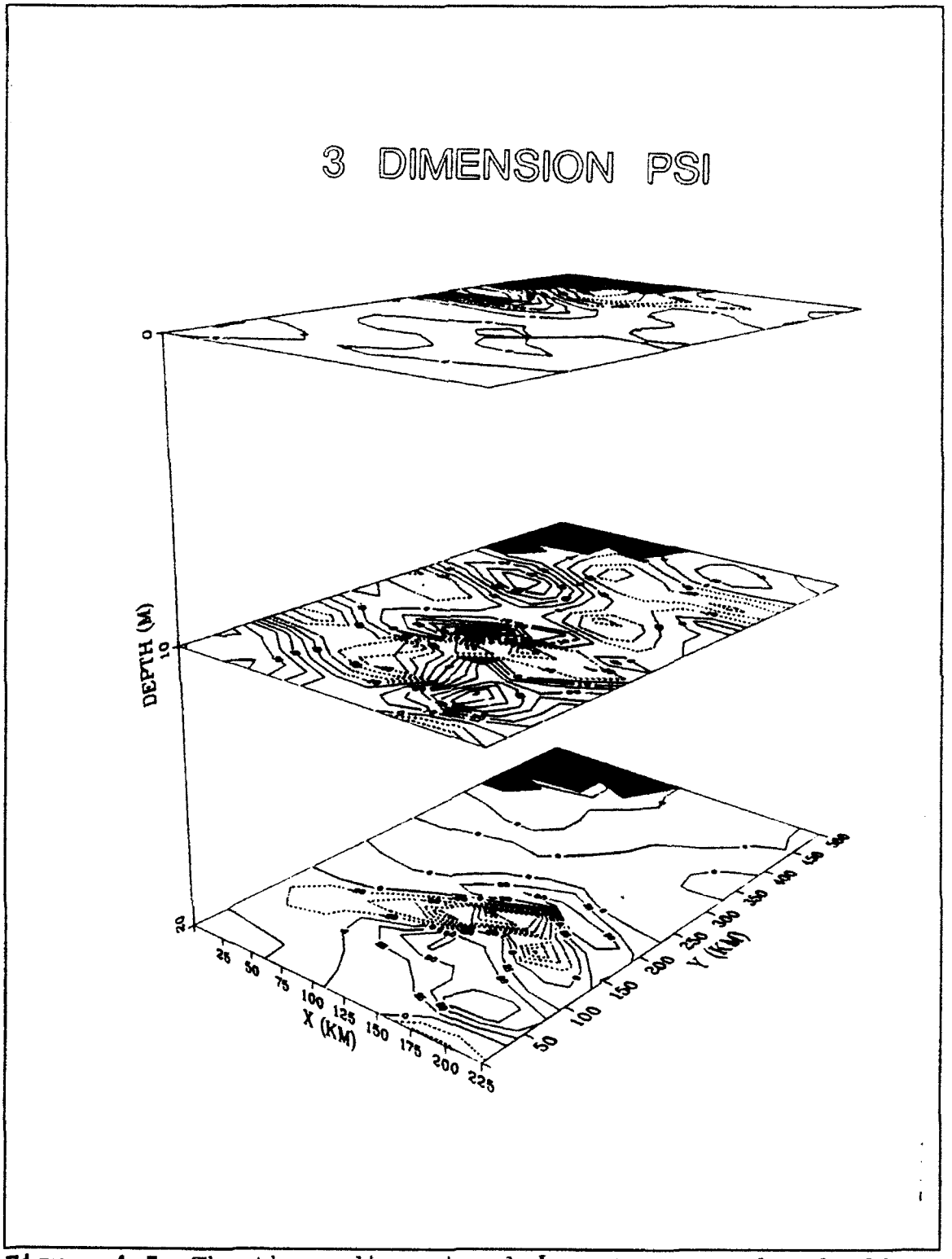

Figure 4.5 The three dimensional Ψ contours at 0, 10, 20 m.

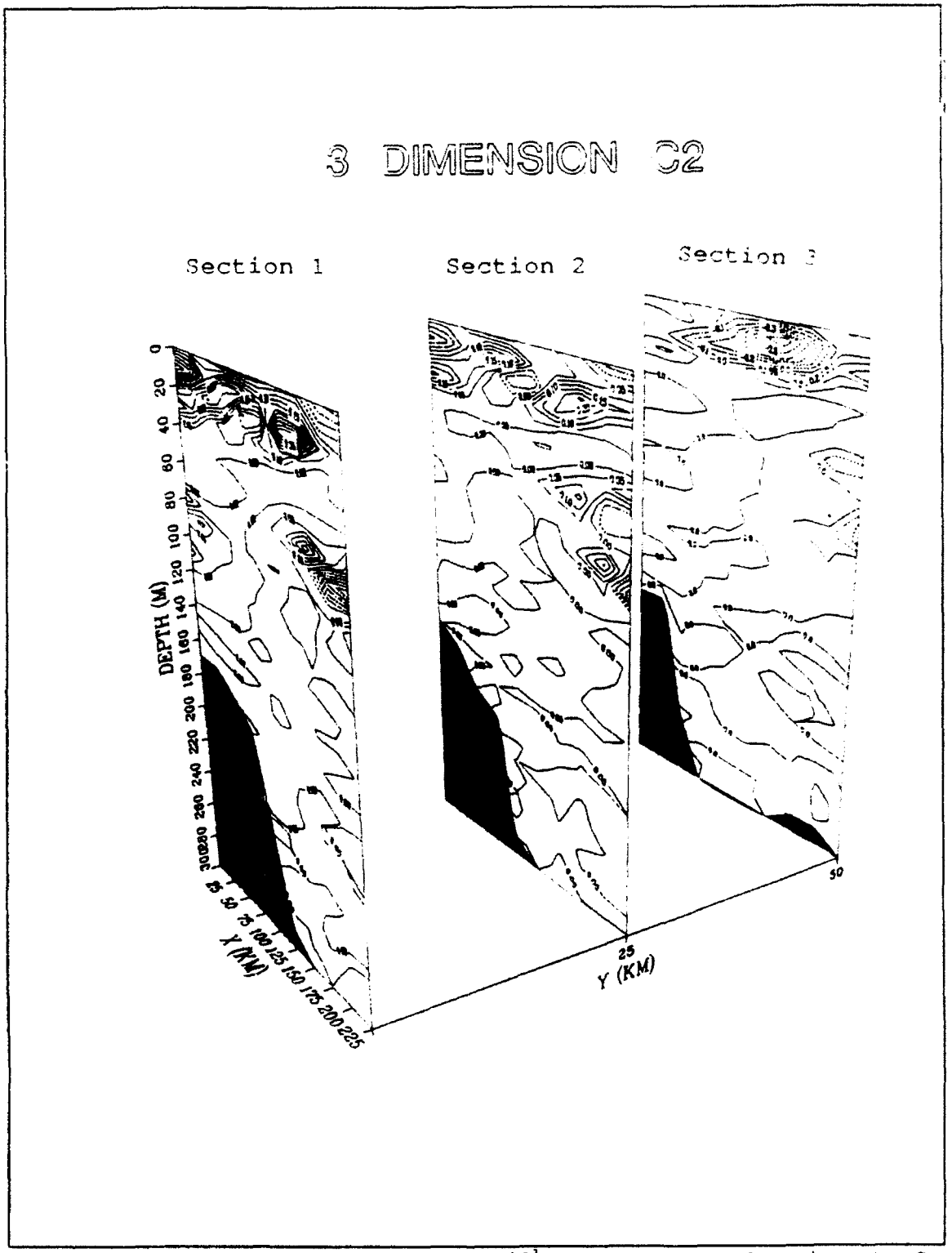

Figure 4.6 Three dimensional C_2/f^3 contours at Section 1, 2, 3. The EPGF passes through Sections 1 and 2.

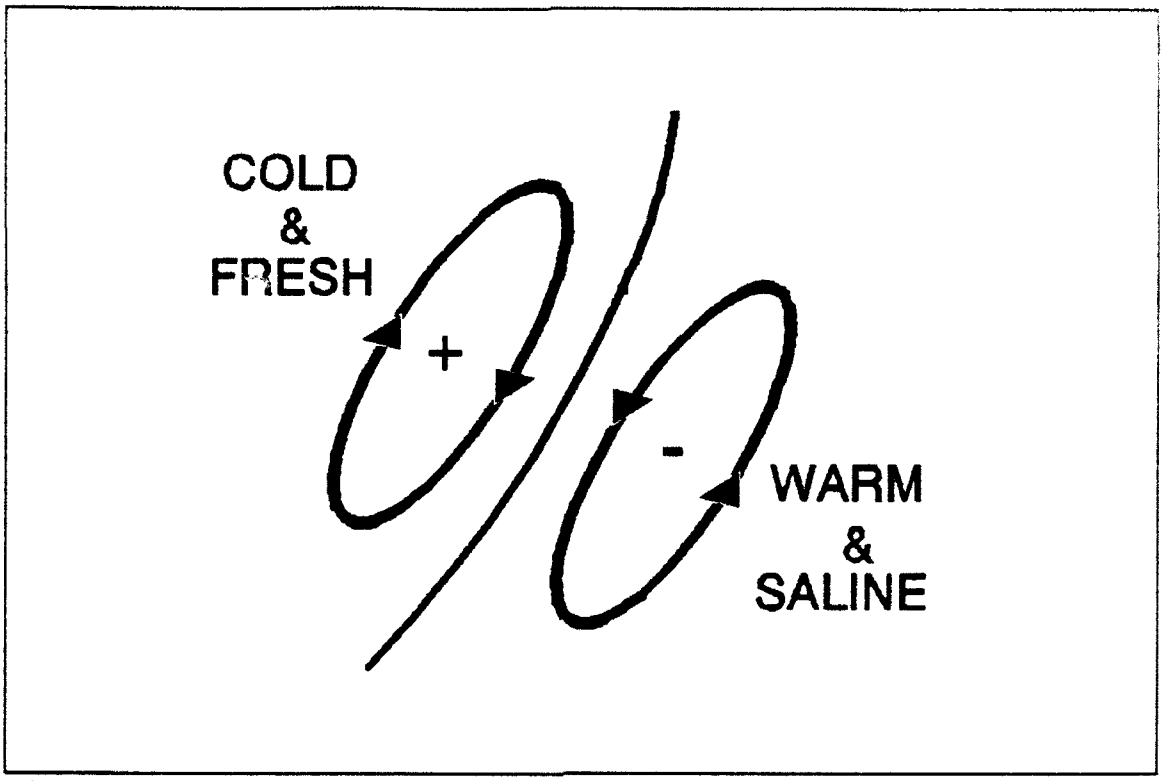

Figure 4.7 A two-cell structure with downward motion occurs in the north-south direction, AIW (warm and saline) at the right, PW (cold and fresh) at the left.

V. SUMMARY, CONCLUSIONS AND RECOMMENDATIONS

A. SUMMARY

A new technique, the 'C-vector method', is employed to define the three-dimensional circulation of the East Greenland Current from CTD and wind data collected during the Northwind 1984 cruise to the Greenland Sea.

Three different types of vertical circulation can be identified by the C-vector method: (1) the wind-driven coastal circulation, (2) an anticyclonic gyre which induces vertical circulation, and (3) a front induced circulation. The results demonstrate that the C-vector method is useful in calculating the ageostrophic circulation using CTD and wind data. The ageostrophic flow can sometimes be significant and the purpose of this study is to particularly emphasize the importance of the ageostrophic circulation in the waters off the east Greenland coast as inferred by the C-vector using CTD and wind data.

B. CONCLUSIONS

- The C-vector method is a very good tool to diagnose the three-dimensional pseudo-vorticity fields in the ocean by using CTD measurements and wind stress data.
- The vertical motion in the ocean can be investigated from the vertical vorticity of C-vector for the total flow, Ψ, value.

- If the quasi-geostrophic assumption can be removed in future work, more realistic results can be obtained.

C. RECOMMENDATIONS

(1) A shortcoming in the calculation of the C-vector was the uncertainty associated with the determination of a reference level or level of no motion. The determination of a reference level still remains disputable because there is no universal method which guarantees this. Density differences between stations in the Greenland Sea study area demonstrate that 300 m is a representative level of no motion for the deep waters. While the density difference stations is not always zero at 300 m, there is a good indication that at this level the currents are very small.

(2) In this study, we didn't solve the dynamical equations. In the future, the pseudo-vorticity equations (8a) to (10c) should be solved under certain boundary conditions to obtain the three dimensional ageostrophic velocity field.

APPENDIX I : THE PSEUDO VORTICITY CONTOUR PLOTS IN X DIRECTION

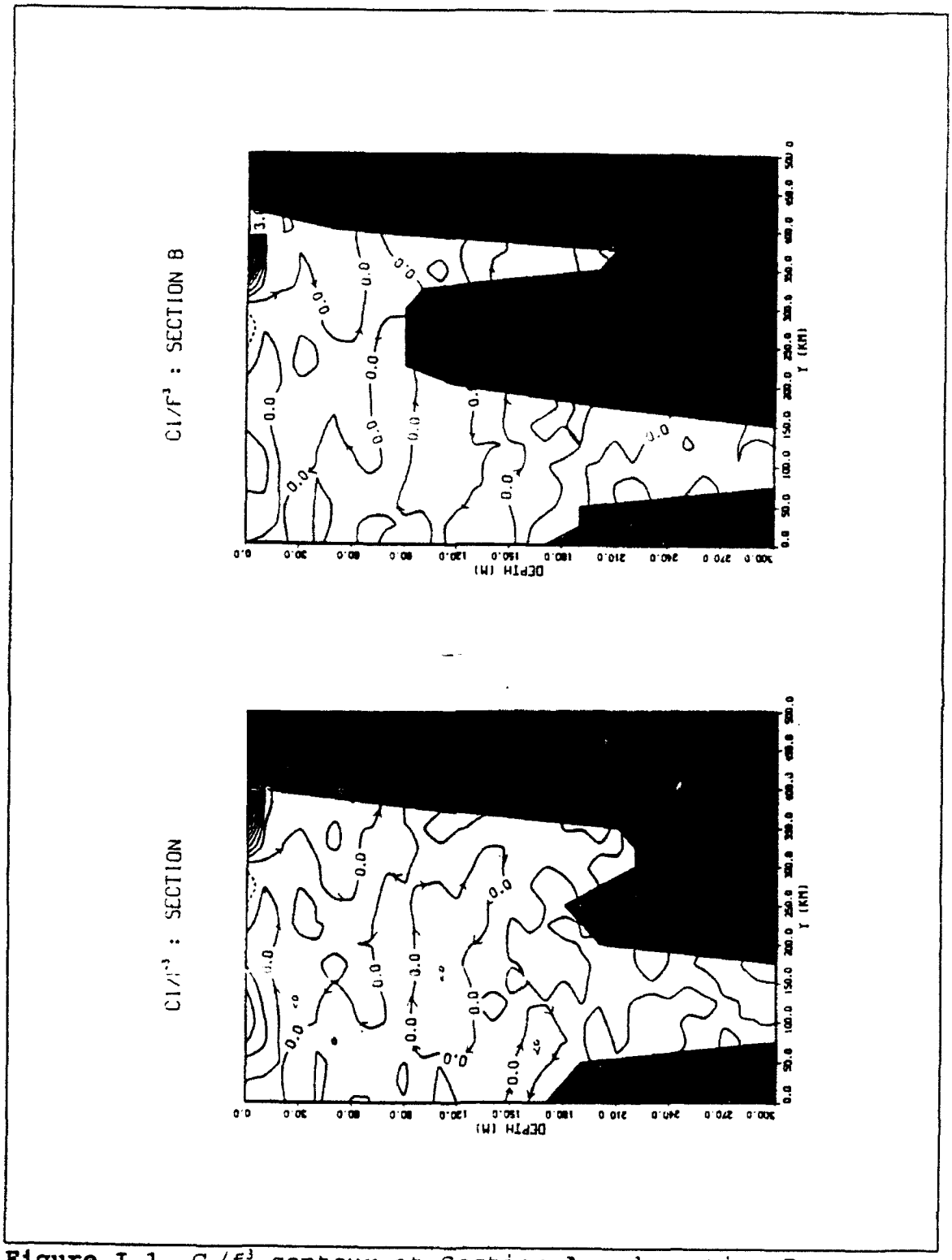

Figure I.1 C_1/f^3 contour at Section A and section B.

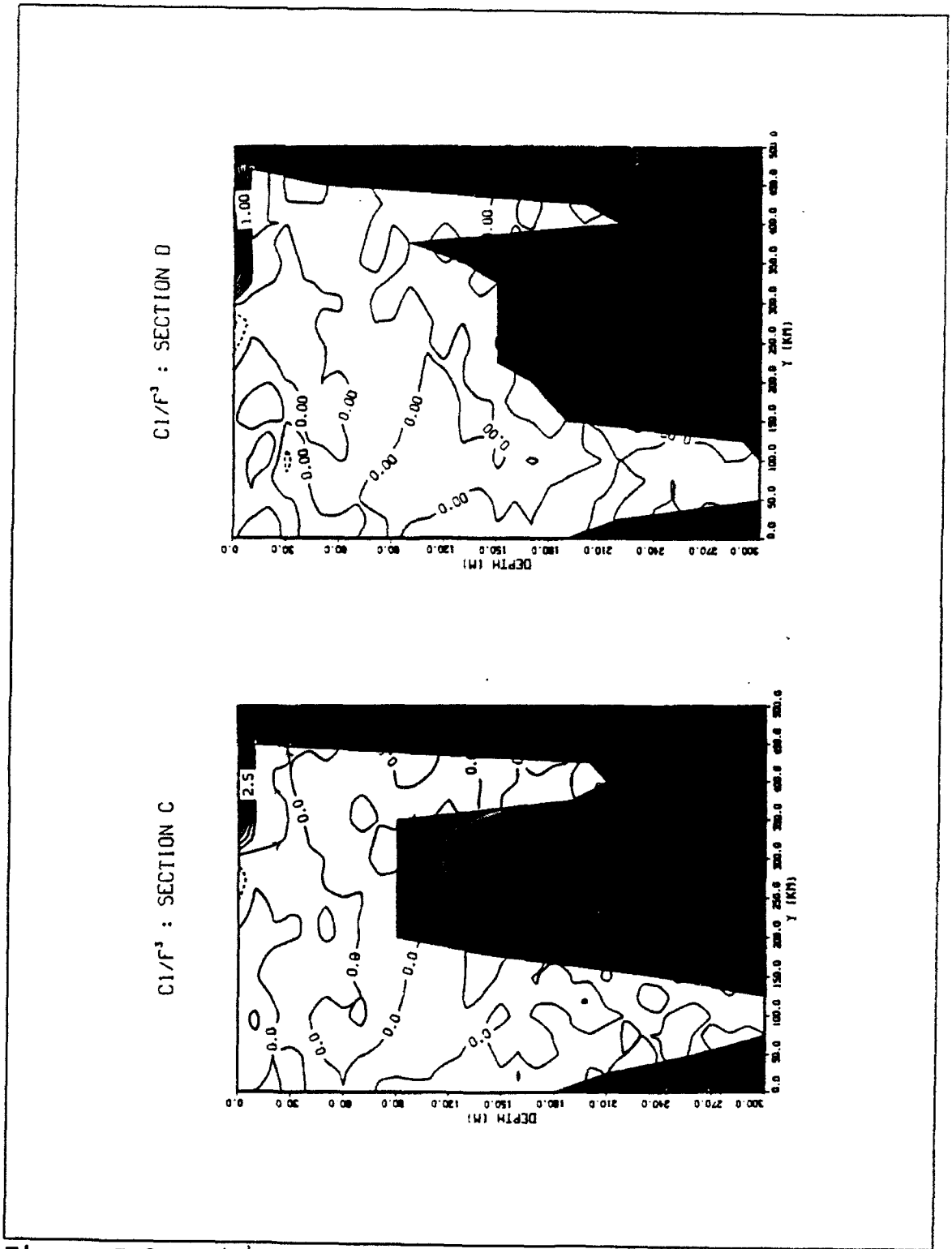

Figure I.2 C_1/f^3 contour at Section C and Section D.

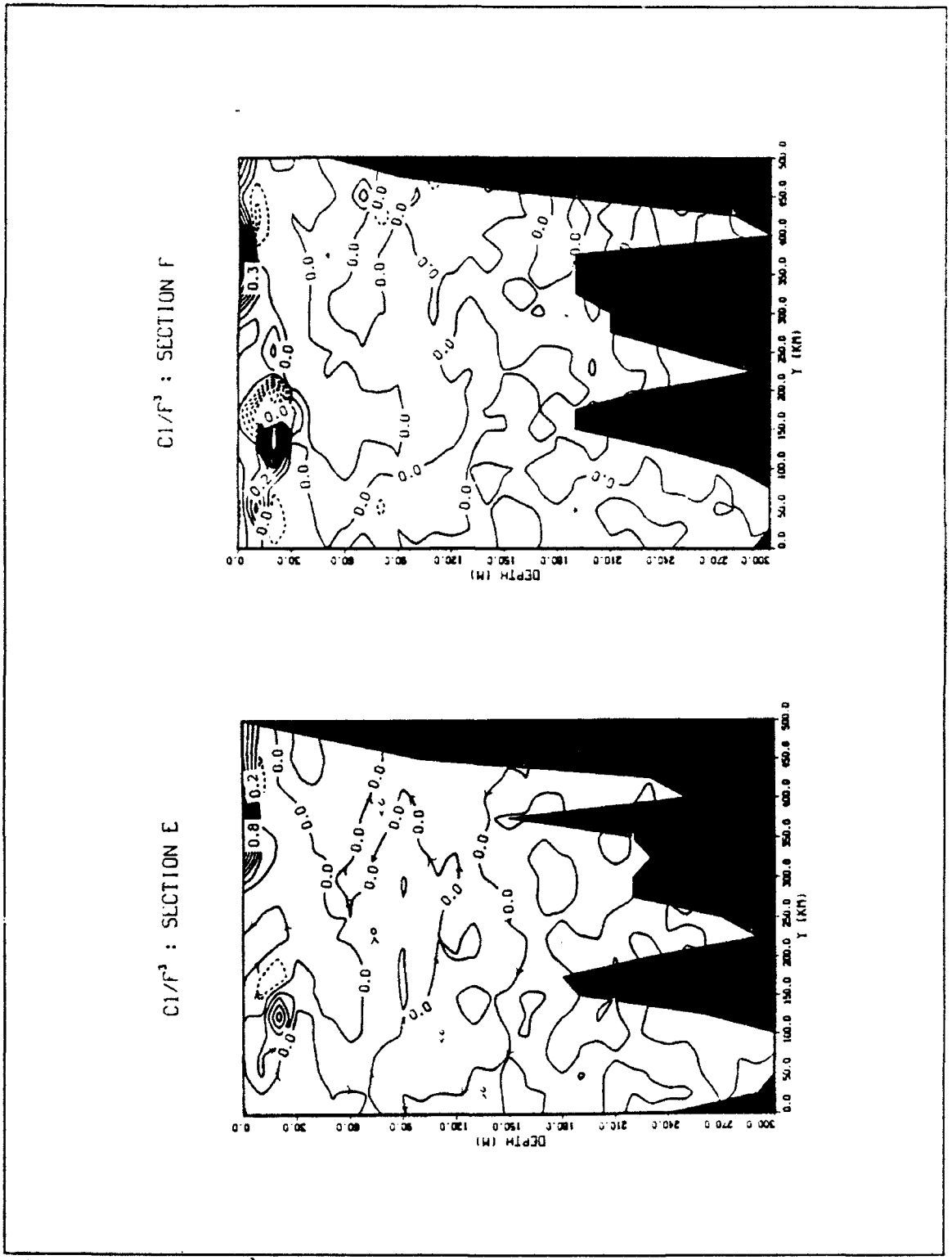

Figure I.3 C_1/f^3 contour at Section E and Section F.

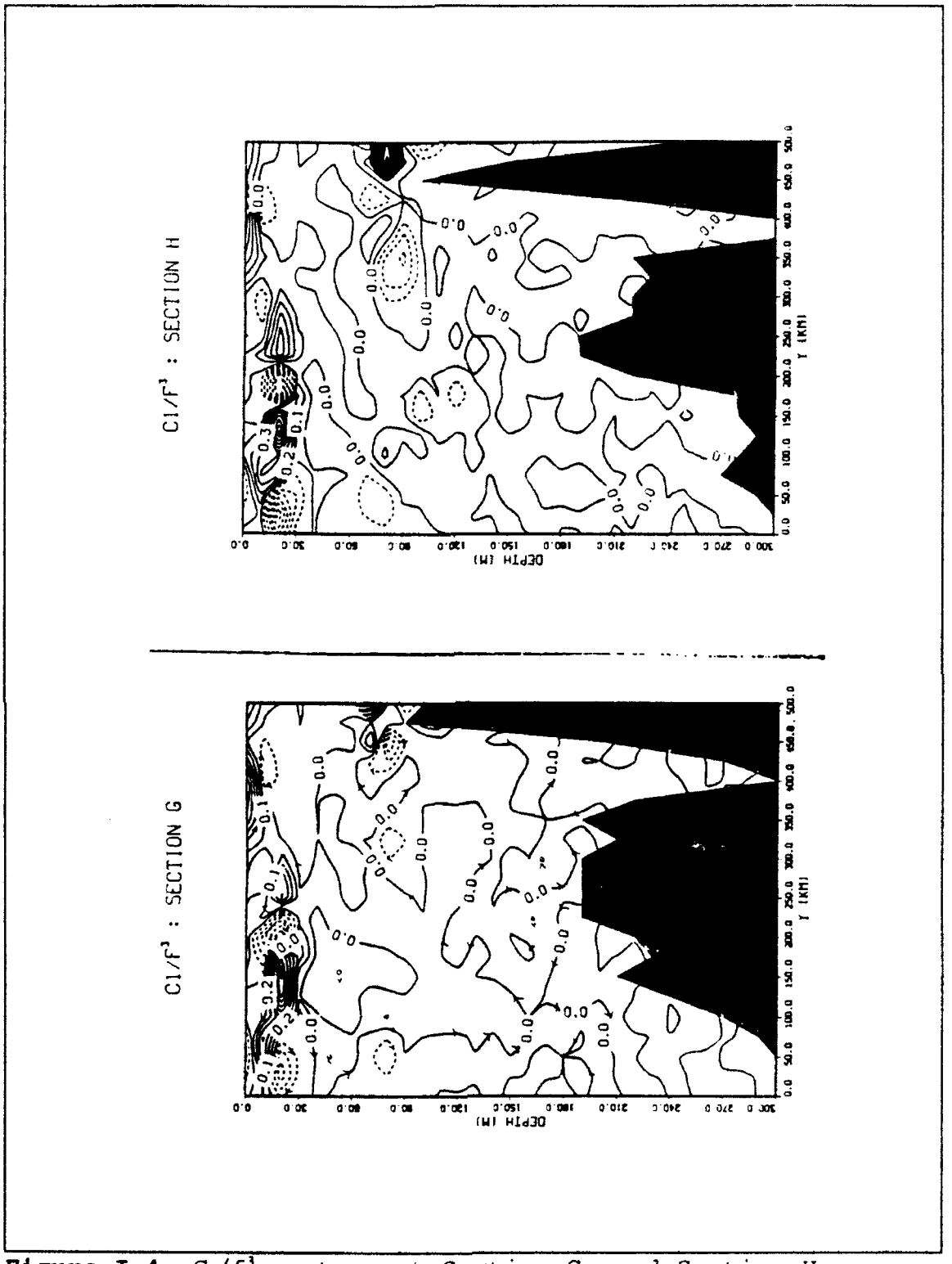

Figure I.4 C_1/f^3 contour at Section G. and Section H.

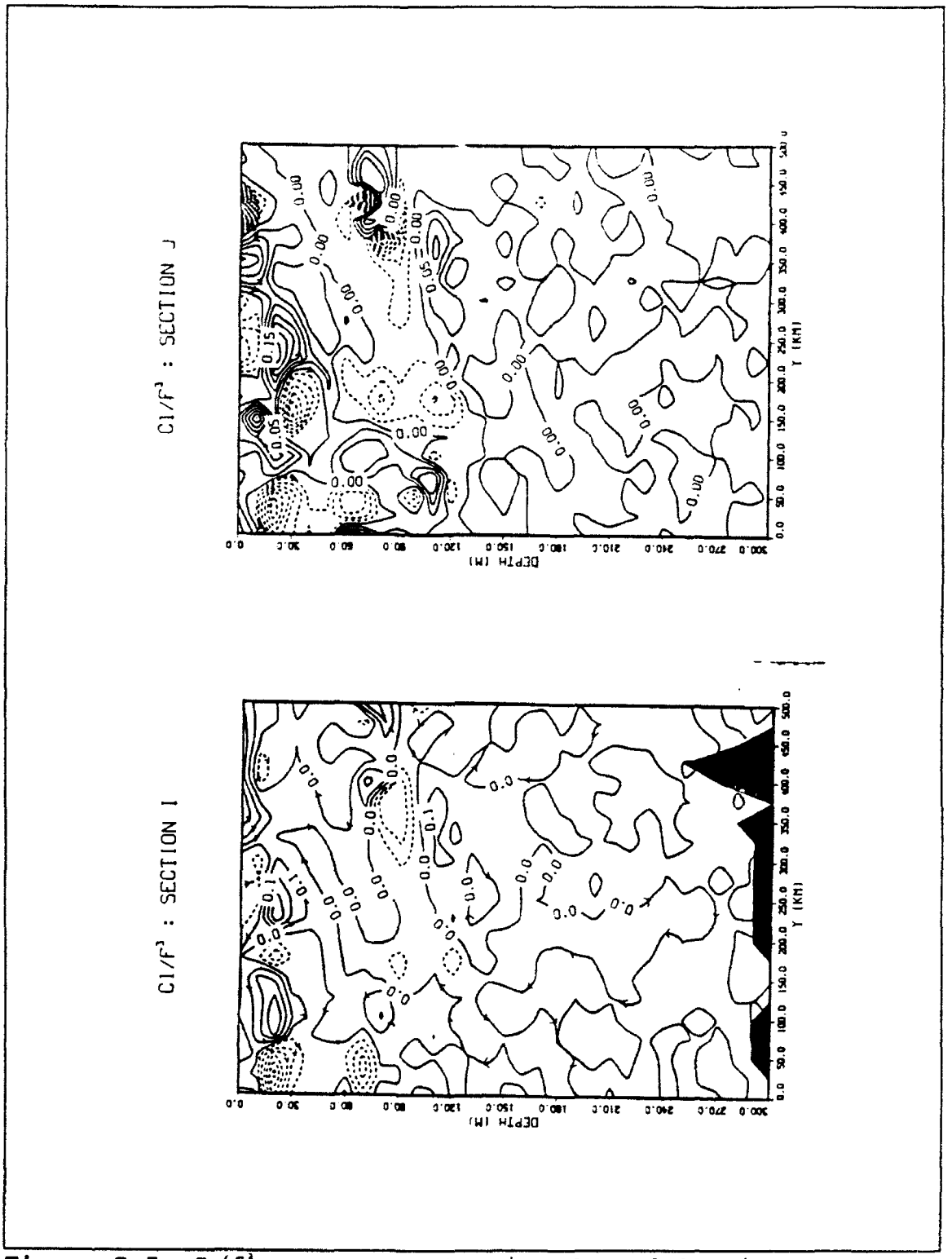

Figure I.5 C_1/f^3 contour at Section I. and Section J.

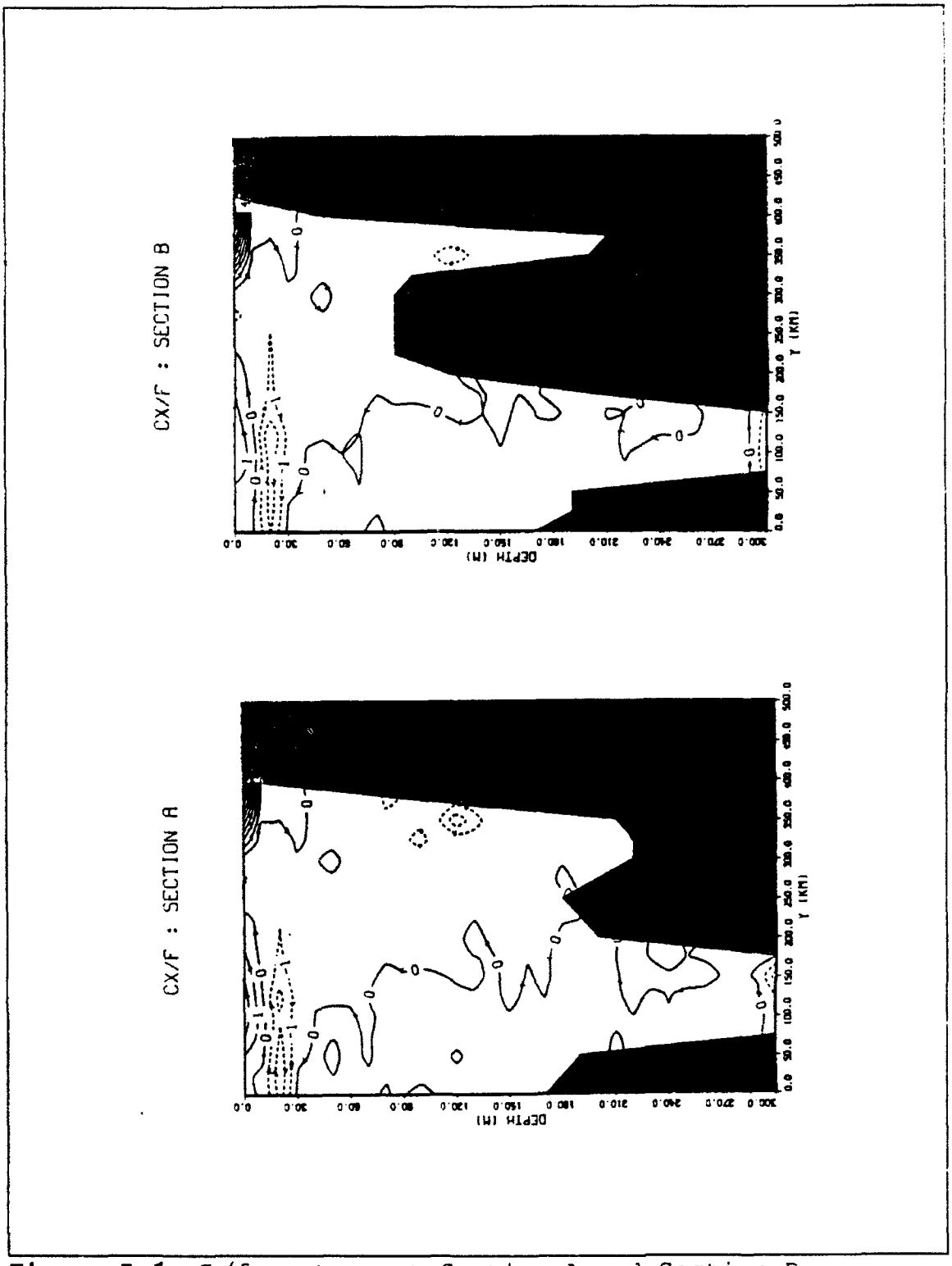

Figure I.6 C_x/f contour at Section A and Section B

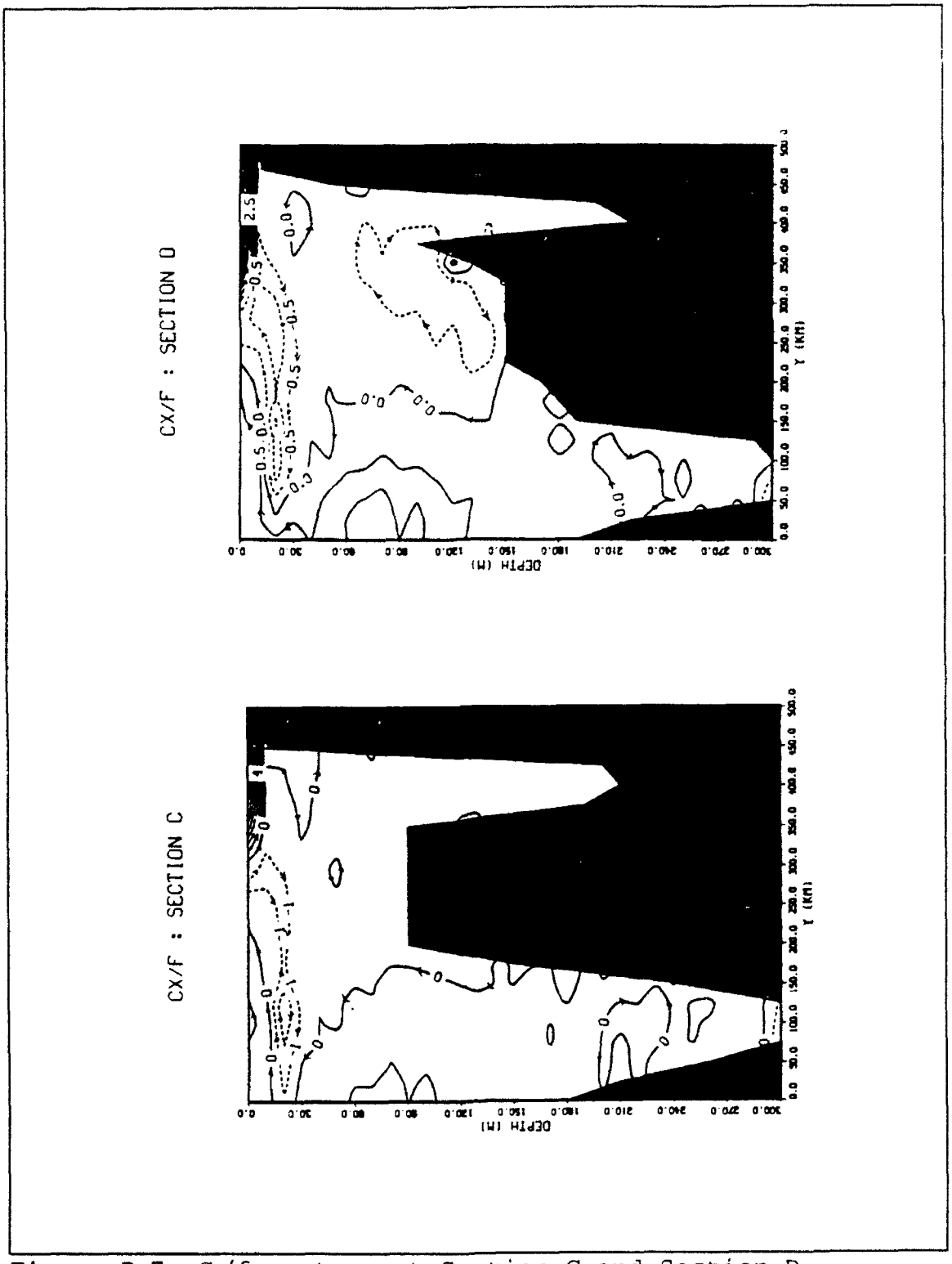

Figure I.7 C_x/f contour at Section C and Section D.

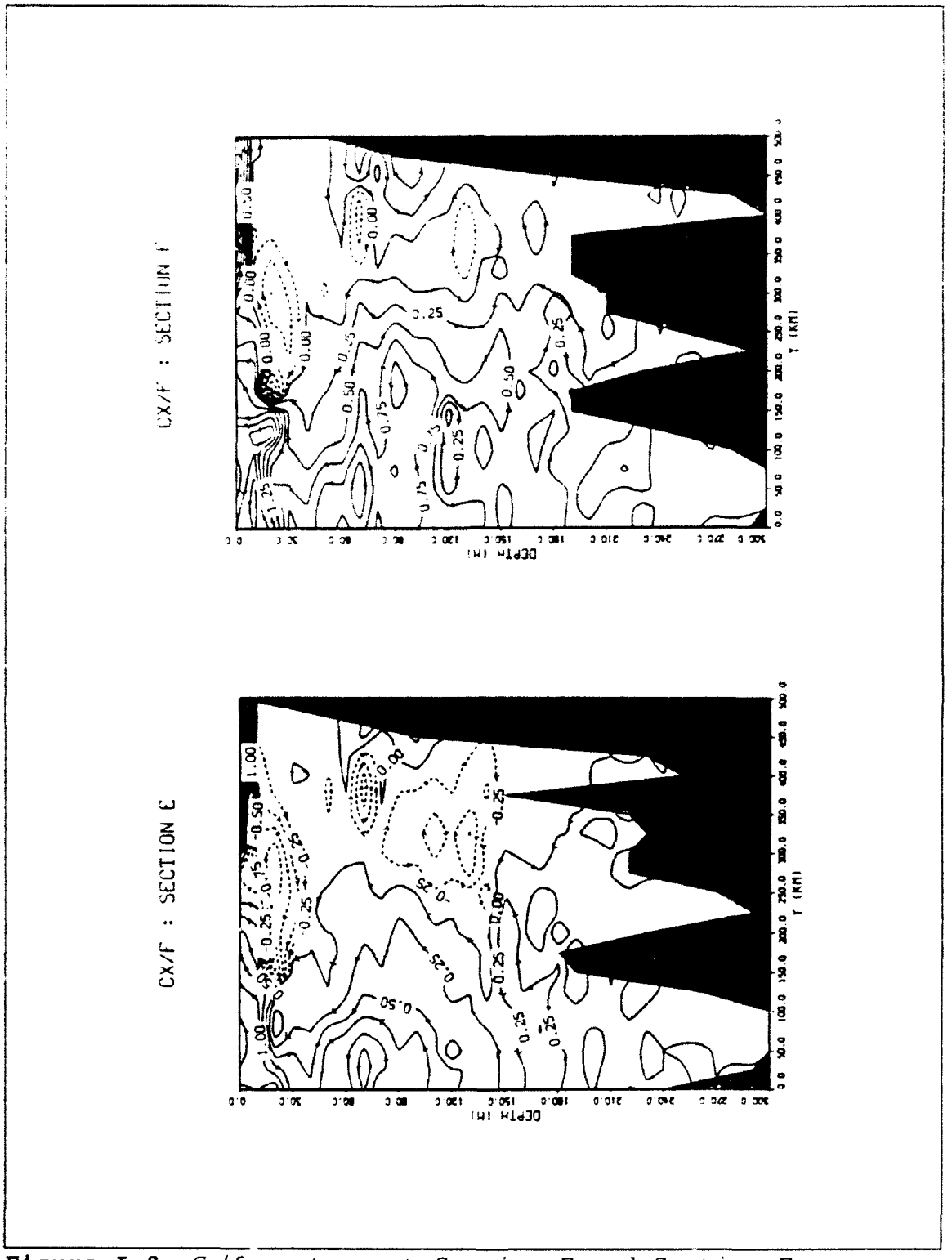

Figure I.8 C_x/f contour at Section E and Section F.

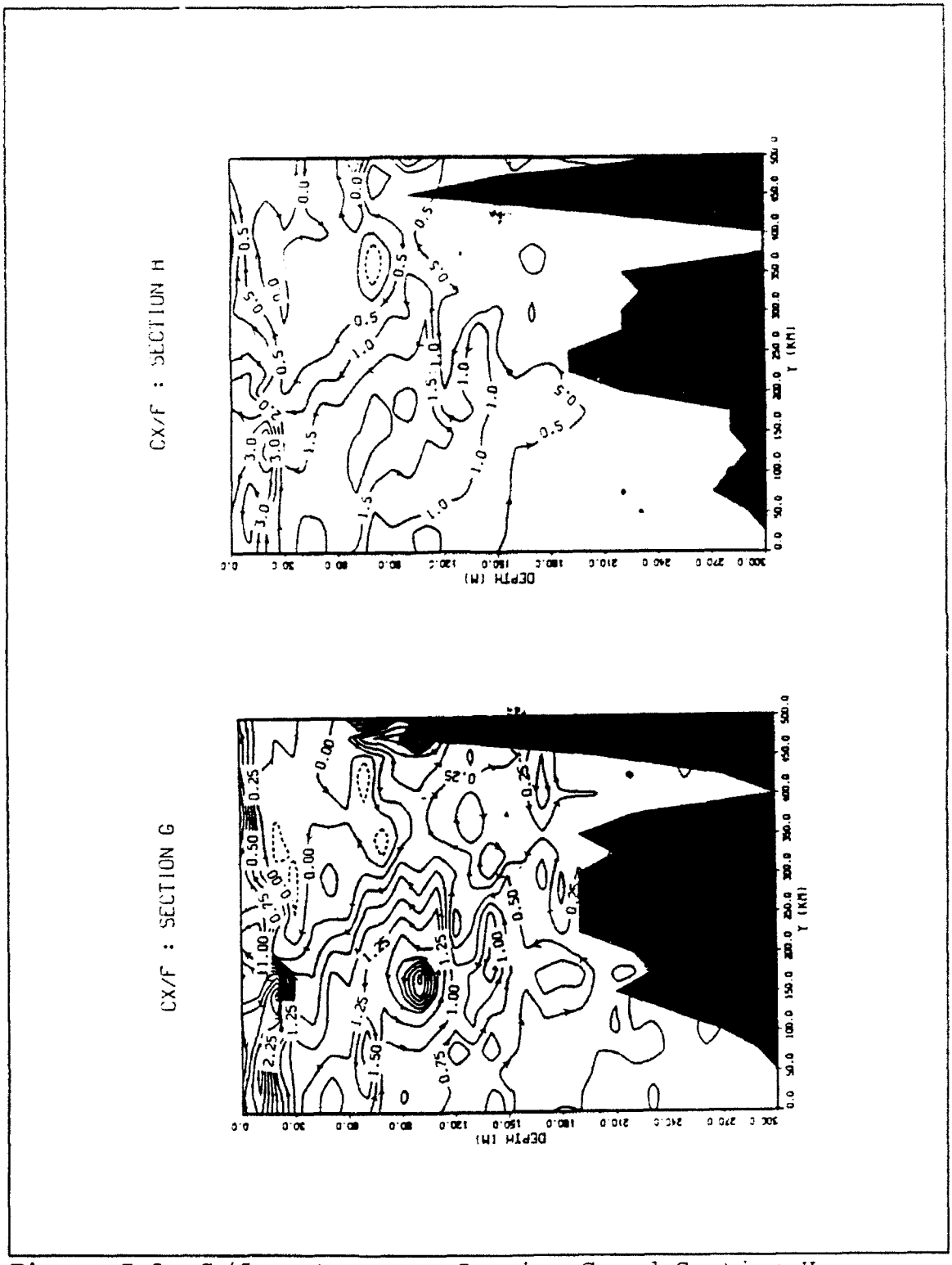

Figure I.9 C_x/f contour at Section G and Section H.

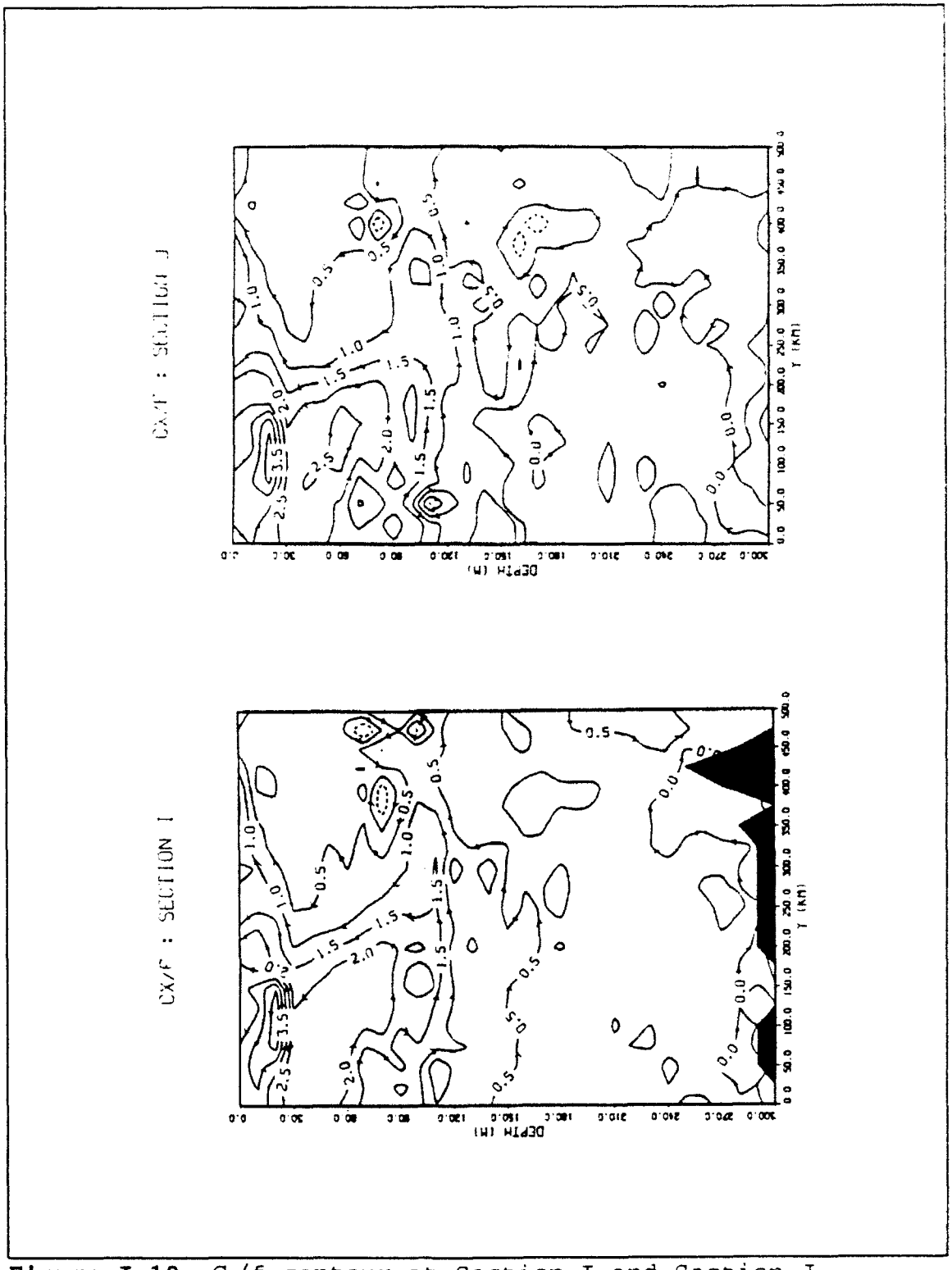

Figure I.10 C_x/f contour at Section I and Section J.

APPENDIX II : THE PSEUDO VORTICITY CONTOUR PLOTS IN Y DIRECTION

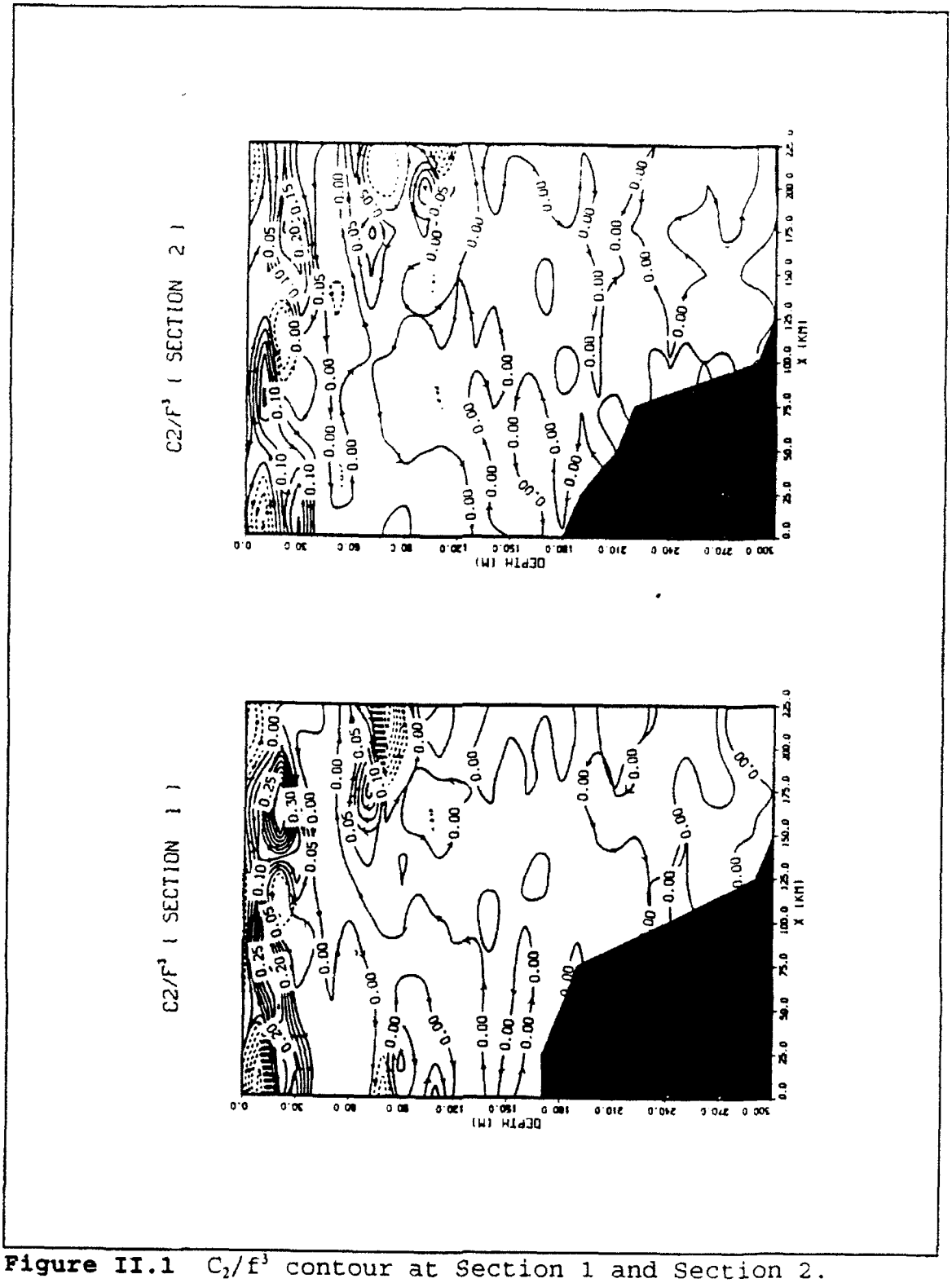

Figure II.1 C_2/f^3 contour at Section 1 and Section 2.

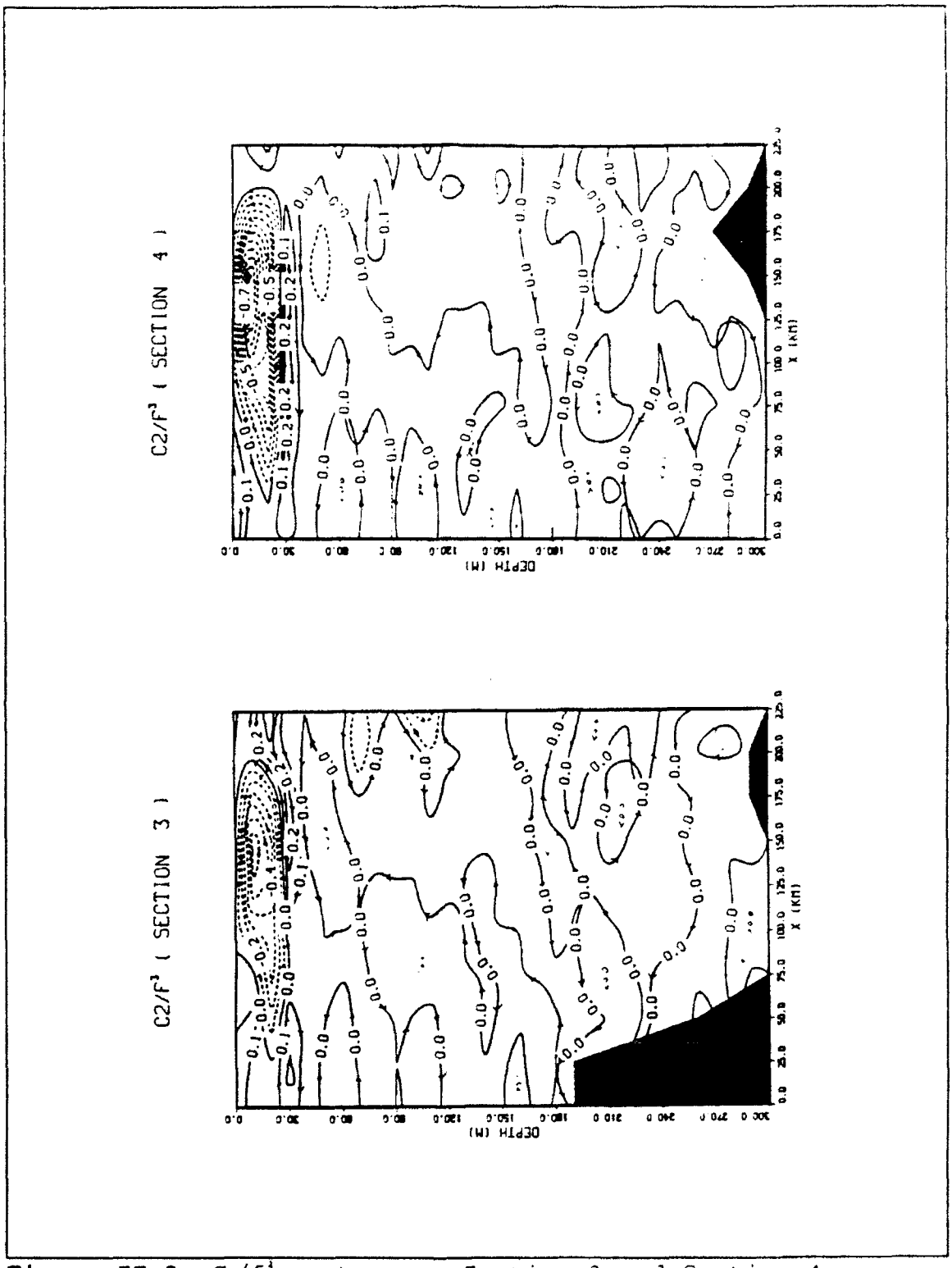

Figure II.2 C_2/f^3 contour at Section 3 and Section 4.

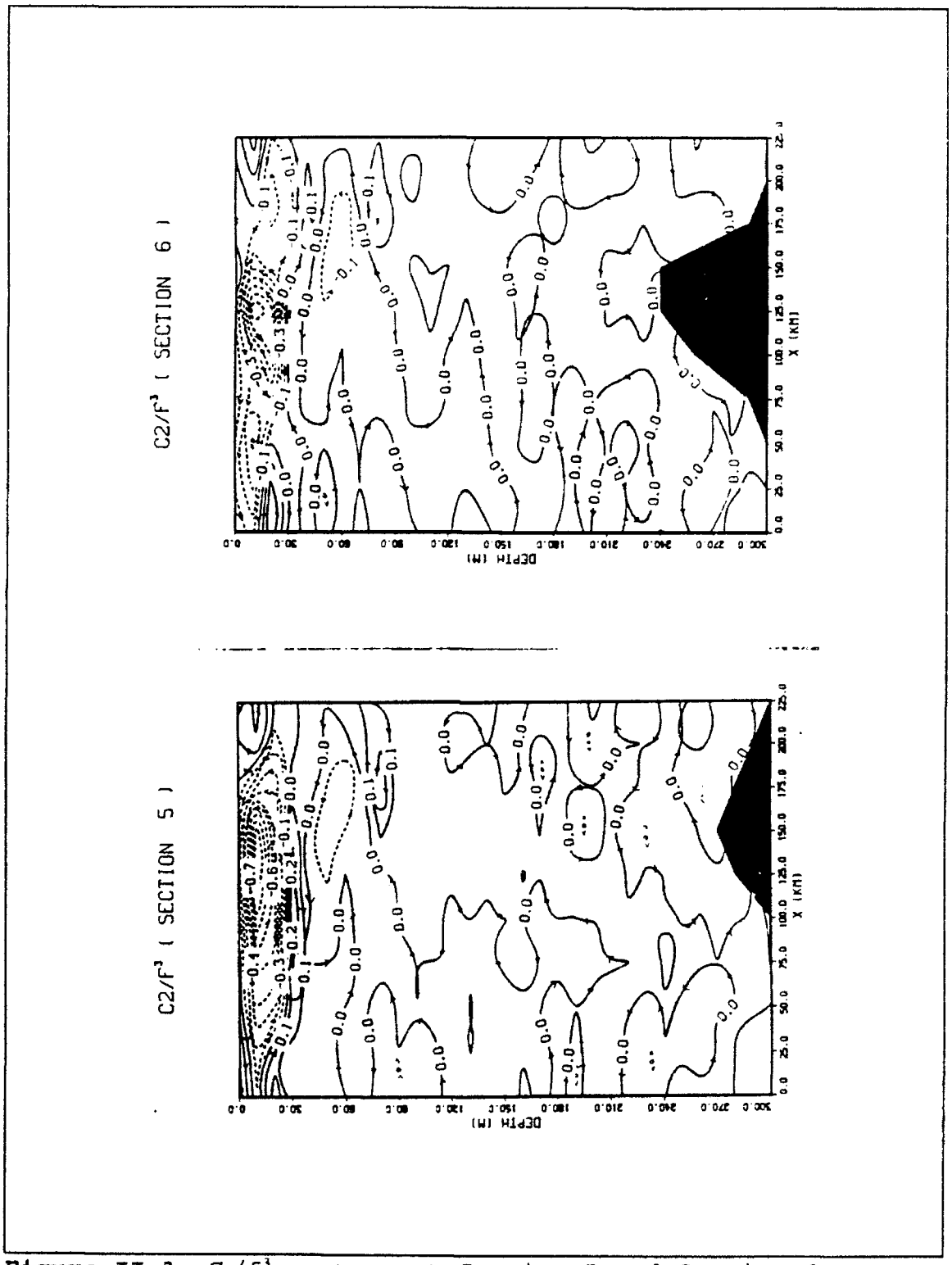

Figure II.3 C_2/f^3 contour at Section 5 and Section 6.

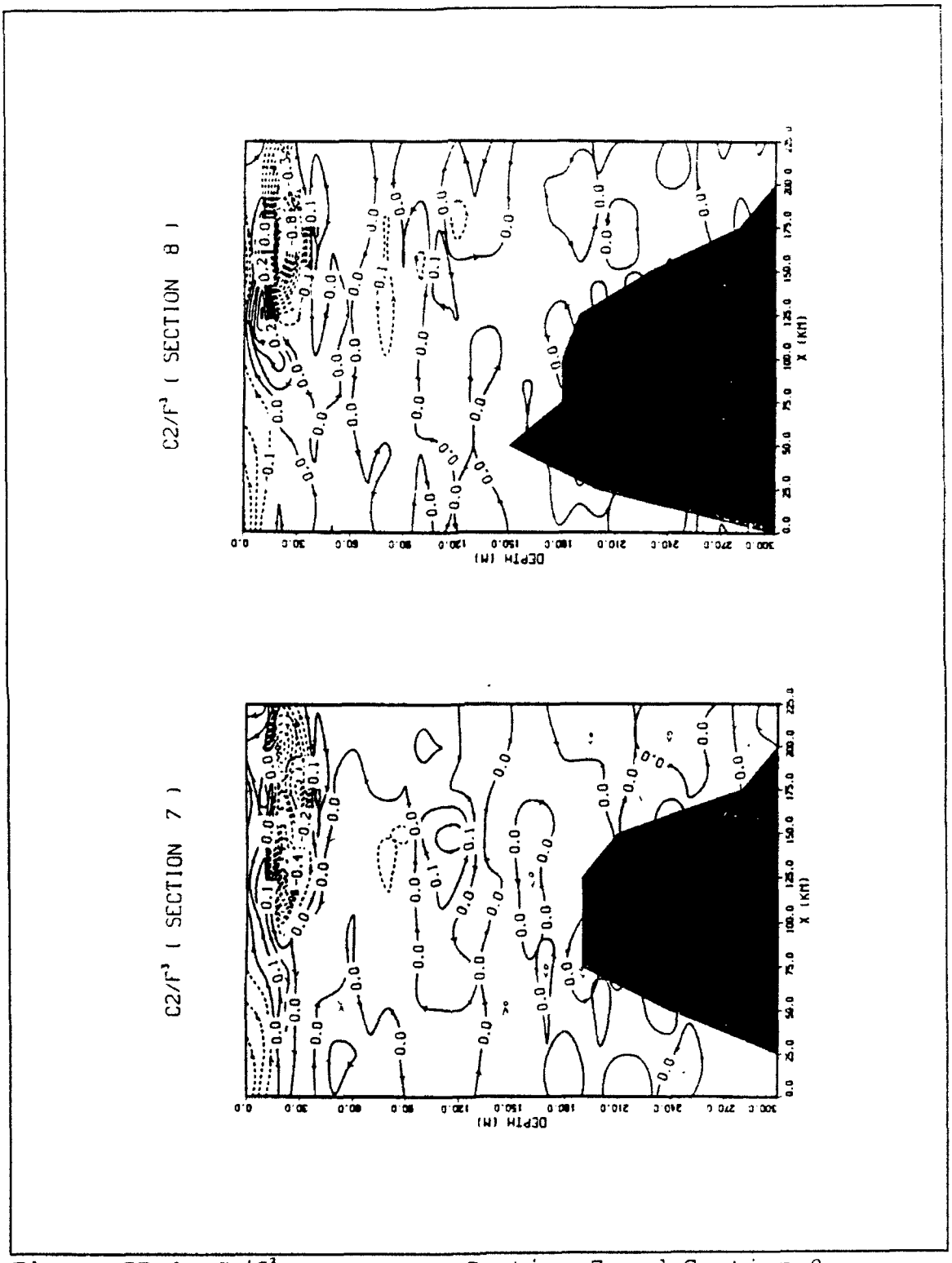

Figure II.4 C_2/f^3 contour at Section 7 and Section 8.

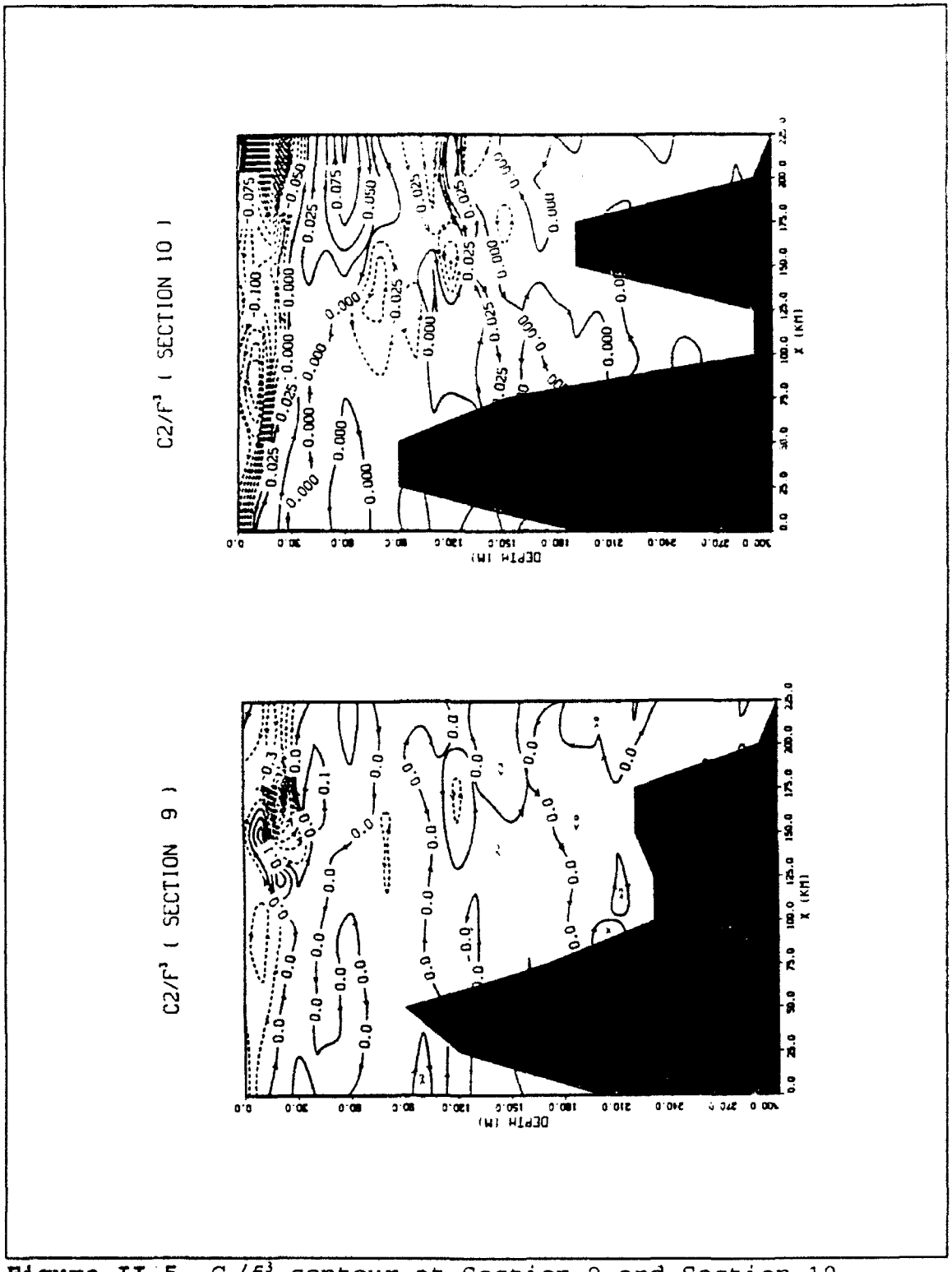

Figure II.5 C_2/f^3 contour at Section 9 and Section 10.

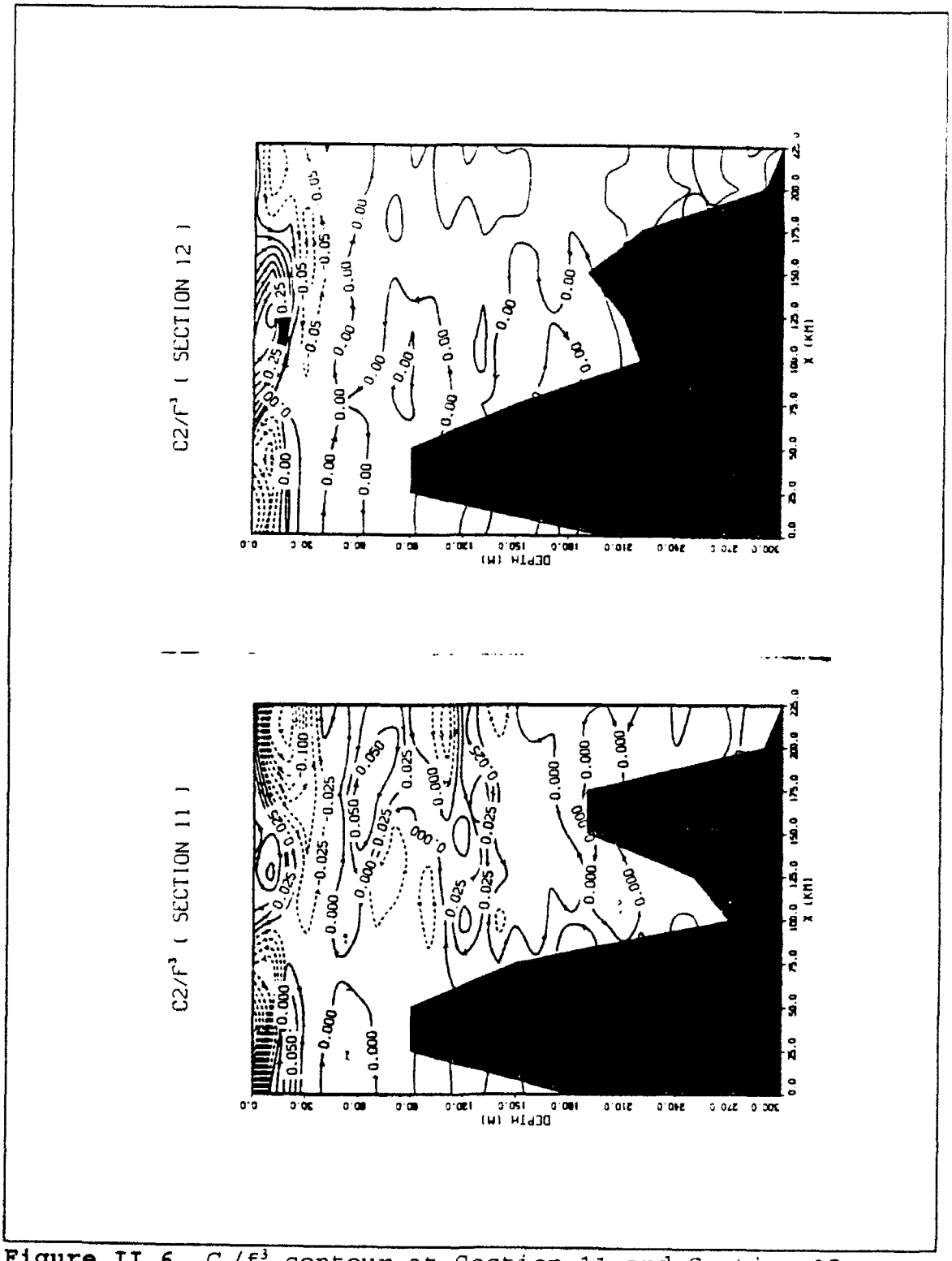

Figure II.6 C_2/f^3 contour at Section 11 and Section 12

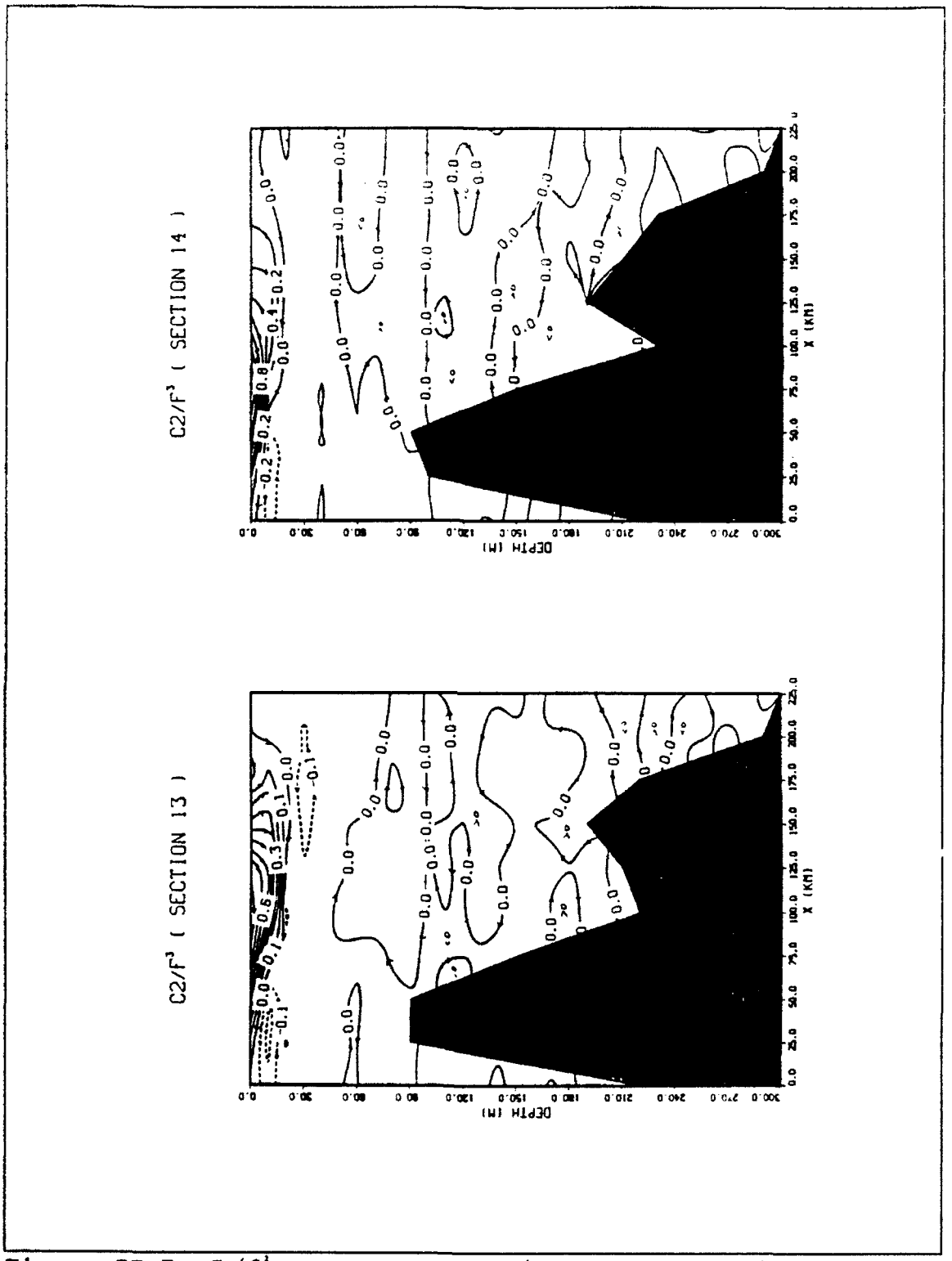

Figure II.7 C_2/f^3 contour at Section 13 and Section 14.

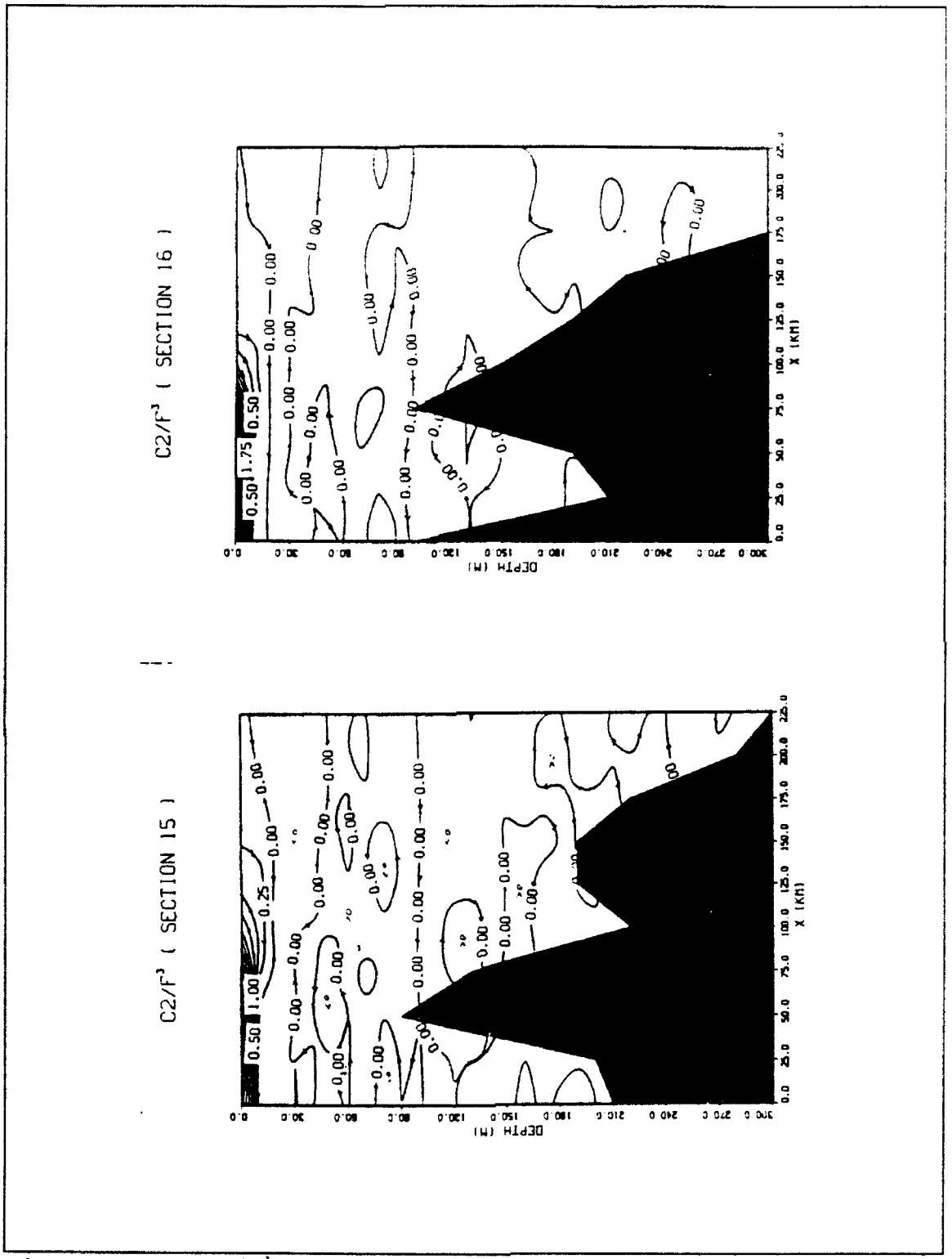

Figure II.8 C_2/f^3 contour at Section 15 and Section 16.

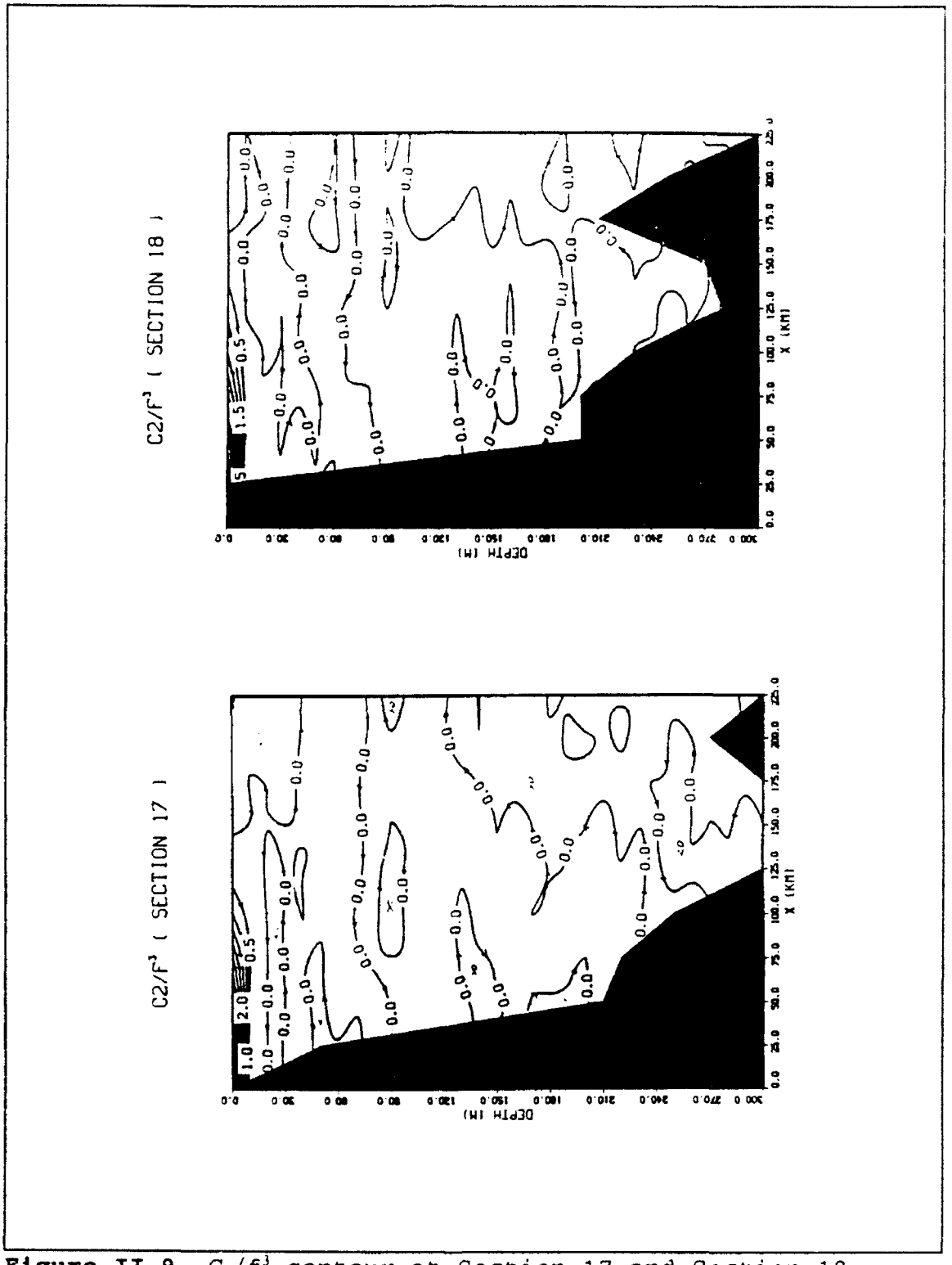

Figure II.9 C_2/f^3 contour at Section 17 and Section 18.

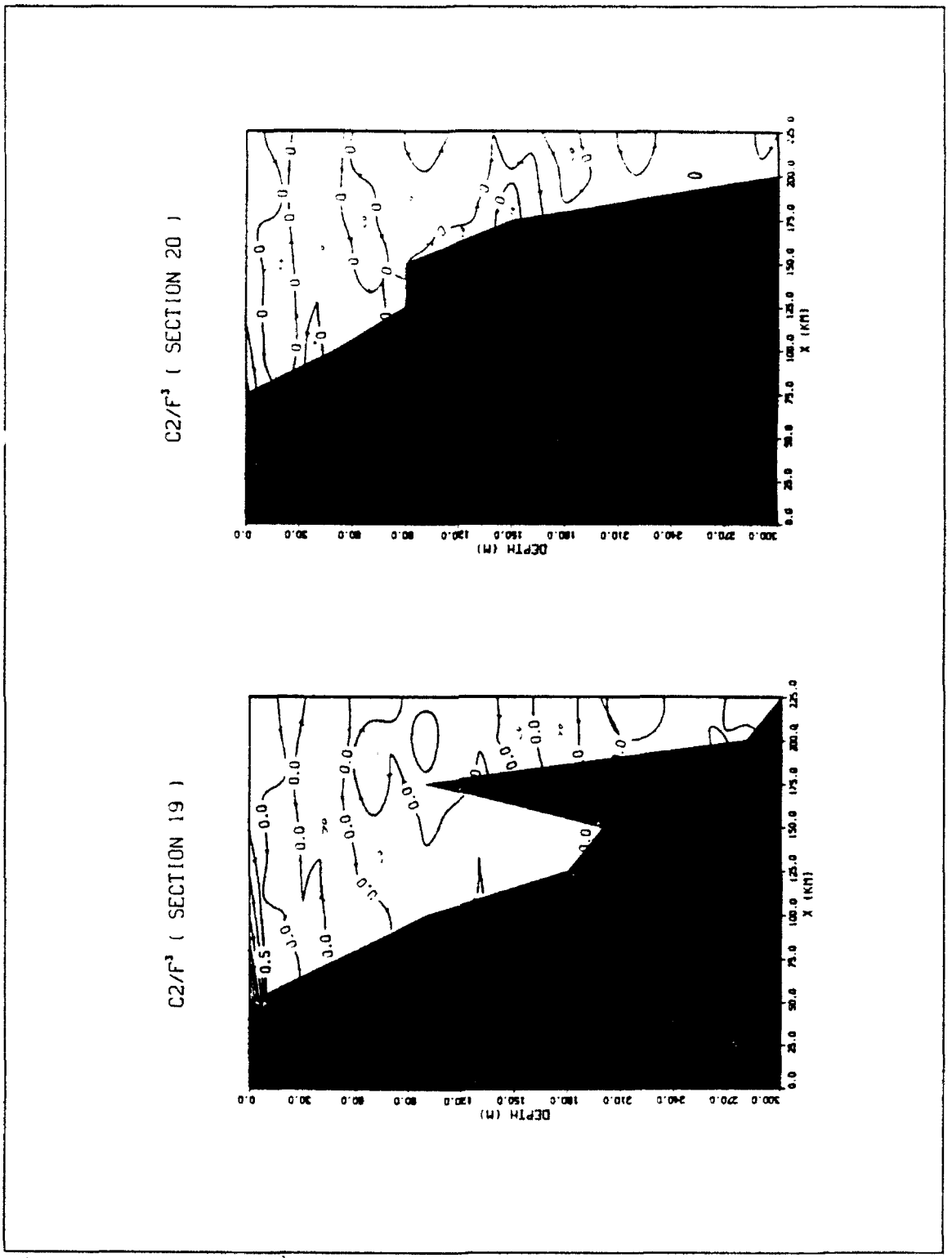

Figure II.10 C_2/f^3 contour at Section 19 and Section 20.

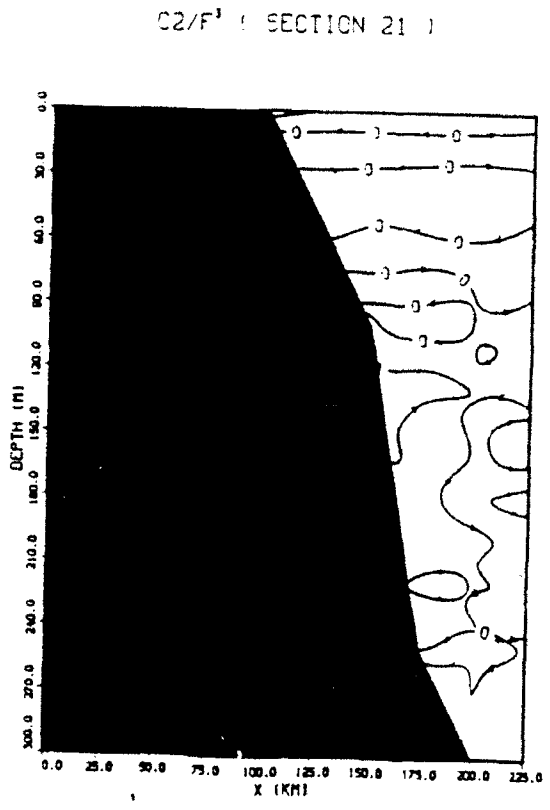

Figure II.11 C_2/f^3 contour at Section 21.

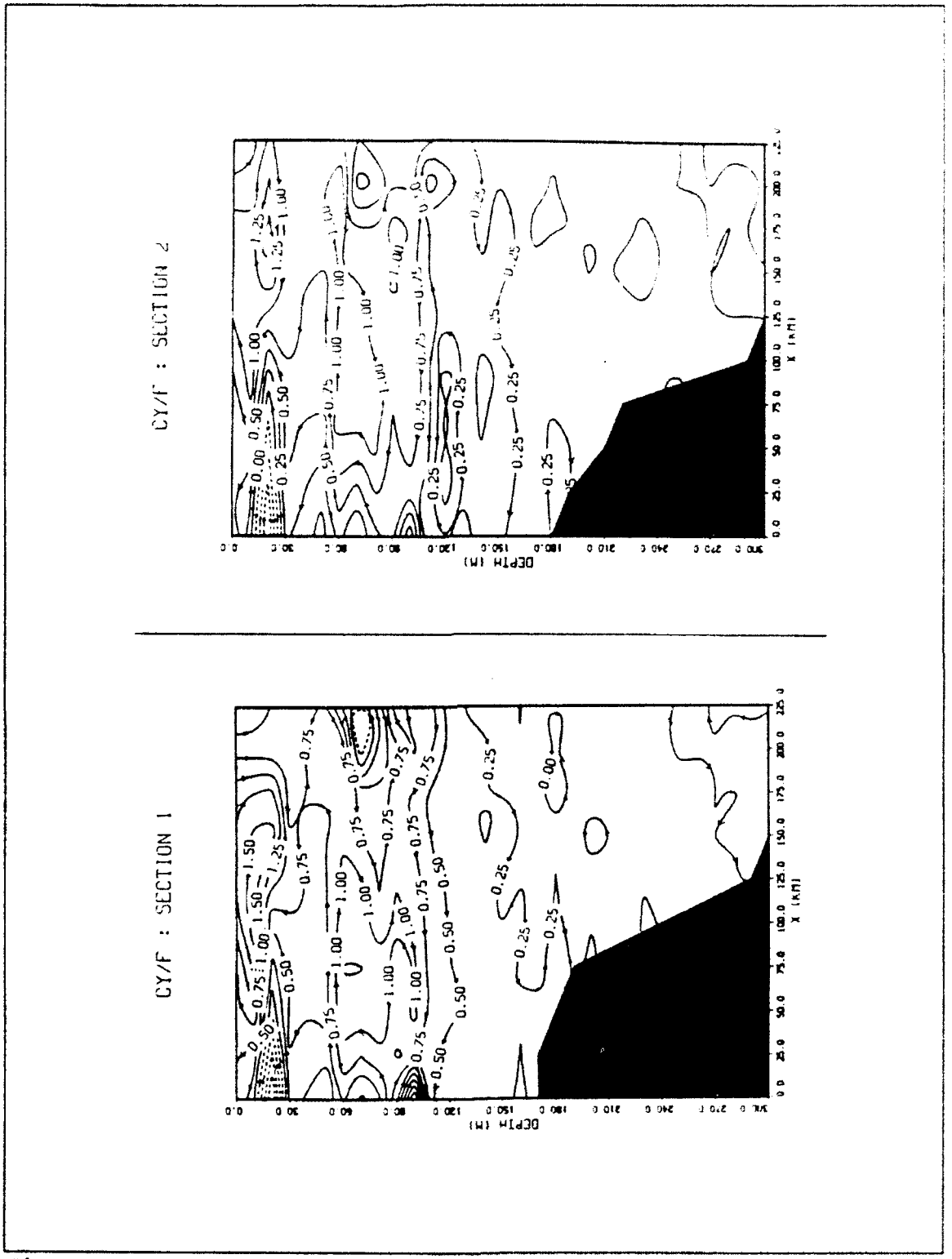

Figure II.12 C_y/f contour at Section 1 and Section 2.

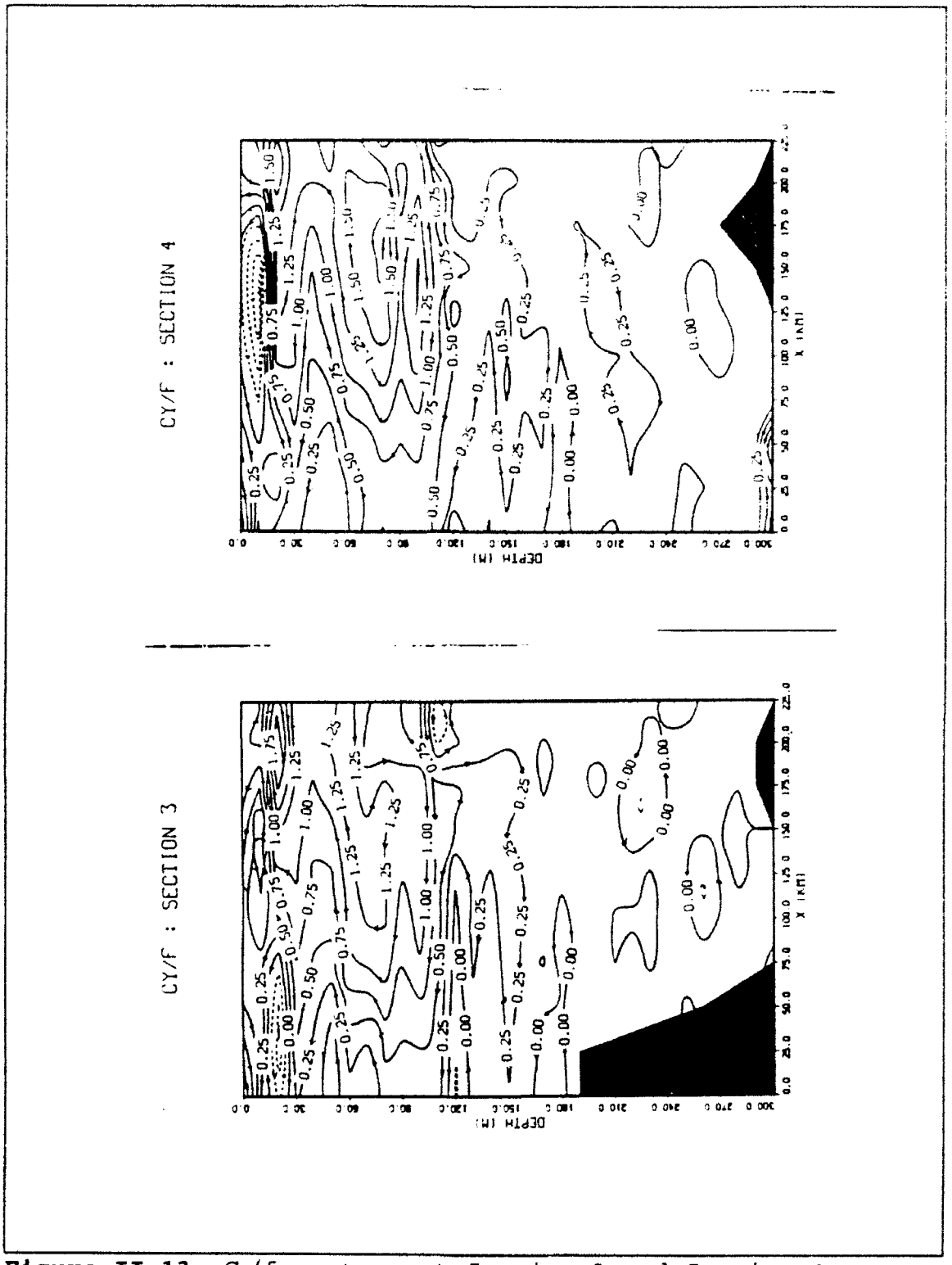

Figure II.13 C_y/f contour at Section 3 and Section 4.

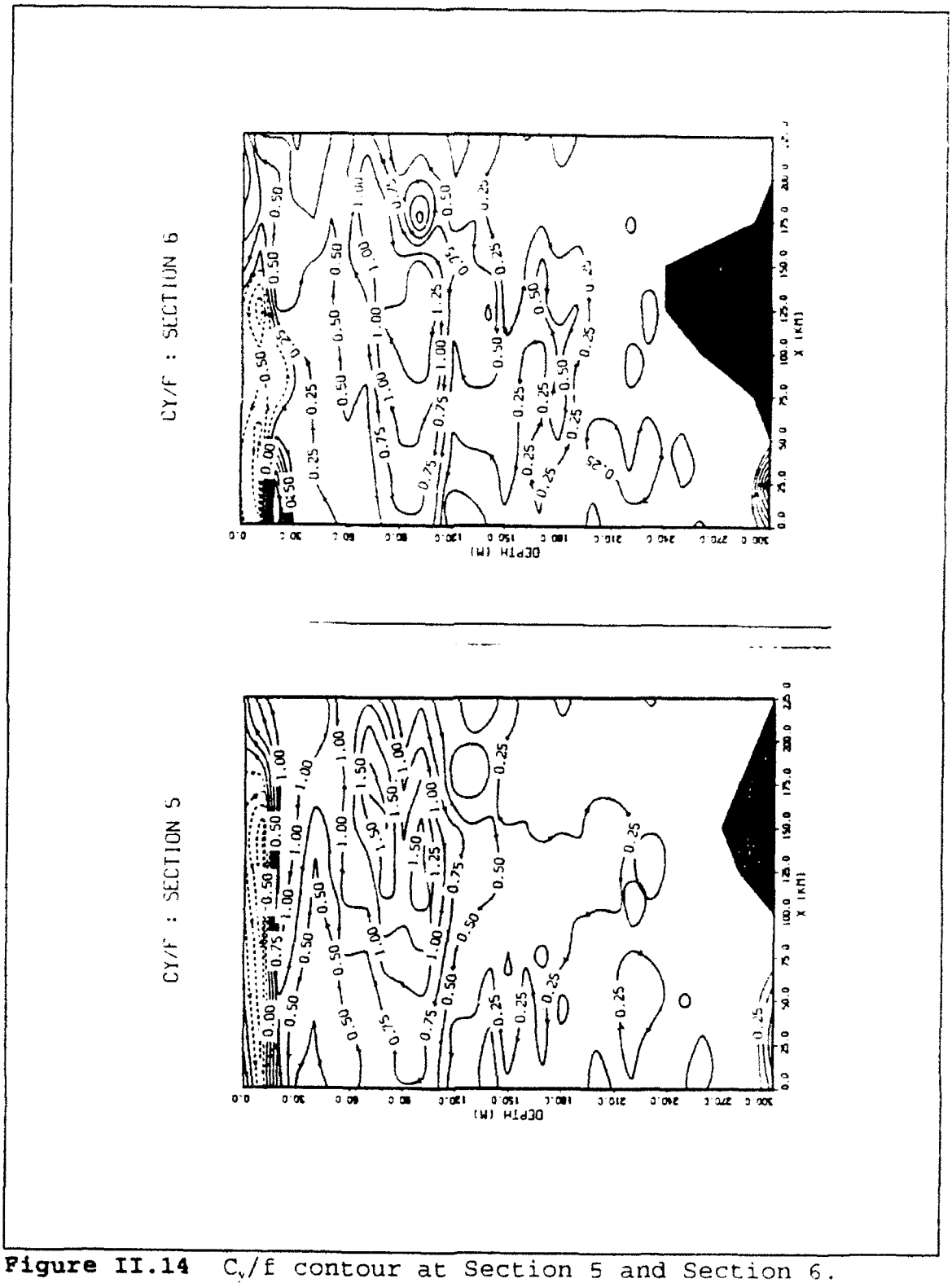

Figure II.14 C_y/f contour at Section 5 and Section 6.

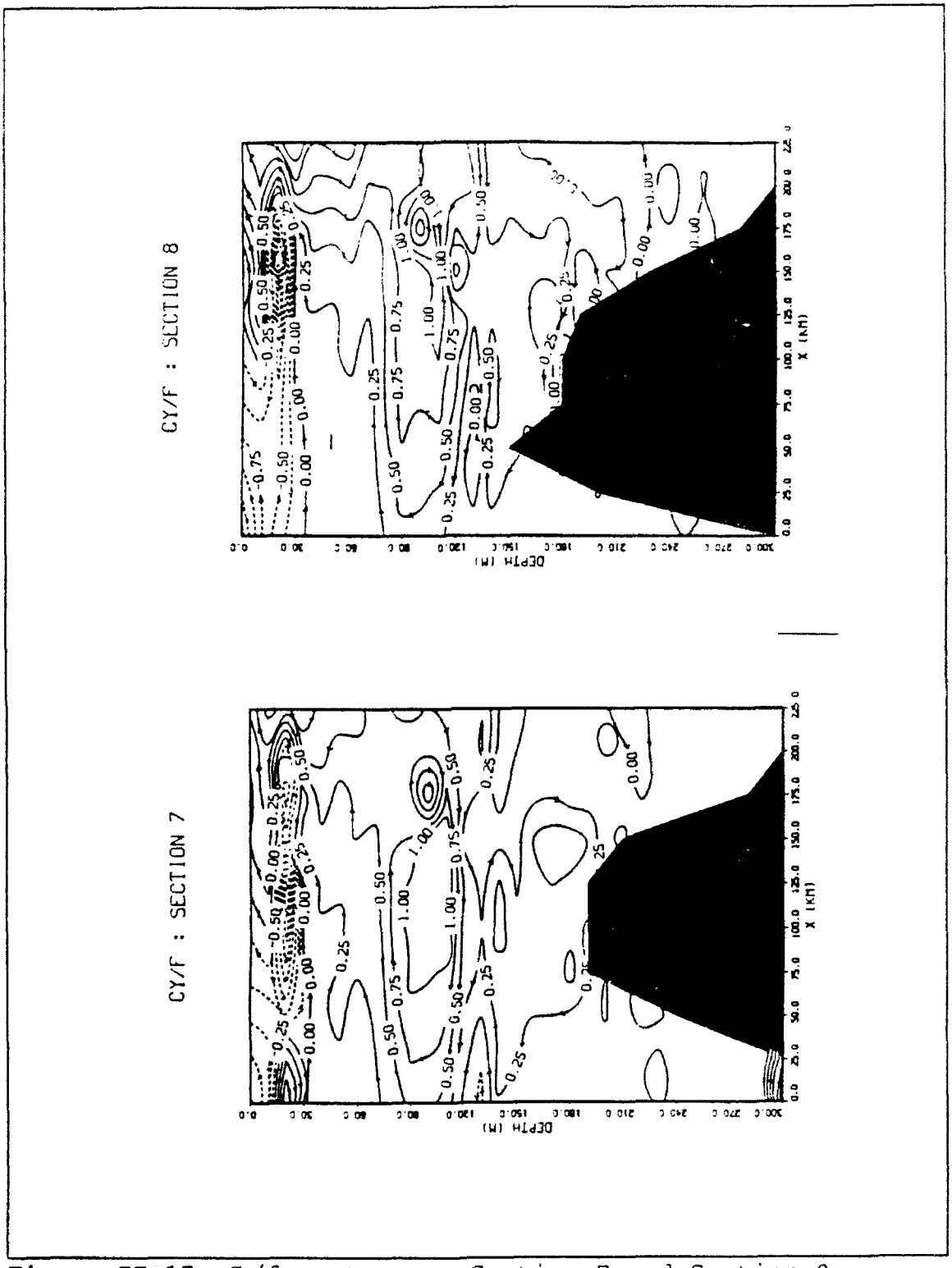

Figure II.15 C_y/f contour at Section 7 and Section 8.

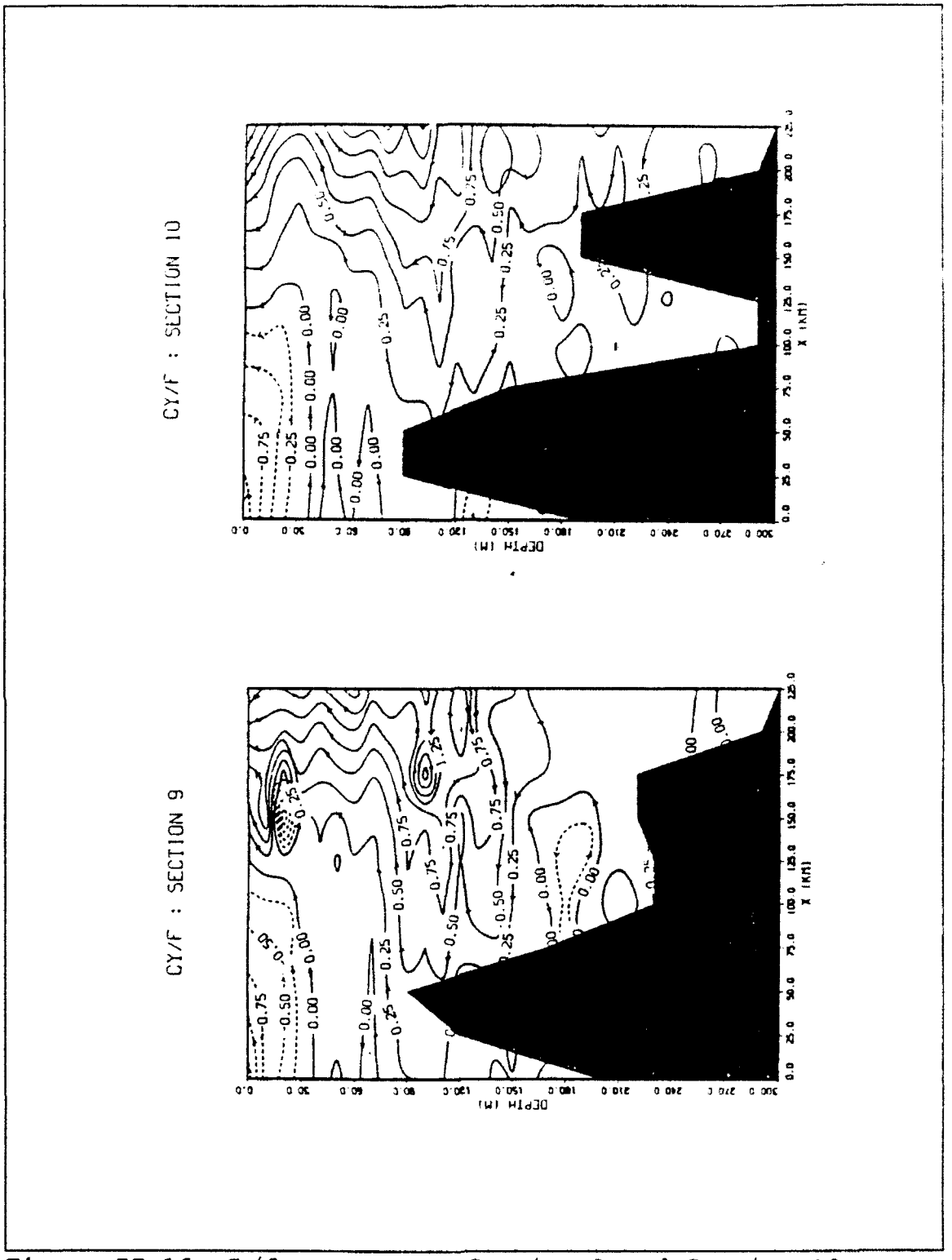

Figure II.16 C_y/f contour at Section 9 and Section 10.

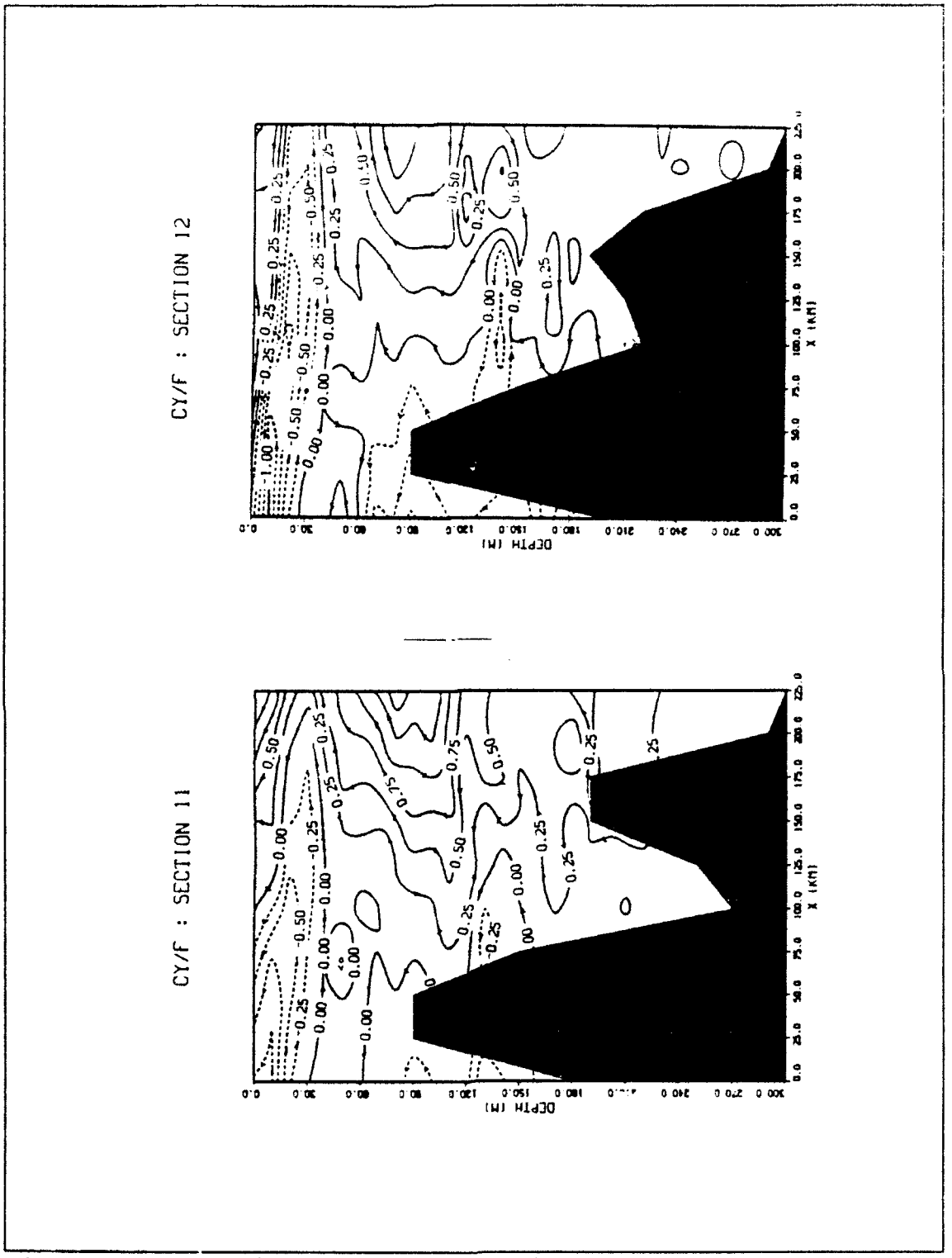

Figure II.17 C_y/f contour at Section 11 and Section 12

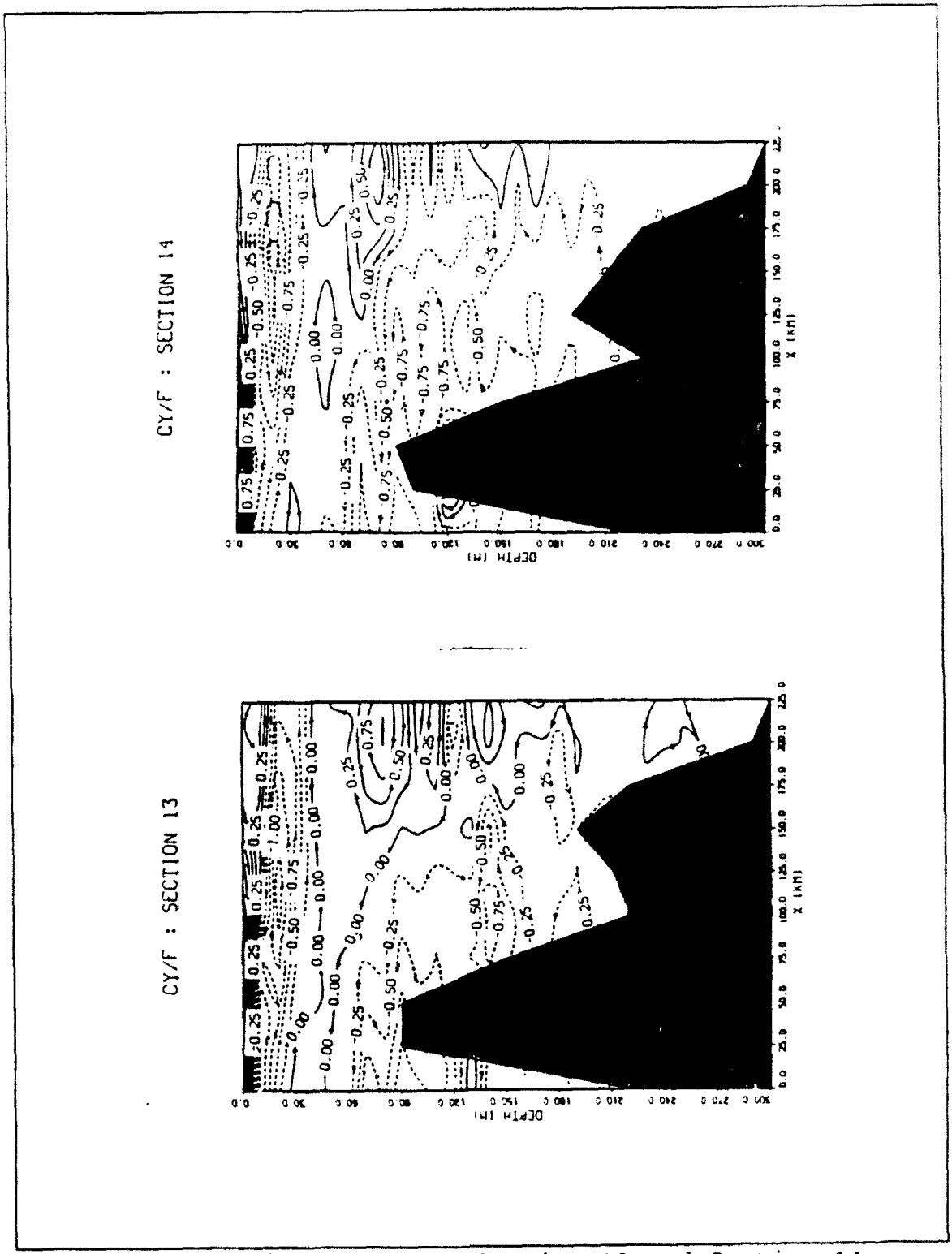

Figure II.18 C_y/f contour at Section 13 and Section 14.

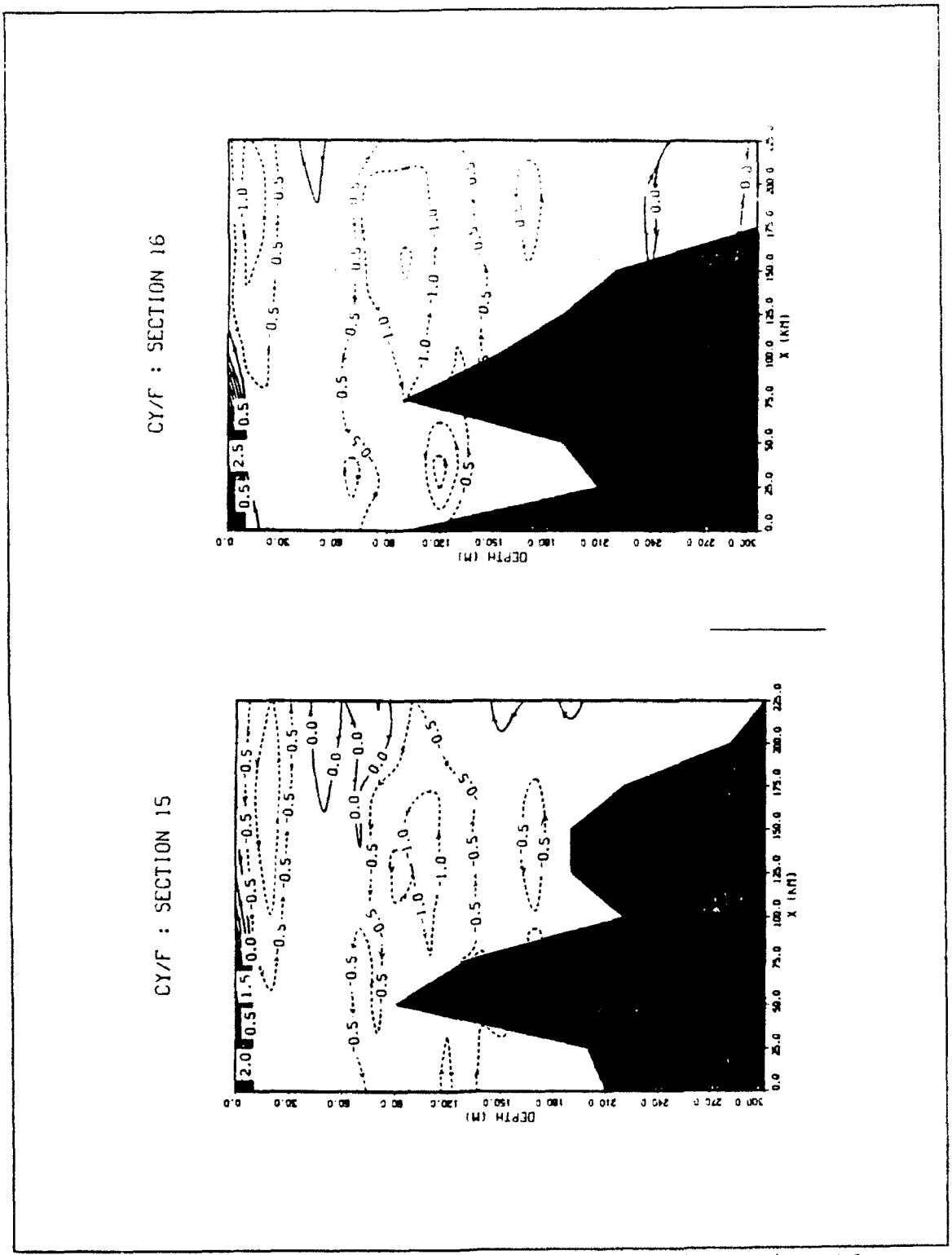

Figure II.19 C_y/f contour at Section 15 and Section 16.

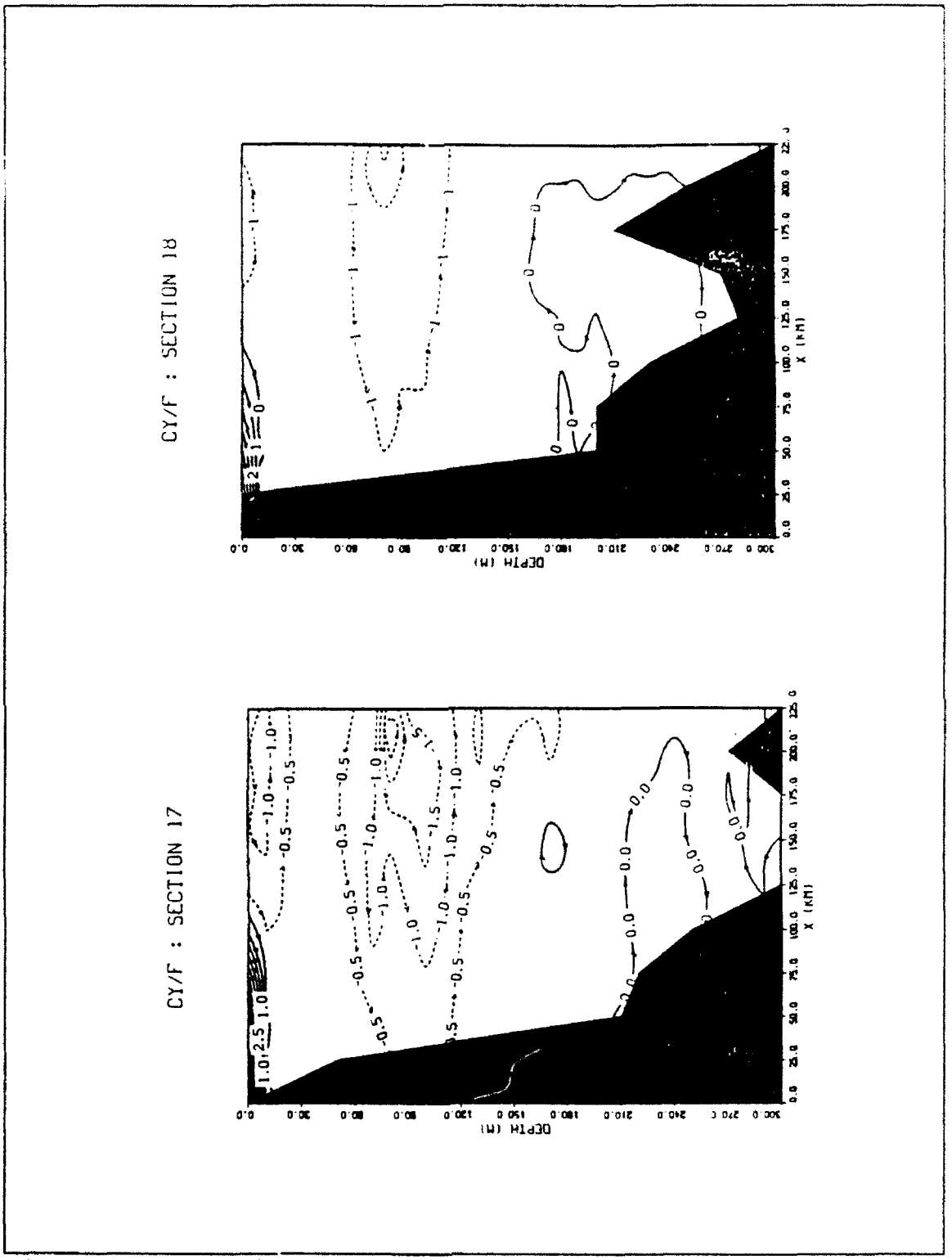

Figure II.20 C_y/f contour at Section 17 and Section 18.

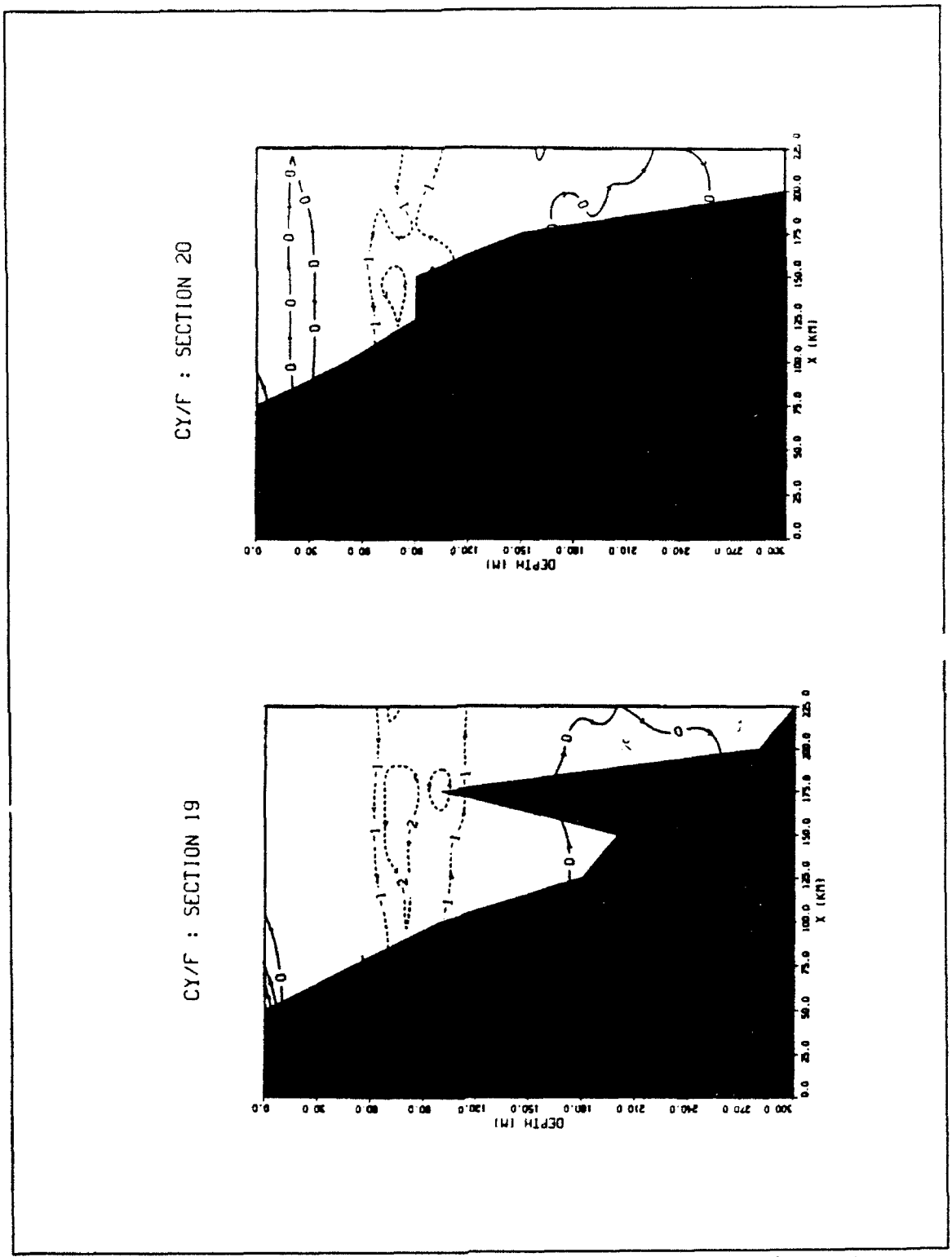

Figure II.21 C_y/f contour at Section 19 and Section 20.

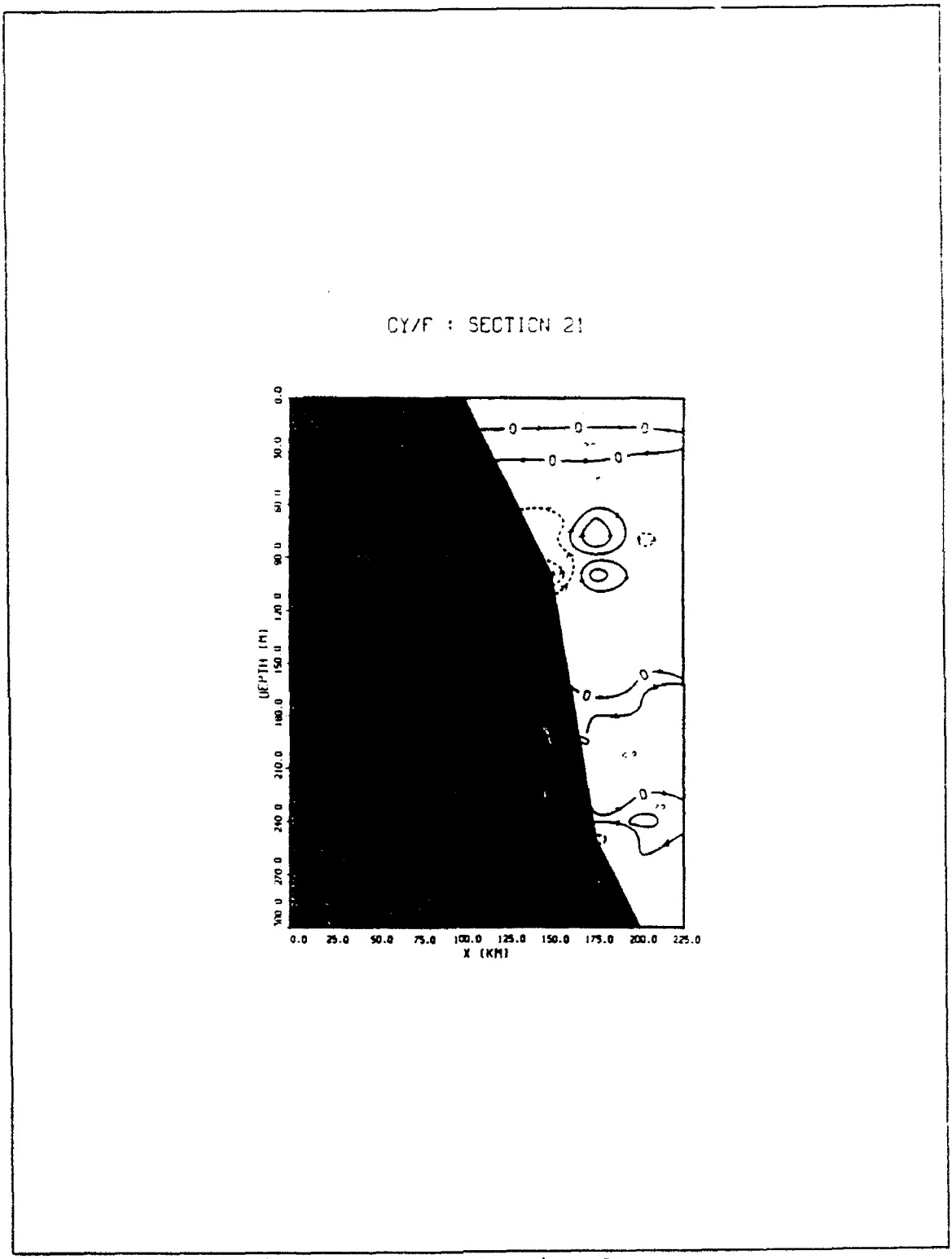

Figure II.22 C_y/f contour at Section 21.

APPENDIX III : Ψ CONTOUR PLOTS

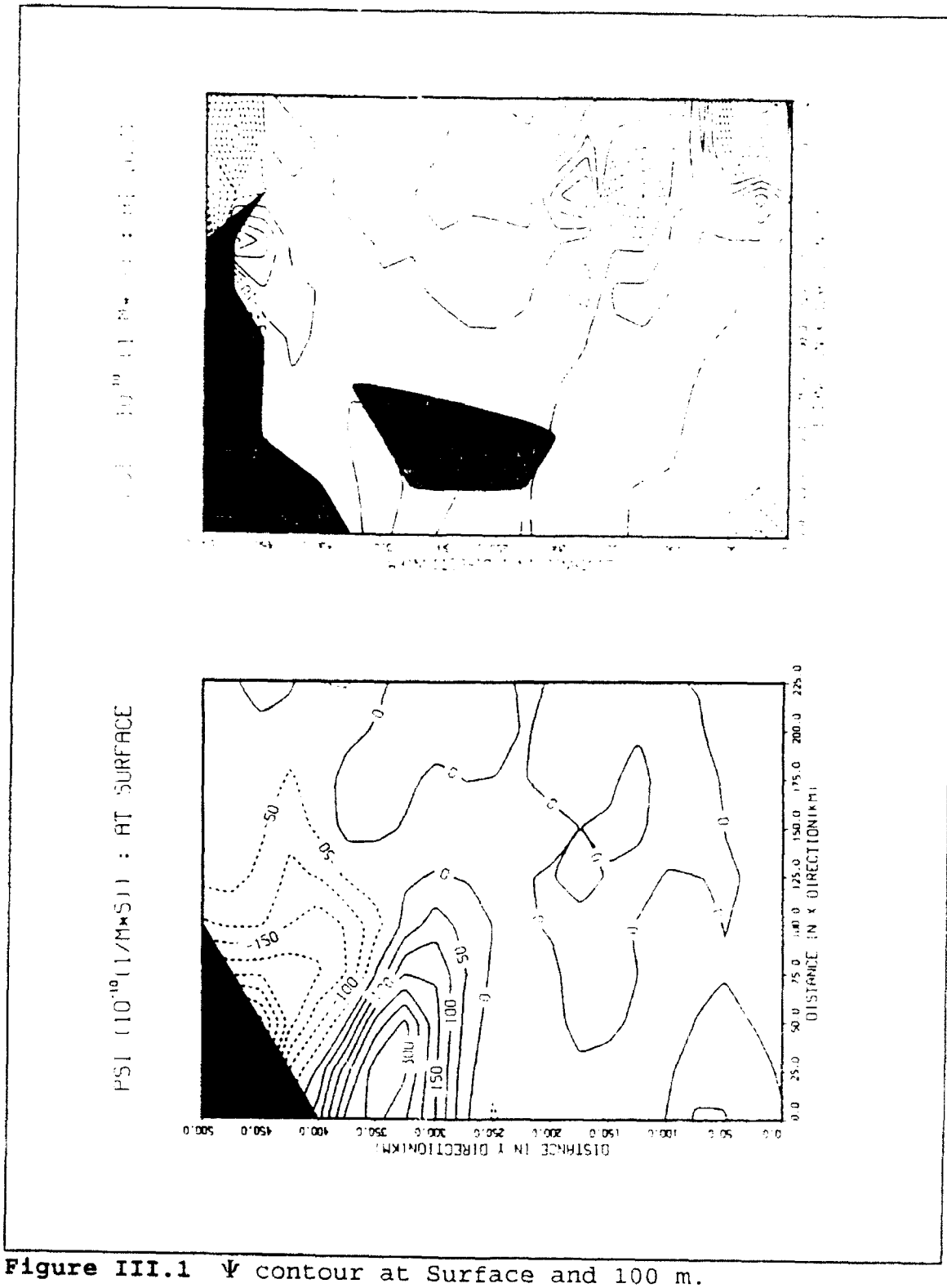

Figure III.1 Ψ contour at Surface and 100 m.

Figure III.2 Ψ contour at 200 m.

LIST OF REFERENCES

Aagaard. K., and L. K. Coachman, The East Greenland Current north of the Denmark Strait, I, Arctic, 21 3), 181-200, 1968a.

Aagaard. K., and L. K. Coachman, The East Greenland Current north of the Denmark Strait, II, Arctic, 21(4), 267-290, 1968b.

Arnone, R. A., D. A. Wiesenburg, and K. D. Saunders, The Origin and Characteristics of the Algerian Current, J. Geophys. Res., 95, 1587-1598., 1990.

Barnes, S. L., A Technique for Maximizing Details in Numerical Weather Map Analyses, J. Appl. Meteor., 3. 396-409., 1964.

Barnes. S. L., Mesoscale Objective Map Analysis Using Weighted Time Series Observations, NOAA Tech. Memo. ERL NSSL-62, 60 pp. [NTIS COM-73-10781], 1973.

Bourke, R. H., J. L. Newton, R. G. Paquette, and M. D. Tunnicliffe, Circulation and Water Masses of the East Greenland Shelf, J. Geophys. Res., 92(C7), 6729-6740, 1987.

Chu, P., C., Three Dimensional Eastern Greenland Sea Circulation Compute from a CTD Data Set, ARCSS Ocean-Atmosphere-Ice Interactors, NSF, pp. 61-64, 1992.

Chu, P., C., Three Dimensional Pseudo-Vorticity Fields in the West Spitsbergen Current, Polar Meteorology and Oceanography, vol. III, pp. 101-104, 1992.

Hoskins, B., J., Draghich I. and Davies H., C., A New Look at the Ω-equation, Quart. J. Roy. Meteor. Soc., 104, 31-38, 1978.

Johnson, G. L., and O. B. Eckhoff, Bathymetry of the North Greenland Sea, Deep-Sea Res., 13, 1161-1173, 1966.

Maddox, R. A., An Objective Technique for Separation Macroscale and Mesoscale Features in Meteorological Data, American Meteorological Society, 108, 1108-1121, 1980.

Muench, R. D., G. S. E., Largerloef, and J. T. Gunn, 1984-85 Current Observations in the East Greenland Current: A Preliminary Description, MIZEX Bull. 7, CRREL Spec. Rep. 86-3, pp. 41-53, U.S. Army Cold Reg. Res. and Eng. Lab., Hanover, N. H., 1986.

Paquette, R. G., R. H. Bourke, J. L. Newton and W. F. Perdue, The East Greenland Polar Front in Autumn, J. Geophys. Res., 90(C3), 4866-4882, 1985.

Perry, R. K., H. S. Flemming, N. Z. Cherkis, R. H. Feden, and P. R. Vogt, Bathymetry of the Norwegian-Greenland and Western Barents Seas, U. S. Naval Research Laboratory - Acoustics Division, Environmental Sciences Group, William and Geintz Map Corporation, Washington, D.C. 1980.

Sutcliffe, R., C., A Contribution to the Problem of Development, Quart. J. Royal., Meteor. Soc. 73, pp 370-383, 1947.

Tintoré, J., D. Gomis, S. Alonso, and G. Parrilla, Mesoscale Dynamics and Vertical Motion in the Alborān Sea, American Meteorological Society, 811-823, 1990.

Tunnicliffe, M. K., An Investigation of the Waters of the East Greenland Current, Master's thesis, 136 pp., Naval Post grad. Sch., Monterey, Calif., 1985,

Xu, Q., Ageostrophic Pseudovorticity and Geostrophic C-Vector Forcing a New Look at the Q-Vector in Three Dimensions, Journal of Atmospheric Science, 49, 981-990, 1992.

INITIAL DISTRIBUTION LIST

1. Colony, Roger — 1
   Polar Science Center, Applied Physics Laboratory
   University of Washington 98105

2. Curry, Judith — 1
   Department of Aerospace Engineering Science
   University of Colorado
   Campus Box 429
   Boulder, Colorado 80309

3. Office of Naval Research (Code 1125 AR) — 1
   Environmental Science Directorate
   800 N Quincy Street, Code 1125
   Arlington, Virginia 22217

4. Defense Technical Information Center — 1
   Cameron Station
   Alexandria, VA 22304-6145

5. Library, Code 52 — 2
   Naval Postgraduate School
   Monterey, CA 93943-5002

6. LCDR. Wei-Szu Li — 1
   21-6f Ruey-Fong St., Ku-San Dist., Kaohsiung,
   Taiwan, R.O.C.

7. Library — 1
   Chung Cheng Institute of Technology
   Tau-Yuen, Taiwan, R.O.C.

8. Department of Oceanography
   Naval Postgraduate School
   Monterey, CA 93943-5000
   Attn: Chairman, (Code OC/Co) — 1
   Attn: Dr. P. C. Chu (Code OC/Cu) — 1

9. Commanding Officer — 1
   Navy Headquarters
   Taipei, Taiwan, R.O.C.

10. Commanding Officer — 1
    Naval Hydrographic & Oceanographic Office
    Tso-Ying, Kaoshiung, Taiwan, R.O.C.

11. Commanding Officer 1
Naval Oceanographic Office
NSTL Station
Bay St. Louis, MS 39522

12. Prof. Untersteiner, Norbert 1
Department of Atmospheric Sciences AK-40
University of Washington
Seattle, Washington 98195

13. Prof. Walsh, John E. 1
University of Illinois
Department of Atmospheric Sciences
105 S. Gregory Avenue
Urbana, Illinois 61801